VNIVERSIDAD NACIONAL AVFNOMA DE MEXICO

UNIVERSIDAD NACIONAL AUTONOMA DE MÉXICO

PROGRAMA DE MAESTRÍA Y DOCTORADO EN INGENIERÍA

INSTITUTO DE INGENIERÍA

Estudio sobre el diseño de observadores no lineales para reactores agitados y tubulares mediante la disipatividad

On the Design of Nonlinear Dissipative Observers for Agitated and Tubular Reactores

T E S I S

QUE PARA OPTAR AL GRADO DE:

DOCTOR EN INGENIERÍA

INGENIERÍA ELÉCTRICA – CONTROL

P R E S E N T A:

ALEXANDER SCHAUM

INSTITUTO DE INGENIERÍA UNAM

TUTOR:

JAIME ALBERTO MORENO PÉREZ

2009

JURADO ASIGNADO:

Presidente: Dr. Espinosa Pérez Gerardo René

Secretario: Dr. Alvarez Calderón Jesus

Vocal: Dr. Moreno Pérez Jaime Alberto

1er. Suplente: Dr. Alvarez Icaza Longoria Luis Agustín

2do. Suplente: Dr. Padilla Longoria Pablo

Lugar o lugares donde se realizó la tesis:

Instituto de Ingeniería - Universidad Nacional Autónoma de México

TUTOR DE TESIS:

Dr. Jaime Alberto Moreno Pérez

_____

FIRMA

Abstract

The application-oriented observer design problem for a practically important class of agitated and tubular reactors is addressed within a unifying design approach. First of all the problem of concentration estimation for a continuous stirred tank reactor (CSTR) with temperature measurements is considered. The designed dissipative observer is combined with a passive state-feedback controller for output-feedback control purposes. The performance of the dissipative-passive output-feedback is analyzed through analytical considerations and numerical simulation studies. The obtained estimator and controller provides an important contribution in the area of chemical process engineering sciences because they combine basic requirements of (i) a systematic design, (ii) convergence improvement, (iii) mathematically rigorous convergence and closed-loop stability criteria with physical meaning, and (iv) ensured performance in a realistic scenario with modeling and measurement errors.

Having the CSTR dissipative observer as methodological point of departure, the result is extended to the consideration of distributed transport and reaction phenomena in an isothermal tubular reactor with concentration point measurements at the boundary and/ or in the domain. A dissipative observer is designed which provides important innovation in the respective are of chemical process engineering studies, because, in comparison to previous studies on this subject reported in the literature, the dissipative observer combines (i) a systematic design, (ii) mathematically rigorous convergence criteria with physical meaning, and (iii) convergence improvement. The performance of the dissipative observer is tested through numerical simulations.

Based on the dissipative observers for the continuous stirred and the isothermal tubular reactor, the problem of estimating the concentration and temperature profile of a non-isothermal tubular reactor with boundary and/ or domain point temperature measurements is addressed. The designed dissipative observer has the same features as the previous ones and thus provides an important contribution in the chemical process engineering field.

On the basis of the obtained dissipative observer design methodology for a class of agitated and tubular reactors, some implications on the design of dissipative observers for more general multi-species transport-reaction system networks are presented.

Resumen

El problema de diseño de observadores para una clase de reactores agitados y tubulares es considerado con un enfoque unificador de diseño. Primero, se considera el problema de estimación de la concentración en un reactor continuo agitado (CSTR por sus signos en inglés) con mediciones de temperatura. El observador disipativo que se diseña es combinado con un control pasivo de retroalimentación de los estados para fines de regulación mediante retroalimentación de salida. El desempeño del controlador disipativo-pasivo es analizado mediante consideraciones analíticas y simulaciones numéricas. El observador disipativo y el controlador dinámico disipativo-pasivo presentan contribuciones importantes en el area de ingeniería de procesos químicos, porque combinan requerimientos básicos como (i) un diseño sistemático, (ii) mejora de convergencia, (iii) criterios de convergencia y estabilidad en lazo cerrado matemáticamente rigurosos y con implicaciones físicas, y (iv) desempeño asegurado en escenarios realistas con errores en el modelo y en las mediciones.

Basandose metodológicamente en el observador disipativo para el CSTR, se extiende el diseño para el caso de transporte y reacción distribuidos en un reactor tubular isotérmico con mediciones de concentración en la frontera y/ o en el dominio. El observador disipativo que se diseña representa una contribución importante en el area de ingeniería de procesos químicos porque, en comparación con los resultados reportados en la literature, combina (i) un diseño sistemático, (ii) rigurosidad matemática en los criterios de convergencia con sentido físico, y (iii) mejora de convergencia. El desempeño del observador es analizado mediante simulaciones numéricas.

Con base en el observador disipativo para el reactor continuo agitado y el tubular isotérmico, se enfoca el problema de estimación de concentración y temperatura para un reactor tubular no-isotérmico con mediciones de temperatura en puntos discretos en la frontera y el dominio. Se diseña un observadore disipativo el cual tiene las mismas caracteristicas que se mencionaron para los casos anteriores, por lo cual representa una contribución importante en el area de ingeniería de procesos químicos.

Basandose en la metodología de diseño de observadores disipativos obtenidos para una clase de reactors agitados y tubulares, se pesentan algunas implicaciones para el diseño de observadores disipativos para redes de sistemas de transporte y reacción con múltiples especies.

Für Romina Elizabeth, unseren Sohn Matthias Federico,
meine Eltern und alle meine Geschwister.

S.D.G.

Acknowledgements

The author gratefully appreciates the continuous assistance and the inspiring discussions with Professor Jaime Alberto Moreno Pérez from the UNAM-México and Professor Jesús Álvarez Calderón from the UAM-Iztapalapa México.

Special thanks to Martin Ott from the University of Stuttgart for the inspiring collaboration and fruitful discussions during his "Diplomarbeit" at the Instituto de Ingeniería at UNAM-México, which enriched the understanding of the tubular reactor observer design studies.

Furthermore, the author thanks Professor Emilia Fridman, from Tel-Aviv University in Israel for the interesting and enriching discussions and her collaboration in our joint scientific publications.

Special acknowledgments to CEP-UNAM and the Coordinación de Posgrado en Ingeniería for financial support.

Contents

List of Figures

Chapter 1

Introduction

In this chapter the consideration of the estimation problem for a class of agitated and tubular reactors is motivated and justified by means of the state-of-the-art in chemical engineering (tubular) reactor observer design in particular and distributed parameter system observer design in general. The approach employed for the solution of the problem is motivated on the basis of results recorded in the chemical engineering literature, and the main contributions are announced.

1.1 Motivation

Modern control applications in the chemical, biological and biochemical process engineering sciences seek for process optimization on the basis of (i) cost efficiency, (ii) product quality, (iii) sustainability, and (iv) robustness. These issues are closely related to the efficiency of the employed control algorithms, in the light of (i) non-wastefulness, (ii) convergence speed, and (iii) robustness oriented convergence properties. Since the early works of Kalman in 1964 [1] and Willems in 1971 [2] it is known that there is a close relation between dissipativity and optimality. This issue has been particularly exploited in the theory of modern nonlinear constructive [3, 4] and passive [5, 6] control. These considerations suggest to approach the above requirements within an energy dissipation framework.

Chemical processes naturally involve many different states, such as temperatures, concentrations and pressures, which interact in complex dynamical networks and the efficient manipulation of given control inputs to such networks requires a high degree of mathematical abstraction. The problem of implementing non-wasteful, fast and robust controllers to achieve high quality products, has to tackle the additional problem that there is an inherent problem in measuring concentrations in chemical reaction networks. In spite of this problematic, in many practically important applications in catalytic chemical and biological reactors, the concentration (or substrate) can be measured [7, 8]. Nevertheless, if such measurements are not at hand, and for systems in which spatially inhomogeneous profiles of temperature and concentration are involved, it becomes necessary to employ state estimators, because it is not possible to measure a complete state profile. This is of particular importance in chemical reactor control applications, since modern (robust and optimal) controllers require knowledge of the complete physical state of the reactor. Depending on the chemical process involved, chemical reactors differ in form, size and operation mode. Two main classes of reactors are given by the tubular and the continuous stirred reactor, being the last one the limit case of the first one in the case of high diffusion (spatial profiles become homogeneous) [9]. The design of an estimator for inference of (eventually spatially inhomogeneous) concentrations on the basis of temperature measurements, thus represents a key element for the entire process design task.

Chemical reactors represent a particular class of transport reaction systems. The dynamic behavior of these systems is completely determined by the continuous interplay between the two basic mechanism of transport and reaction, in the under-

standing that the phenomenological behavior depends on the type of reaction and the kind of transport at place. There are many different kinds of linear and nonlinear transport processes characterizing important classes of systems. For instance, tubular reactors are often driven by diffusive-convective transport [10, 7], or by purely convective (plug-flow) transport [10, 11] corresponding to high flow velocities, while nonlinear transport phenomena such as convective acceleration, characterize e.g. the Korteweg-de Vries(-Burger) equation [12] or the Kuramoto-Shivashinsky equation [13, 14], used to describe flow and flame expansions for instance. In the case of very high diffusion, the tubular reactor corresponds to the continuous stirred reactor [9, 10] and is described by a corresponding ODE model [10, 15]. In the present study, the attention is restricted to linear diffusive-convective constant parameter transport phenomena in agitated and tubular reactors. With respect to the reaction, only pointwise reaction rates are considered, in the understanding that the reaction rate's value at each point of the system extension, is determined by the state values in this point, and does not depend on spatial changes in the states. From a phenomenological viewpoint, one can make the following interpretation of these basic process mechanisms:

- *Diffusion*: A phenomenon caused by Brownian motion of particles within a conductive media (molecules in a fluid, etc.). Diffusion is a natural mass and energy dissipating mechanism, in the understanding that it tends to homogenize the spatial distribution of the considered variables.

- *Advection and Convection*: A phenomenon due to energy and heat transport by a larger-scale motion of currents in the transporting media. Such currents may be caused e.g. by gradients in density or pressure. Due to the motion of the transporting media such mechanisms naturally dissipate mass and energy.

- *Reaction*: A kinetic degradation of some reactants to products by molecular transformations. Reactions may have different properties and the corresponding kinetic rate expressions attain different algebraic forms. Of particular interest for the present study is a differentiation of the nature in terms of *reversibility* and *inhibition*. Reversibility is a property inherent to the reaction mechanism and causes different effects in the corresponding kinetic rate. Inhibition is normally caused by the consumption of a resource necessary for the reaction (e.g. the surface of a catalyst, the concentration of certain enzymes). Both effects

may cause non-monotonic behavior of the kinetic rate: for reversible reactions passing a certain threshold concentration causes a decrease in the degradation and additionally favors the return path of the reaction direction, while inhibition obviously implies a certain threshold where the reaction rate reaches a maximum due to high concentration of the reactants while, passing it, there is too much reactant to ensure the same reactivity with respect to its concentration. Typical rates corresponding to such phenomena are the Haldane-type kinetics [16, 17] in biochemical engineering and Langmuir-Hinsheldwood type kinetics [18, 19] in chemical engineering processes. Saturation phenomena of similar type may also lead to monotonic behavior with slowly decreasing rate as for example known from Monod-type kinetics [8]. These effects may cause regional differences between production or consumption phenomena.

The interplay of diffusive-convective transport with chemical reaction thus introduces a complex interaction of mass and energy consuming (dissipating) and mass and energy producing (or consuming) mechanisms. Consequently the phenomenological behavior depends on the considered process characteristics in terms of: conductivity, permeability, flow velocity (as a result of construction, operation mode, and control), reaction enthalpy, etc. Some of these parameters are explicitly depending on the process and control design while others are inherent to the desired operation mode. The analysis of the different kinds of mechanisms at play is therefore of fundamental interest as it reveals inherent possibilities for, and requirements on the design of the process in the way that the interplay of them enables, or destructs the desired performance. This applies also for the design of a state estimator, in the understanding that: (i) the data-assimilation scheme has to improve the stabilizing and diminish the destabilizing mechanisms at play , (ii) accordingly the sensors have to be chosen (if possible) to obtain from, the less necessary number, the maximal possible information content on the critical elements in the system dynamics, (iii) the gain tuning should exploit the natural dissipation mechanisms in the sense of an optimal innovation, and (iv) the influence of uncertainties and errors has to be analyzed carefully, in particular those related to the possibly destabilizing mechanisms.

1.2 Methodological Approach

Based on the above discussion, the requirements on a chemical reactor observer for concentration and temperature profile estimation, has to satisfy basic requirements: (i) systematic design, (ii) simple implementation and tuning, (iii) some optimality criteria, (iv) mathematical rigor, (v) exploitation of process inherent structural mechanisms, and (vi) certain ensured robustness issues. As has already been mentioned, dissipativity, in an abstract system theoretic sense, has turned out to be a key element between some of these requirements [1, 2, 3, 5, 6]. In this spirit the present study is based on the employment of concepts from, the physically motivated dissipativity theory. In order to employ these concepts, a combination of modern estimation theory and Lyapunov-type stability theory is combined with chemical engineering physical knowledge and mathematical analysis. This complex objective is focussed on employing an inductive three-step approach, based on the fact that the agitated reactor is a physical limit case of the tubular reactor [9].

In this spirit, first, the limit case corresponding to high diffusion of the non-isothermal tubular reactor with temperature measurements is considered, i.e. the non-isothermal continuous stirred tank reactor (CSTR). The basic dissipation mechanisms are identified and exploited for the design of an exponentially stable observer. In order to analyze the behavior of the designed observer in combination with a passive (robust, optimal) controller, an exothermic CSTR with non-monotonic kinetics is considered in the understanding that this kind of kinetics implies difficult observer and control design problems [19, 20, 21, 22].

Next, an isothermal tubular reactor with concentration measurements is considered, in the understanding that (i) the analysis of this case allows for extending the main components of the design methodology to the distributed case, and (ii) there exist important application examples and studies based on concentration measurements in chemical and biological system sciences (e.g. [23, 24, 25, 26, 27])

Then, the non-isothermal tubular reactor with temperature measurements is considered, in the sense that, based on the previous steps, the solution of this complex problem reduces to the consideration of the coupling phenomena while the methodological tools for the analysis and design have already been identified and analyzed in the preceding studies.

Based on these particular cases, next, the corresponding state of the art in the particular area is identified.

1.3 State of the Art

1.3.1 Estimation and control of non-monotonic CSTRs

From experimental and numerical estimation studies on reactors with non-monotonic Langmuir-Hinshelwood [28] or Haldane-type kinetics [16, 8, 29] it is known that the concentration can, in principle, be estimated: (i) with convergence speed fixed by the inverse residence time [28] (or dilution rate [8]), using an open-loop (OL) observer driven by a mass balance-based reaction rate inference, and (ii) with adjustable convergence speed, using an Extended Kalman Filter (EKF) driven by the actual measurement. By construction, the OL observer (referred to as asymptotic in the bioreactor engineering literature) is more robust than its EKF counterpart, in the sense that the OL observer does not need the reaction kinetic model, and the EKF is quite model dependent (including rate function derivatives).

From a control perspective, the output-feedback (OF) control problem, has been addressed by implementing a state-feedback (SF) controller with: (i) an OL (or asymptotic) observer to attain regulation at maximum reaction rate with convergence speed fixed by the dilution rate, or (ii) an EKF to achieve regulation at reaction rate sufficiently below its maximum in order to have local observability and adjustable convergence speed [29, 22].

These considerations manifest, that the slow OL and fast EKF estimators represent extreme cases of an inherent compromise between reconstruction speed and robustness, which has not been formally considered in terms of suitable observability and controllability properties. Furthermore they motivate the design of an observer with: (i) convergence rate between the fast (EKF) and slow (OL) convergence rates attainable with the mentioned observers, (ii) robustness behavior between the strong (EKF) and weak (OL) model dependencies, and (iii) functioning which includes the robust open-loop observer as a particular case and the combination of the observer with a passive, optimal, nonlinear controller for OF control purposes.

1.3.2 Estimation of Tubular Reactors

In the understanding that the tubular reactor is a distributed parameter system, there are, in principle, many different methods which apply to it.

Most of the reported studies are based on *a priori* spatial truncations of the distributed parameter model followed by the employment of lumped observer design

methods (e.g. [7, 30, 31, 32]). This *early-lumping* (EL) approach yields good performance from an application point of view, but it implies different inherent problems: (i) structural properties depend on the truncation method [7, 11], (ii) stability of the truncation does not necessarily imply stability of the distributed model [33], and many design degrees of freedom have to be handled due to high-dimensional model approximations [34].

In the seek of maximal mathematical rigor, different methods have been developed to perform the observer design based on the original PDE model. Respectively, this approach is called *late-lumping* (LL).

For the linear case, since the 1970's, (i) modal (spectral decomposition) approaches have been reported (e.g. [35, 36, 37, 38, 39]), and (ii) stochastic Kalman filters have been employed (e.g. [40]).

For bilinear systems a modal approach with collocated measurement injection in the boundary has been proposed recently [26].

For integro-differential systems, [41] proposed a backstepping observer design.

For nonlinear PDE systems, since the late 1970's, (i) a physical-heuristic approach has been employed [42, 43, 44, 45], (ii) open-loop (OL) (or asymptotic) observers have been introduced [46, 47, 48, 49, 50], (iii) Approximate Inertial Manifolds (AIM) have been applied [51, 11], (iv) linear-quadratic-regulator-type observers have been reported [52], and (v) stochastic Kalman filters have been designed [53]. From these approaches, the physically-heuristic, OL, AIM, and Kalman filters have been applied to tubular reactor studies.

The physically-heuristic approach as well as the OL approach are based on interpolation of the temperature profile between the measurement points. This implies some problems: (i) a mathematically rigorous convergence analysis becomes difficult, (ii) the interpolation requires many measurements and implies many degrees of freedom, and (iii) in the OL case, the concentration convergence is fixed by the process itself and cannot be improved.

The approach using AIMs, yields rather complex analytic expressions for the approximated lumped model which become even more complicated when considering nonlinear, non-monotonic concentration and temperature dependencies of the reaction kinetic rate.

The EKF on the other hand is based on a linearization of the nonlinear model around a given trajectory and consequently the convergence result is basically of

local character [7].

Summarizing, the two main approaches applied to tubular reactors are: (i) *a priori* truncation-based EL approaches, and (ii) approaches based on the original PDE model (LL). All approaches reported in the literature on the tubular reactor estimation problem present a lack of some main requirements as there are (cp. e.g. [54, 11, 55])

- a systematic and mathematically rigorous, non-local design
- simple implementation and explicit solvability conditions
- physical insight
- convergence improvement.

Furthermore, none of the reported studies considered explicitly the implications of non-monotonic reactions. In the studies which apply to the non-monotonic case, no specific analysis has been presented, identifying the inherent limitations and requirements implied by the non-isotonicity feature.

1.4 Contribution

Having as point of departure the previous studies on the design of observers (and controllers) for agitated and tubular reactors, the main contributions of this thesis consist in:

- design of a dissipative observer for a non-monotonic continuous stirred reactor which yields (i) systematic design, (ii) identification of capabilities and limitations, (ii) convergence conditions with physical meaning, (iv) tuning guidelines, and (v) convergence improvement
- combination of the dissipative observer with a nonlinear passive (optimal, robust) state-feedback (SF) controller for output-feedback (OF) stabilization of a non-monotonic exothermic jacketed reactor at maximum production rate, yielding (i) solvability conditions with physical meaning, (ii) rigorous closed-loop stability criteria, (iii) tuning guidelines, and (iv) performance recovery of ideal SF

- concentration profile estimation of an isothermal tubular reactor with boundary and/ or domain point concentration measurements, with (i) systematic design criteria, (ii) mathematical rigor, (iii) explicit convergence conditions with physical meaning, and (iv) convergence improvement

- temperature and concentration profile inference of a non-isothermal tubular reactor with temperature point measurements at the boundary and/ or in the domain, allowing for (i) systematic design approach, (ii) rigorous convergence criteria, (iii) physical implications on process design, and (iv) convergence improvement

In all cases the implications of the reaction kinetics' isotonicity feature are discussed and the corresponding limitations are identified.

These problems are tackled by the combination of (i) chemical engineering sciences (e.g. [10, 9, 7, 15]), (ii) system-theoretic and physical concepts of dissipation (e.g. [2, 56, 57, 58, 59]), and (iii) estimation and control theory of linear and nonlinear lumped and distributed parameter systems (e.g. [3, 6, 34, 38, 39, 60]).

In particular, the continuous stirred reactor observer design uses the recently proposed design methodology for lumped dissipative observers [61, 62]. For the isothermal tubular reactor estimation problem, the conceptual ideas of the previous design are extended for the consideration of distributed transport and reaction phenomena, and combined with basic ideas of linear distributed parameter systems estimation (and control) theory [34, 37, 60], and the convergence analysis is based on DPS stability theory [63, 64, 60, 65, 59, 66]. The analysis of the non-isothermal tubular reactor is based on the previous results for the continuous stirred and the isothermal tubular reactor, which are combined and extended for the consideration of the coupling effects present in the non-isothermal tubular case.

A particular effort throughout this work is spend on addressing the particular problems within a unifying design framework, in the understanding that the continuous stirred and the isothermal tubular reactor represent particular limiting cases of the non-isothermal tubular reactor [10, 9, 47].

In this spirit, the design methodology introduced for the non-isothermal tubular reactor estimation study and the corresponding limit cases represents another contribution of the thesis, in the understanding that it allows for (i) systematic design, (ii) mathematical rigor, (iii) physical insight, and (iv) performance improvement.

Finally, this methodology is put into a more general context of multi-species transport reaction system networks and combined with a system-theoretic dissipativity framework, to obtain general convergence criteria.

1.5 Summary

Based on the respective state-of-the-art in observer design in chemical process engineering sciences and distributed parameter systems, the considered agitated and tubular reactor estimation problems have been motivated and justified. The methodological approach which will be followed has been motivated in general terms, and the main contributions have been announced.

Chapter 2

Estimation Problem

In this chapter the estimation problem for a class of chemical reactors is formulated, including the consideration of three specializations of the regarded system class: (i) the non-isothermal stirred tank reactor with temperature measurement as the limiting case of the tubular reactor with high dispersion, (ii) the isothermal case of the tubular reactor with boundary and/ or domain point concentration measurements, and (iii) the non-isothermal tubular reactor with boundary and/ or domain temperature measurements. Each of these problems constitutes a relevant study subject in chemical process systems engineering. Furthermore, the first two problems are inductive methodological steps towards the consideration of the non-isothermal tubular reactor class, and represent a step towards the development of a general purpose methodology for transport-reaction systems.

2.1 Non-isothermal tubular reactor

In the spirit of its unifying character, the model of the non-isothermal tubular reactor is presented and subsequently the particular application examples are presented as limit cases of the tubular reactor corresponding to high diffusion and isothermal reaction.

2.1.1 Modelling

The basic constellation of a non-isothermal tubular reactor is sketched in Figure 2.1. The reactor consists of the reaction tube, covered by the cooling jacket. The

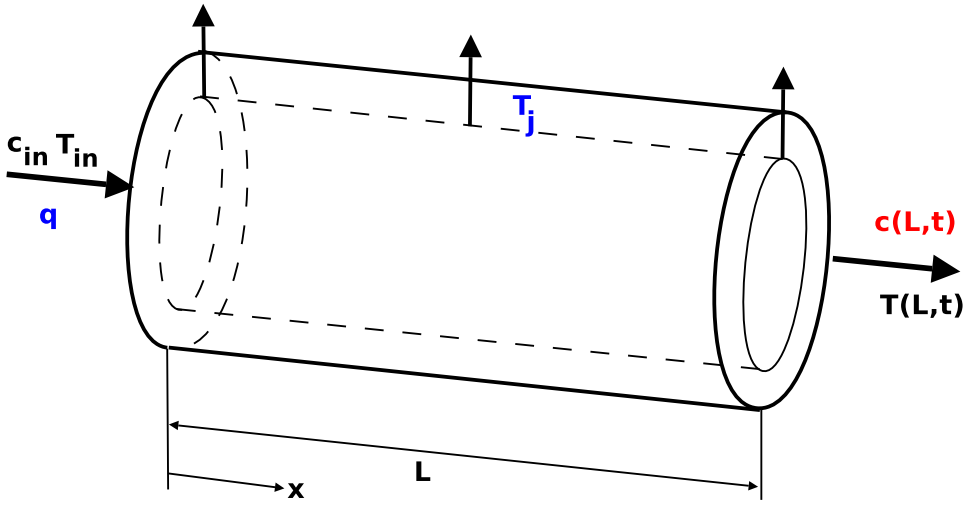

Figure 2.1: Basic constellation of a jacketed non-isothermal tubular reactor.

reactor is fed with a flow with corresponding reactant concentration and fluid temperature. The cooling jacket is fed with cooling fluid in parallel or counterflow with respect to the reactor fluid. The reactor interior may be filled with a catalytic bed (packed-bed reactor) or be empty (empty tube). Mass and energy are transported through the reactor by two mechanisms: (i) diffusion (up- and downstream transport), and (ii) convection (down-stream transport). Along the reactor extension, the reactant is transformed to product through the chemical reaction. The reaction heat produced within the reactor is transferred to the cooling jacket, a process supposed to be instantaneous (infinite radial diffusion), and an energy interchange with the jacket takes place. At the outlet of the reactor no changes take place and the further processing of the product with remaining reactant depends on the design of the

complete process.

Based on these general considerations, next, the mass and energy balance are shortly presented without going into detail, in order to establish the system dynamics, based on which the estimation problem is formulated.

2.1.2 Mass balance

Consider the tubular reactor with length L, and superficial area A, in which a reagent R with concentration $c = [R]/[R]^0$ (referred to pure reagent $[R]^0$), is fed into with an inflow stream of flowrate $q\,[l/s]$ and transported through the reactor by the corresponding convective stream with superficial velocity $v = q/A$, dispersed through the interior with proportionality factor D, and decreased continuously by the reaction to product P with kinetic rate $kr(c,T)$, depending on (i) the concentration c, (ii) the temperature T of the reaction mixture, and (iii) the reaction frequency (proportionality) factor k. Taking into account that the total mass flow through the system is characterized by the combination of dispersion (expressed by Fick's law of diffusion) and convection (characterized by the advective superficial flow), i.e.

$$\mathcal{F}_m(\xi,\tau) = D\frac{\partial c(\xi,\tau)}{\partial \xi} - vc(\xi,\tau), \tag{2.1}$$

the mass balance in the interior ($\xi \in (0,1)$) of the reactor is given by

$$\begin{aligned}\frac{\partial c(\xi,\tau)}{\partial \tau} &= \frac{\partial \mathcal{F}_m(\xi,\tau)}{\partial \xi} - kr(c(\xi,\tau),T(\xi\tau)) \\ &= D\frac{\partial^2 c(\xi,\tau)}{\partial \xi^2} - v\frac{\partial c(\xi,\tau)}{\partial \xi} - kr(c(\xi,\tau),T(\xi,t))\end{aligned} \tag{2.2}$$

for $\tau > 0$. Furthermore, it is assumed that the spatial change at the inlet depends on the concentration difference between feed concentration and actual reactor concentration at $\xi = 0$, while at the outlet of the reactor no changes take place. These considerations are mathematically expressed in Danckwerts boundary conditions [67]

$$\xi = 0: \quad D\frac{\partial c(0,\tau)}{\partial \xi} - vc(0,\tau) = -vc_{in}(\tau), \quad \xi = L: \quad \frac{\partial c(L,\tau)}{\partial \xi} = 0, \quad t \geq 0. \tag{2.3}$$

The evolution of the mass component in time additionally depends on the initial profile $c(\xi,0) = c_0(\xi), \quad \xi \in [0,L]$.

2.1.3 Energy Balance

Considering two types of energy transport through the reactor, (i) diffusion with constant $\alpha\,[m/s^2]$, corresponding to Fourier's law, and (ii) convection due to advective transport according to the fluid flow through the reactor with the superficial velocity $v = \frac{q}{A}$, the total (thermal) energy flow is given by

$$\mathcal{F}_E(\xi,\tau) = \alpha\frac{\partial T(\xi,\tau)}{\partial \xi} - vT(\xi,\tau). \tag{2.4}$$

Furthermore, a continuous change of energy is induced by (i) interchange of heat through a diathermal wall with transport coefficient U and area A_U, and (ii) exothermic (or endothermic) reaction with the reaction enthalpy $(-\Delta H)\,[J]$ and reaction frequency $k\,[1/s]$. Correspondingly, the energy balance reads

$$\begin{aligned}\rho c_p\frac{\partial T(\xi,\tau)}{\partial \tau} &= \frac{\partial \mathcal{F}_E(\xi,\tau)}{\partial \xi} - UA_U(T(\xi,\tau)-T_j) + (-\Delta H)\,kr(c(\xi,\tau),T(\xi,\tau)) \\ &= \alpha\frac{\partial^2 T(\xi,\tau)}{\partial \xi^2} - v\frac{\partial T(\xi,\tau)}{\partial \xi} - UA_U(T(\xi,\tau)-T_j) + (-\Delta H)\,kr(c(\xi,\tau),T(\xi,\tau)),\end{aligned} \tag{2.5}$$

for $\xi \in (0, L)$. Furthermore the possible temperature values and gradients on the boundary are related by Danckwert's boundary conditions [67]

$$\xi = 1:\ \alpha\frac{\partial T}{\partial \xi} = v(T - T_{in}), \quad \xi = L:\ \frac{\partial T}{\partial \xi} = 0, \tag{2.6}$$

where $T_{in}(\tau)$ is the feed temperature. The initial condition is given by a profile $T(\xi, 0) = T_0(\xi)$.

2.1.4 The non-isothermal tubular reactor model

Combination of the mass balance (2.2)-(2.3) with the energy balance (2.5)-(2.6) and using the chemical process engineering parametrization [7, 68, 69]

$$\begin{aligned} &x = \frac{\xi}{L}, \quad t_D = \frac{L^2}{D}, \quad t_c = \frac{L}{v}, \quad t_R = \frac{1}{k}, \\ &t = \frac{\tau}{t_D}, \quad P_e = \frac{t_D}{t_c}, \quad D_a = \frac{t_D}{t_R},\ P_{eT} = \frac{t_D}{t_c}, \\ &L_e = \frac{1}{\rho c_p},\ \eta = \frac{UA_U}{V\rho c_p},\ \beta = \frac{(-\Delta H)}{\rho c_p} \end{aligned} \tag{2.7}$$

yields the non-isothermal tubular reactor model

$$\begin{aligned}\frac{\partial c}{\partial t} &= \frac{1}{P_{ec}}\frac{\partial^2 c}{\partial x^2} - \frac{\partial c}{\partial x} - D_a r(c,T)\\ \frac{\partial T}{\partial t} &= \frac{L_e}{P_{eT}}\frac{\partial^2 T}{\partial x^2} - L_e\frac{\partial T}{\partial x} - \eta(T-T_j) + \beta D_a r(c,T)\end{aligned} \tag{2.8}$$

for $x \in (0,1)$, $t > 0$, boundary conditions

$$x = 0: \quad \begin{aligned}\frac{1}{P_{ec}}\frac{\partial c}{\partial x} &= c - c_{\in}\\ \frac{1}{P_{eT}}\frac{\partial T}{\partial x} &= T - T_{\in},\end{aligned} \quad , \quad x = 1: \quad \begin{aligned}\frac{\partial c}{\partial x} &= 0\\ \frac{\partial T}{\partial x} &= 0,\end{aligned} \tag{2.9}$$

for $t \geq 0$, and initial profiles $x \in [0,1]: c(x,0) = c_0(x), \quad T(x,0) = T_0(x)$. This set of equations describes the considered dynamics of the non-isothermal tubular reactor with axial dispersion and forms the basis of the model-based observer design problem formulated in the next section.

2.1.5 The estimation problem

The estimation problem corresponding to the non-isothermal tubular reactor consists in inferring the concentration and temperature profiles from boundary and/ or domain point temperature and or concentration measurements. Generally speaking, the problem of estimating spatially distributed state profiles includes decisions on

(i) estimation model

(ii) data-assimilation scheme

(iii) sensor location.

In the present context of the non-isothermal tubular reactor estimation problem, these issues obtain the following basic interpretation:

ad (i): design of the observer on the basis of the distributed model (*late lumping*) or use of a spatial discretization (*early lumping*).

ad (ii): choice of an explicit correction mechanism from an infinite number of possible spatial distributions and measurement coupling combinations.

ad (iii): analysis of the information content of the measurement, in dependence on the sensor location, to choose an optimal sensor location in terms of estimation performance (convergence speed and robustness).

The corresponding decisions should be taken in the light of particular requirements as there are (i) simple and cheap implementation, (ii) mathematical rigor and ensured performance, (iii) convergence improvement, and (iv) explicit convergence criteria with physical meaning.

Based on these considerations: (i) the *late lumping* approach is employed to enable maximal mathematical rigor based on physical insight to the reactor dynamics, (ii) the data-assimilation scheme is considered as an important design degree of freedom, in the sense of comparing some particular possibilities in order to get close to an optimal choice (in the above mentioned sense of desired performance), and (iii) the sensor location is identified as a key issue for the design of an estimator but no analytical analysis method is employed for the location of the sensor, but only general considerations are performed.

2.1.6 The methodological approach

In order to address the estimation problem of the regarded chemical reactor class described by the equation set (2.8)-(2.9), in the spirit of a unifying framework, the following particular cases are considered as specializations of the non-isothermal tubular reactor estimation problem.

1.) Non-isothermal stirred tank reactor with temperature measurement: As it is well-known [9], in the limit case of infinite diffusion, the tubular reactor dynamics are perfectly well described by the dynamics of a continuous stirred tank reactor (CSTR). The consideration of the estimation problem for the non-isothermal CSTR permits to address two main issues:

- identify the main mechanisms at play in terms of mass and energy transport phenomena and chemical reaction, and exploit them in order to obtain mathematically rigorous convergence criteria coupled with simple tuning guidelines
- analyze the application of the designed state estimation scheme for output-feedback (OF) purposes, combining the dissipative observer with a passive nonlinear state-feedback (SF), to obtain rigorous and simple convergence conditions with physical interpretation

2.) Isothermal tubular reactor with concentration measurement: The consideration of the inference of the concentration profile from boundary and/ or domain point concentration measurements enables to identify two basic issues:

- analysis and assignment of the energy-dissipation properties corresponding to distributed diffusive-convective transport
- handling the spatially distributed nature of the influence of the chemical reaction on the convergence properties

3.) Non-Isothermal tubular reactor with temperature measurement: Based on the preceding results obtained for the non-isothermal CSTR with temperature measurement and the isothermal tubular reactor with concentration measurements, the problem of concentration and temperature profile inference for the non-isothermal tubular reactor based on temperature point measurements at the boundary and/ or in the domain relies in the consideration of two different kind of coupling phenomena:

- linear coupling through the correction injection mechanism
- nonlinear coupling through the chemical reaction

Correspondingly, the particular study cases allow for a step-by-step identification and solution of the main problems which have to be addressed for the consideration of the non-isothermal tubular reactor estimation problem.

Furthermore, *each problem in itself represents a contribution with respect to previous studies in the stirred and tubular reactor fields.*

In the sequel the particular estimation problems are presented.

2.2 Non-isothermal stirred tank reactor

2.2.1 The estimation model

It is known [9] that the dynamics of a tubular reactor with infinite diffusion are completely described by the model of a continuous stirred tank reactor (CSTR). In a more realistic scenario, considering the case that the process conditions lead to high diffusion coefficients and the flow velocity is considerably small, in the understanding that the diffusion-characteristic (Einstein) time $t_D = L^2/D$ is much less

than the convection-characteristic time $t_c = L/v$ and thus energy and mass are dispersed rapidly through the reactor, the spatially distributed profile rapidly tends to a spatially constant profile. If furthermore a mixing mechanism is employed, a homogeneous spatial distribution can be assumed without loss of important information [10, 7, 68]. Under this assumption the mass and energy balances naturally lead to the model of a Continuous Stirred Tank Reactor (CSTR). Figure 2.2 shows the basic

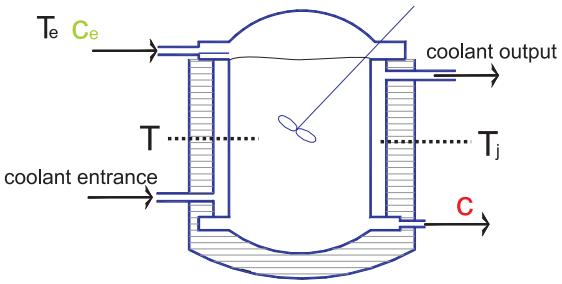

Figure 2.2: Configuration of the *continuous stirred tank reactor* (CSTR).

configuration of a CSTR.

Using the standard notion in chemical engineering sciences of the dilution rate or inverse residence time $\theta = \dfrac{1}{t_R} = \dfrac{q}{V}$, the CSTR model equations are given by

$$\begin{aligned} \dot{c} &= \theta(c_e - c) - r(c, T, p_r), \quad c(0) = c_0 \\ \dot{T} &= \theta(T_e - T) - \eta(T - T_j) + \beta r(c, T, p_r), \quad T(0) = T_0, \\ y &= T \end{aligned} \tag{2.10}$$

with parameter vector $p = (p_a^T, p_r^T)^T$, $p_a = (c_e, \beta, \eta)^T$ being the vector with the feed concentration (c_e), the adiabatic temperature rise (β) and the heat transfer coefficient (η). Note that the reaction rate expression is given by $r = kR$. It is known [70] that the trajectories of the reactor (3.1) are restricted to the compact interval $\Xi = [0, 1] \times [T^-, T^+]$, where $T^- = \min(T_e, T_c)$ (or $T^+ = \max(T_e, T_c) + \beta$) is the minimum (or maximum) possible temperature determined by mass-heat conservation and thermodynamic's second law arguments.

The consideration of the non-isothermal CSTR estimation problem based on temperature measurements allows to identify

- the main mechanisms at play in terms of transport and reaction phenomena
- the main issues corresponding to the application of an energy-based dissipative observer

- the main interplay between system inherent transport and reaction mechanisms and the imposed correction mechanism
- a methodological framework to analyze the nonlinear dissipation components corresponding to the chemical reaction.

Furthermore, it enables the analysis of the application of the designed observer for OF control purposes. Therefor, the dissipative observer is combined with a passive nonlinear SF controller. This allows to

- exploit the structure-oriented approach of the dissipative observer based on an explicit energy and dissipation characterization
- analyze the performance of the OF controller employing Lyapunov's direct method.

Methodologically speaking, the stirred tank estimation (and control) problem is addressed by combining dissipativity, (passivity,) and chemical reaction engineering tools.

2.3 Isothermal tubular reactor

2.3.1 The estimation model

Assuming a constant temperature profile corresponding to an isothermal reaction, the estimation model, with boundary and/ or domain point concentration measurements follows from the mass balance (2.2)-(2.3)

$$\frac{\partial c(x,t)}{\partial t} = \frac{1}{P_{ec}}\frac{\partial^2 c}{\partial x^2} - \frac{\partial c}{\partial x} - D_a r(c(x,t), T(x,t)) \tag{2.11}$$

for $t > 0, \quad x \in (0,1)$, boundary conditions

$$x = 0 : \frac{1}{P_{ec}}\frac{\partial c(0,t)}{\partial x} = (c(0,t) - c_{in}(t)), \quad x = 1 : \frac{1}{P_{ec}}\frac{\partial c(1,t)}{\partial x} = 0 \tag{2.12}$$

for $t \geq 0$, initial profile $x \in [0,1] : c(x,0) = c_0(x)$ and measurement vector

$$y(t) = [c(0,t),\, c(\xi,t),\, c(1,t)]^T, \tag{2.13}$$

where $\xi \in (0, 1)$ is the domain-sensor location.

It is noteworthy, that the isothermal tubular reactor case represents also an important class in bio-systems engineering (see e.g. [27, 25]).

The isothermal reactor estimation problem will be addressed by extending the stirred transport-reaction dissipation concept to distributed diffusive-convective transport, and exploiting the sector characterization of the stirred case, adapting it to the distributed case.

Mathematically speaking, standard tools from functional analysis and related Lyapunov-type methods are employed to perform the technical part including the convergence assessment and the derivation of explicit solvability conditions with physical meaning.

2.4 Non-isothermal tubular reactor with temperature measurements

The non-isothermal tubular reactor estimation problem is based on the mass and energy balance (2.8)-(2.9), and the assumption that only point temperature measurements at the boundary and in some point of the domain are available.

Having as point of departure the preceding non-isothermal agitated and isothermal tubular reactor studies, the main issues which have to be addressed for the non-isothermal tubular reactor consist in the coupling by the reaction kinetics, and the artificial coupling introduced by the correction mechanism.

2.5 Implications for a class of more general transport reaction systems

Finally, some implications and considerations for transport-reaction distributed systems in general are discussed, based on a generalized model including several species which dynamically interact through various simultaneous reactions.

This issue allows to establish the basis for a more general observer design methodology for larger classes of transport-reaction systems. For this purpose, the basic features of the developed design methodology for the isothermal and the non-isothermal tubular reactor are extended to a more general abstract dissipativity

framework. The approach combines dissipativity, passivity and chemical reaction engineering tools with functional analytic methods.

2.6 Practical Stability Framework

The underlying practical stability framework, employed for the subsequent observer (and control) design studies is presented. The employment of the concept of practical stability for the chemical reactor estimation (and control) studies is motivated by the fact, that the real process has to be supposed to be subject to (i) errors in the parameters and the measurements, and (ii) disturbances in the exogenous load, which are unknown. The corresponding robustness oriented stability property, enables to analytically delimit an ensured convergence behavior in a real-world application.

Consider the (tubular or continuous stirred) reactor with constant ($\tilde{p}$) parameter, time-varying reactor temperature measurement $\tilde{y}$, time-varying exogenous load (feed) $\tilde{d}$, and actuator bounded errors. The *actual reactor system dynamics* are given by

$$\frac{\partial z}{\partial t} = f(z, d + \tilde{d}(t), u + \tilde{u}(t), p + \tilde{p}), \quad z(0) = z_0, \quad y = Cx + \tilde{y}(t), \quad z = x \tag{2.14}$$

where $z = [c, T] \in Z$ is the (possibly spatially distributed) state vector in the state space Z (an euclidean or L^2 space), $d \in \mathbb{R}^k$ is the exogenous (possibly distributed) load, $u \in \mathcal{U}$ is the (possibly distributed) control input, an element of the input space $\mathcal{U}$ (including possibly space and time varying functions), and p is the constant parameter vector of the reactor dynamics. Consider that all errors and disturbances are bounded

$$||\tilde{p}|| \leq \delta_p, \quad \left|\left|\tilde{d}(t)\right|\right|_{\sup} \leq \delta_d, \quad ||\tilde{u}(t)||_{\mathcal{U}} \leq \delta_u, \quad ||\tilde{y}(t)||_{\sup} \leq \delta_y,$$

where δ_p, δ_d, δ_u and δ_y are the error sizes, and $||\cdot||$ is the Euclidian (vector) norm, $||\cdot||_{\sup}$ is the supremum norm of a real valued function, and $||\cdot||_{\mathcal{U}}$ is the norm corresponding to the input (function) space $\mathcal{U}$ (normally a L^2-space in space and time). In deviation form, referred to the steady state $\bar{z}$, the preceding reactor system (2.14)

is written as follows

$$\frac{\partial e}{\partial t} = f_e[e, \tilde{u}_e(t)],\ e(0) = e_0,\ e = z - \bar{z},\ \tilde{u}_e = (\tilde{p}^T, \tilde{d}^T, \tilde{u}^T)^T,\ f_e(0,0) = 0. \quad (2.15)$$

The definition of *nonlocal input-to-state (IS) stability* [71, 72, 3], which underlies the present study, is stated next.

Definition 2.1. *The steady-state $e = 0$ of system (2.15) is said to be* ***practically uniformly stable*** *if an admissible disturbance size (δ_{ue}) produces an admissible state deviation size (ε_z): given $(\delta_{ue}, \varepsilon_z)$ there is a KL-class (increasing-decreasing) function τ and a K-class (increasing) function α so that the state responses of system (2.15) are bounded as follows*

$$\begin{aligned} ||e_0||_Z \leq \delta_0, ||\tilde{u}_e(t)||_{\mathcal{U}e} \leq \delta_{ue} \Rightarrow ||e(t)||_Z &\leq \tau(||e_0||_Z, t) + \alpha(||\tilde{u}_e(t)||_{\mathcal{U}e}) \\ &\leq \tau(\delta_0, 0) + \alpha(\delta_{ue}) = \varepsilon_z \end{aligned} \quad (2.16)$$

where τ (or α) bounds the transient (or asymptotic) component of the response.

The (necessary and sufficient) Lyapunov characterization of the ISS property is given by [72]

$$\alpha_1(||e||_Z) \leq V(e) \leq \alpha_2(||e||_Z), \quad \dot{V} = -\alpha_3(||e||_Z) + \alpha_4(||\tilde{u}_e||_{\mathcal{U}e}) \quad (2.17)$$

where V is a positive definite radially unbounded function and $\alpha_1, \cdots, \alpha_4$ are K-class functions. Henceforth, practical uniform stability will be simply referred to as *practical (P) stability.*

Furthermore, a particular Lyapunov-like exponential stability result is employed frequently. Consider the state space Z, an euclidean or L^2 space, with norm $||\cdot||_Z$. Let $E(e)$ be a functional which defines a norm equivalent to $||\cdot||_Z$, in the understanding that there exist $m_1, m_2 > 0$ such that

$$m_1 ||e||^2 \leq E(e) \leq m_2 ||e||^2. \quad (2.18)$$

Then the following result holds.

Lemma 2.1. *Let $E(e)$ be a functional which fulfils (2.18). Furthermore, let $\dot{e} =$*

$f(t,e)$, $e(0)=e_0$ with $e(t)\in Z\,\forall t\geq 0$, so that $f(t,0)=0$, $\forall t\geq 0$. If it holds that

$$\frac{dE(e)}{dt}\leq -2\lambda E,\quad \lambda>0, \tag{2.19}$$

then it follows

$$||e(t)||\leq a\,||e_0||\,e^{-\lambda t},\quad a=\sqrt{m_2/m_1}. \tag{2.20}$$

Proof. It follows from the comparison principle [73], that $E(e(t))\leq E(e_0)e^{-2\lambda t}$ and with (2.18), property (2.20) follows. □

2.7 Summary

The estimation problem addressed in the present study has been formulated, and the corresponding P-stability framework has been presented. Three particular study objects have been identified: (i) the non-isothermal CSTR with temperature measurement, as the limiting case of high dispersion of a tubular reactor, (ii) the isothermal tubular reactor with concentration measurements, and (iii) the non-isothermal tubular reactor with temperature measurements.

The particular advantages of considering these specializations of the non-isothermal tubular reactor estimation problem allow to solve the distributed estimation problem in an inductive way, in the understanding that

- the consideration of the lumped CSTR estimation problem with temperature measurement enables the identification of a methodological framework to exploit the process inherent mechanisms of (i) transport, and (ii) reaction, in order to obtain (a) mathematically rigorous convergence criteria, and (b) physically meaningful solvability conditions.

- the isothermal tubular reactor with concentration measurements includes the basic distributed mechanisms at play in all tubular reactors with diffusive-convective transport, and thus allows to extend the previously identified methodological framework to the case of distributed diffusive-convective transport, and enables the analysis of the distributed nonlinear kinetic influence on the convergence behavior.

- the estimation problem for the non-isothermal tubular reactor with temperature measurements reduces to the analysis of the influence of the coupling effects between the concentration and temperature dynamics, and the extension of the methodological treatment of the nonlinear kinetic influence of the reaction to the case that the distributed reaction mechanism depends on more than one state variable.

Each of these problems constitutes an important field of actual studies in the chemical process engineering sciences and offers an interesting contribution with respect to the preceding literature.

Additionally, the consideration of these particular study cases will enable to conclude the work with some implications for a more general class of systems, which includes the regarded cases as specializations. These considerations represent an interesting contribution in the field of observer design methodologies for (distributed) transport-reaction systems.

Chapter 3

The non-isothermal stirred tank reactor

In this chapter the concentration estimation problem is addressed for the high-dispersion limiting case of the non-isothermal tubular reactor: the non-isothermal continuous stirred tank reactor with temperature measurement.

The purpose is twofold: (i) a methodological step towards the consideration of the tubular reactor and (ii) the resolution of estimation and control problems in the light of previous studies in chemical reactor systems engineering.

First, the reactor inherent energy interchange mechanisms are analyzed and their importance for the observer design are discussed. Next, based on the notions of observability and detectability, the dissipative observer is introduced exploiting the reactor's transport and reaction mechanisms, applying Lyapunov's second method to obtain convergence conditions coupled with simple tuning guidelines.

Finally, the dissipative observer is combined with a nonlinear passive SF controller to yield an OF controller with closed-loop stability conditions and simple tuning guidelines. The results are illustrated through numerical simulations.

3.1 Introduction

The consideration of continuous stirred tank reactors (CSTRs) represents an important first step in the consideration of the tubular reactor problem, in the understanding that a tubular reactor with infinite diffusion (and thus instantaneous complete dispersion of information through the reactor) is perfectly well described by the model of a CSTR [9]. Therefore, the consideration of the lumped ODE model of the CSTR already allows to identify the main issues connected with chemical reactors in terms of

- advection-type mass and energy transport
- diffusion-type energy transport through the reactor wall
- reactive mass and energy consumption or production,

and to identify a methodological framework which permits to exploit their continuous interplay to obtain explicit solvability conditions with physical meaning.

According to (3.1) the CSTR is described by the set of ODEs

$$\begin{aligned} \dot{c} &= \theta(c_e - c) - r(c, T, p_r), \quad c(0) = c_0 \\ \dot{T} &= \theta(T_e - T) - \eta(T - T_j) + \beta r(c, T, p_r), \quad T(0) = T_0. \end{aligned} \tag{3.1}$$

For the given purpose, an abstract energy interchange framework is employed to analyze the intrinsic process characteristic mechanisms, namely transport and reaction, and their influence on the estimation error dynamics. The particular issues addressed in this chapter are the following:

(i) analysis of the natural estimation error dissipation of the CSTR (to be defined) is analyzed in a Lyapunov-like energy dissipation framework, in order to characterize divergence and convergence sources and to compare the respective elements with convergence superhavit with those of convergence deficit,

(i) identification of the observability properties of the non-isothermal CSTR with temperature measurement and non-monotonic reaction,

(ii) design of a dissipative observer for the CSTR exploiting the process inherent transport and reaction mechanisms, in the sense of improving the energy interchange mechanisms, yielding (i) systematic design, (ii) simple convergence conditions with physical meaning and (iii) tuning guidelines,

(iii) combination of the dissipative observer with a passive nonlinear state-feedback control to stabilize the SS with maximum reaction rate of the reactor, which is possibly open-loop unstable, and not locally observable.

For the purpose of constructing the dissipative observer, establishing explicit convergence criteria, and applying it to a challenging OF control problem, the conceptual framework of dissipativity (in a physical and system-theoretic sense) is combined with modern control theory, and physical experience from chemical engineering sciences in a mathematically rigorous way.

3.2 Natural Error Dissipation

In this section, the underlying transport and reaction mechanisms and their interplay are characterized in a Lyapunov-like energy dissipation framework with emphasis on (i) physical meaning, (ii) identification of divergence versus convergence sources, as well as superhavit versus deficit, and (iii) compensation possibilities.

3.2.1 Deviation Dynamics

Consider a copy of the CSTR (3.1) with an initial deviation $e_0 = \hat{x}_0 - x_0$, $\hat{x}_0$ being the initial condition of the deviated dynamics, and driven by the same input signal $u(t) = [\theta(t),\, T_j(t)]^T$ as the actual reactor. The corresponding dynamics of the reactor copy read

$$\begin{aligned} \dot{\hat{c}} &= \theta(c_e - \hat{c}) - r[\hat{c}, \hat{T}, p_r], \hat{c}(0) = \hat{c}_0 \\ \dot{\hat{T}} &= \theta(T_e - \hat{T}) - \eta(\hat{T} - T_c) + \beta r[\hat{c}, \hat{T}, p_r], \hat{T}(0) = \hat{T}_0. \end{aligned} \tag{3.2}$$

In order to identify the main divergence versus convergence sources in the reactor dynamics, the deviation (error) dynamics are considered.

3.2.2 Error Dynamics

From the subtraction of (3.1) and (3.2) the deviation or error dynamics follow (with $\epsilon_c \triangleq \hat{c} - c$, $\epsilon_T \triangleq \hat{T} - T$)

$$\begin{aligned} \dot{\varepsilon}_c &= -\theta\varepsilon_c - \rho(c, T; \varepsilon_c, \varepsilon_T), & \varepsilon_c(0) &= \varepsilon_{c0} \\ \dot{\varepsilon_T} &= -(\theta + \eta)\,\varepsilon_T + \beta\rho(c, T; \varepsilon_c, \varepsilon_T), & \varepsilon_T(0) &= \varepsilon_{T0}, \end{aligned} \tag{3.3}$$

$$\rho\,(c, T; \varepsilon_c, \varepsilon_T) \triangleq r\,(c + \varepsilon_c, T + \varepsilon_T, p_r) - r\,(c, T, p_r)\,. \tag{3.4}$$

Note that there is a direct correspondence of the mass and heat transfer and dilution characterizing the original reactor (3.1), whereas the nonlinear kinetic influence in the dynamics are determined by the difference between the reaction rate's value of the reactor (3.1) and its copy (3.2). Furthermore, one appreciates that the only coupling between both state variables consists in the dependence on the nonlinear kinetic rate. The basic underlying interplay between heat and mass transport and the kinetic mechanism is shown in Figure 3.2. To obtain insight into the basic stabilizing

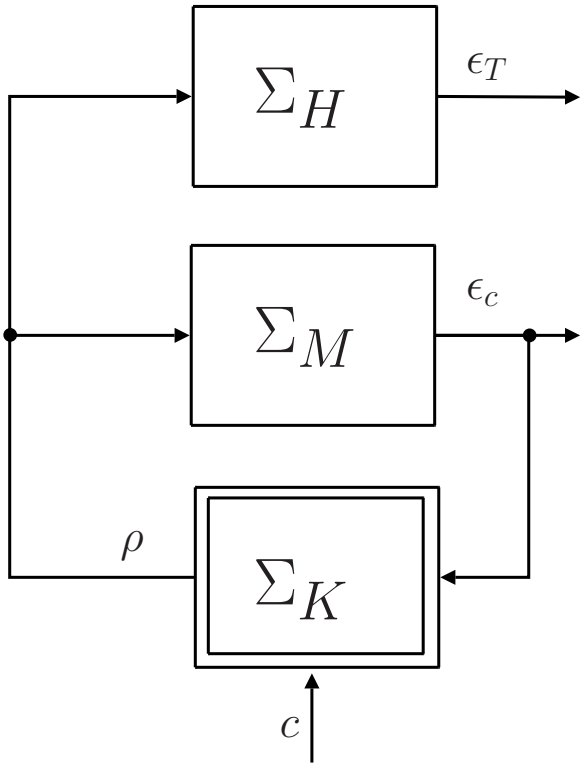

Figure 3.1: Basic interconnection structure of the error dynamics (3.3), with $\Sigma_H : \rho \mapsto \epsilon_T$, $\Sigma_M : \rho \mapsto \epsilon_c$, $\Sigma_K : (\epsilon_c, c) \mapsto \rho$.

and destabilizing mechanisms, the error dynamics (3.3) are analyzed in a Lyapunov energy dissipation framework.

3.2.3 A qualitative analysis of the error dissipation and convergence

In order to identify the main mechanisms in the reactor natural error dynamics (3.3), in the sense of divergence versus convergence sources, a Lyapunov-like energy approach is considered. For this purpose the simple quadratic error Lyapunov function candidate is used

$$E = \frac{1}{2}\left(\varepsilon_T^2 + \varepsilon_c^2\right), \tag{3.5}$$

The corresponding error dissipation is

$$\dot{E} = -[\theta + \eta]\epsilon_T^2 - \theta\varepsilon_c^2 + [\beta\epsilon_T - \varepsilon_c]\rho. \tag{3.6}$$

The first term in the error dissipation (3.6) represents the natural dissipation due to energy interchange of the tank without considering reaction, and the second term represents, accordingly, the dilution of a substance in the reactor. The influence of the chemical reaction kinetics on the error dissipation is reflected in the last terms.

The linear heat and mass dissipation mechanisms are obviously sources of convergence, while the influence of the kinetics on the dissipation has to be analyzed with more detail. In order to identify the basic influence of the kinetic rate on the error dissipation, consider a first order kinetics of the type

$$r(c, T) = kce^{-\gamma/T}. \tag{3.7}$$

Accordingly, the nonlinear function $\rho(c, T; \varepsilon_c, \varepsilon_T)$ obtains the following form[1]

$$\rho(c, T; \varepsilon_c, \varepsilon_T) = k\varepsilon_c e^{-\gamma/T} + k\hat{c}\frac{\gamma}{\tau^2}e^{-\gamma/\tau}\varepsilon_T, \quad \tau = T + \eta\varepsilon_T,\ 0 < \eta < 1.$$

[1] $\rho = k\left([c+\varepsilon_c]e^{-\gamma/(T+\varepsilon T)} - ce^{-\gamma/T}\right) = k\left([c+\varepsilon_c]\left\{e^{-\gamma/(T+\varepsilon T)} + e^{-\gamma/T} - e^{-\gamma/T}\right\} - ce^{-\gamma/T}\right) = k\varepsilon_c e^{-\gamma/T} + k\hat{c}\frac{\gamma}{\tau^2}e^{-\gamma/\tau}\varepsilon_T, \quad \tau = T + \eta\varepsilon_T,\ 0 < \eta < 1.$

and it follows that the above dissipation (3.6) obtains the form

$$\dot{E} = -\left[\theta + \eta - \beta\hat{c}\frac{\gamma}{\tau^2}\right]\epsilon_T^2 + \left[\beta k e^{-\gamma/T} - k\hat{c}\frac{\gamma}{\tau^2}e^{-\gamma/\tau}\right]\varepsilon_T\varepsilon_c - \left[\theta + k e^{-\gamma/T}\right]\varepsilon_c^2.$$

For strongly exothermic reactions, the adiabatic temperature rise β is respectively high, so that the corresponding coefficient for the temperature error dissipation can be positive, i.e. the kinetic influence can destabilize the error dynamics. The concentration error itself corresponds to a strict dissipation, because the reaction rate dependence on the concentration is monotonic. Note that, generally speaking, for every monotonic dependence of the reaction rate $r(\cdot)$ on the concentration, the appearing term $\rho\varepsilon_c$ is always positive and correspondingly these terms represent convergence sources, whereas, for a non-monotonic reaction rate dependence on concentration, this term is negative for some concentration pairs $(c, \hat{c})$ (because the slope becomes negative after passing the concentration which corresponds to maximum rate), and consequently the respective quadratic term represents an additional source of error divergence.

Furthermore, one can show that even for the simple first order kinetics (3.7), there are parameter constellations for which three equilibrium states of the reactor exist, one unstable and two stable steady states (corresponding to ignition and extinction regimes) [10, 74]. The corresponding area of attraction of each of these stable equilibria are separated by a separatrix. The corresponding phase portrait is illustrated in Figure 3.7. For the generation of this phase portrait the following parameters were used: $\theta = 1, c_{in} = 1, \eta = 1, T_j = 350K, T_e = 350K$. One appreciates the convergence to the ignition and extinction respective regimes, and concludes that, near the separatrix, for every (arbitrary close) initial condition pair $(x_0, \hat{x}_0)$, where x_0 and $\hat{x}_0$ correspond to different sides of the separatrix, the corresponding trajectories will always converge to distinct equilibria. This shows that the error between trajectories corresponding to initial conditions in areas of attraction corresponding to different equilibrium profiles will never converge. This phenomenon is actually a consequence of the kinetic influence on the energy interchange mechanisms in the reactor, in the sense of high sensitivity with respect to small changes in initial thermal energy content in the reactor. These qualitative considerations are actually valid for large classes of different kinetic types (see e.g. [10]), and in particular for non-monotonic kinetics.

The conclusions obtained from this introductory qualitative analysis are twofold:

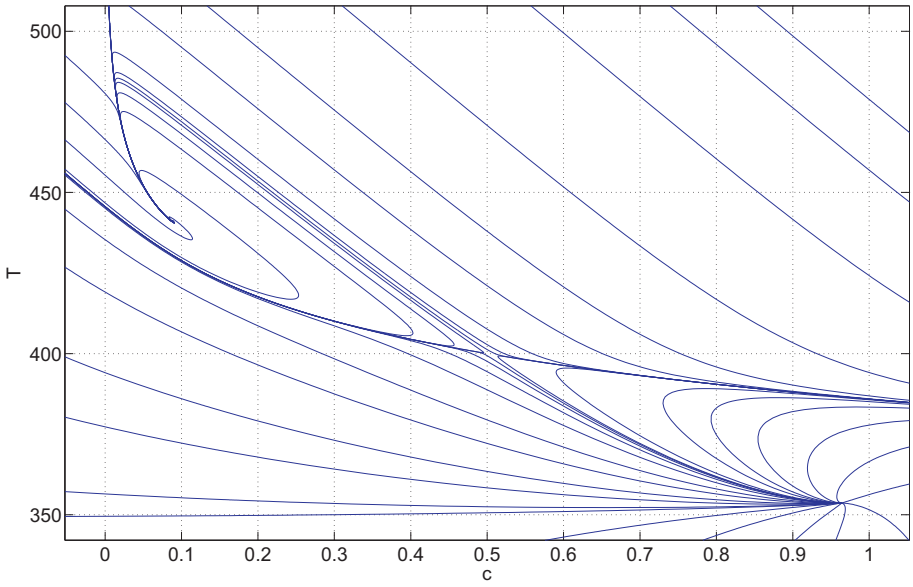

Figure 3.2: Phase portrait corresponding to the reactor dynamics with first order monotonic kinetics (3.7).

- on the one hand, they reveal which are the basic stabilizing and destabilizing mechanisms of the error dynamics, and consequently which mechanisms improve the convergence of the natural estimation and which obstruct them, so that it becomes clear that *there is a need of introducing additional coupling elements in the estimator* (3.2) in order to permit a compensation of convergence deficit by the mechanisms which correspond to convergence superhavit,

- on the other hand, they show that the consideration of non-monotonic reaction rate dependencies on concentration implies that the compensation of the destabilizing behavior of the kinetic mechanism is a quite more challenging task as in the case of a monotonic reaction rate dependency.

Motivated by the last issue, the subsequent analysis focuses on the consideration of reaction rates with non-monotonic concentration dependence. First, a system inherent possibility to estimate the concentration based on the measurement of the temperature, namely the detectabilty of the nonlinear reactor is addressed [75, 76, 77].

3.2.4 Observability and Detectability

Note that in the most widely studied case of a reactor (3.1) with a *monotonic (increasing) reaction rate* dependency on concentration, the reactor is locally and globally observable, in the sense that all initial states are distinguishable for every input function [21], meaning that different initial states produce different measurements for the same input signal. Moreover, the first approximation (Taylor linearization) of the system around any state $\bar{x} \in X$ is observable, and consequently, completely uniformly observable, implying that a high-gain [78] or geometric [79] convergent observer can be designed.

Considering a non-monotonic reaction, the reaction rate function grows with the temperature T, and grows with concentration c up to a concentration value c^* where the reaction rate reaches its maximum value, and decreases with concentration for values larger than c^*. Technically speaking, the rate function $r(c, T, p_r)$ depends isotonically on the temperature T, and non-monotonically on the concentration c, according to the expressions

$$\begin{aligned}
&\frac{\partial r}{\partial T}(c, T, p_r) > 0 \quad \forall\ T \in [T^-, T^+], \\
&\frac{\partial r}{\partial c}(c, T, p_r) > 0\, c \in [0, c^*), \\
&c^* = \mu(T, p_r),\ \frac{\partial r}{\partial c}(c^*(T), T, p_r) = 0, \\
&\frac{\partial r}{\partial c}(c, T, p_r) < 0, \quad c \in (c^*, 1]
\end{aligned}$$

where T^- (or T^+) is the minimum (or maximum) possible temperature determined by mass-heat conservation and thermodynamic's second law arguments [70], and μ is the algebraic function which sets the concentration c^* associated with the maximum rate r^* depending on the prescribed temperature T. For each T, the graph $(c, r(c, T))$ over $[0, \mu(T)]$ (or $[\mu(T), 1]$) is the isotonic (or antitonic) branch of the reaction rate function over $[0, 1]$ (see Figure 3.3).

However, as mentioned above, in the reactor case with *non-monotonic reaction rate*, the situation is quite different. On the one hand, the reactor (3.1) is *not locally observable* about any steady-state $\bar{x}$ with maximum reaction rate $\bar{r}^*$, as the reactor's first approximation does not meet Kalman's observability condition [77, 80] because $\dfrac{\partial r}{\partial c}(\bar{c}^*, \bar{T}^*, p_r) = 0$. On the other hand, the reactor has bad inputs [76]. This phenomenon resides in the physical fact that the same reaction rate value is produced

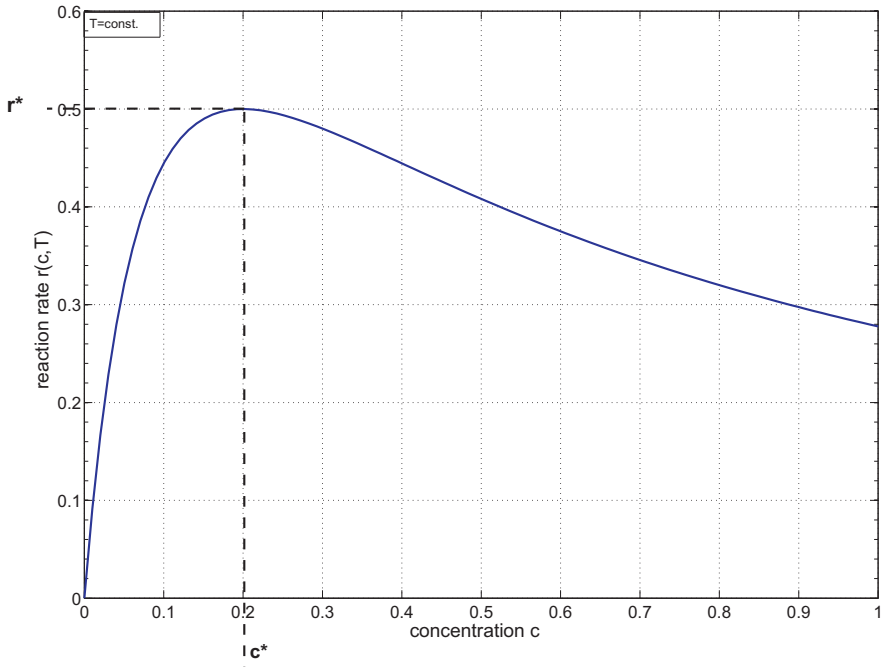

Figure 3.3: Non-monotonic kinetics.

by the same temperature and two different concentrations, one in the isotonic branch of r and one in the antitonic one (see Figure 3.3):

$$r[c_1(t), T(t), p_r] = r[c_2(t), T(t), p_r],\ c_1 \in [0, c^*],\ c_2 \in [c^*, 1],\ c^* = \mu(T).$$

The existence of bad inputs implies that the reactor (3.1) is not globally observable, and consequently that it is not possible to construct a globally convergent observer with assignable convergence velocity for every input. As mentioned before, the lack of (global) observability rules out the possibility of most nonlinear observer design methods, among them being the high-gain [78], Lipschitz, error linearization observers, as well as geometric estimators [79]. On the other side, recall the concentration error dynamics (3.3) with the bad input $(\theta, T_j, c_e)(t)$ and two different (indistinguishable) concentration initial conditions (c_{10} and c_{20}) and corresponding error $\epsilon_c = \hat{c} - c$

$$\begin{aligned} \dot{\epsilon_c}(t) &= -\theta\epsilon_c - \rho(c, T; \epsilon_c, 0), \\ &= -\theta\epsilon_c \\ \rho(c, T; \epsilon_c, 0) &= r(c + \epsilon_c, T, p_r) - r(c, T, p_r) = 0, \end{aligned} \tag{3.8}$$

which we refer to as *indistinguishable dynamics* [81, 79, 75, 21]. Given that, by process design specifications and restrictions, the reactant feed flowrate q (3.1) is greater or equal than a lower saturation limit q^-, the (possibly time-varying) dilution rate θ input has the same feature:

$$\theta(t) \geq \theta^- = q^-/V > 0. \tag{3.9}$$

From this *process design consideration*, in conjunction with the particular form (3.8) of the reactor indistinguishable dynamics, it follows that the reactor model (3.1) is *globally detectable* for any input, and for any possible indistinguishable motion pair (generated by any bad input). This, in turn, implies two important conclusions on inherent estimation capabilities and limitations, regardless of the particular data assimilation scheme employed:

1. In the presence of bad inputs over a certain time interval, the convergence rate attainable with any observer is fixed by the process itself and cannot be modified by the designer. This means that the maximal ensured global convergence speed corresponds to the inverse residence time $\theta(t)$.

2. In the absence of bad inputs over a certain time interval, the convergence rate can be made faster than the natural dilution rate input $\theta\,(t)$, depending on the employment of an adequately designed estimator.

From a phenomenological point-of-view it can be stated that *the detectability corresponds to the strict consumption of the energy corresponding to indistinguishable trajectories. The condition on the flow-rate $q \geq q^-$ corresponds to the persistence of physical dissipation due to a convection-kind mechanism. This shows that the persistence of flow (dilution) condition $q \geq q^-$ actually ensures the energy dissipation along all indistinguishable trajectories, in the understanding that the nonzero flow condition $\theta > 0$ is met by the continuous stirred tank reactor class.*

This detectability characterization (i) sets inherent capabilities and limitations of any observer design, (ii) draws a conceptual connecting point between process and control design via the detectability property, and (iii) establishes the conceptual point of departure for the design of the dissipative observer.

3.2.5 Discussion

In the context of the previously discussed subject of steady-state multiplicity, the detectability property has to be understood on the basis that indistinguishable trajectories correspond to the same temperature. As the different equilibria of the reactor (3.1) correspond to different temperature regimes, the multiplicity issue does not affect the detectability properties of the reactor, because trajectories converging to different SS are not indistinguishable.

The presented considerations show that there is a basic interplay between the process inherent physical mechanisms, characterizing the dissipation properties of the error dynamics, as there are (i) linear transport of heat and mass (systems Σ_H and Σ_M, respectively), and (ii) nonlinear kinetics (system Σ_K). Furthermore, as there is no inherent interchange mechanism between the convergence superhavit of the linear temperature transport mechanism and deficit of the linear mass transport, and nonlinear kinetic mechanisms, the over-all dissipation is almost characterized by the properties of the kinetic mechanism because of nonlinear coupling effects. It results that there is a need of (i) improving the dissipation of the linear transport subsystem, and (ii) compensating the convergence deficit of the kinetic mechanism, in the sense of enabling an over-all strict dissipation via a compensation of convergence deficit by the heat mechanism with convergence superhavit.

3.3 Dissipative Observer

The preceding reactor detectability assessment in the light of the present estimation problem naturally fits with the conditions required for the consideration of a dissipative observer [61, 62], because of two reasons: (i) the functioning of a dissipative observer does not depend on the fulfillment of a complete observability property , and (ii) the structure-oriented approach of the dissipative observer sets a tractable manner to address the difficult exploitation of the process inherent linear transport and nonlinear reaction mechanisms.

3.3.1 Observer Construction

To begin, assume for the moment that the model parameters and the exogenous inputs are exactly known and that the measurements at the inlet and outlet are errorless (in the understanding that this assumption will be relaxed later), and consider

the observer with the standard linear-additive measurement injections ($y = T$) in the concentration-temperature dynamics and one peculiar injection in the concentration argument of the reaction rate (as proposed in [62, 82]):

$$\begin{aligned}\dot{\hat{c}} &= \theta(c_e - \hat{c}) - r[\hat{c} - \kappa_r(\hat{T} - y), y, p_r] - \kappa_c(\hat{T} - y), \hat{c}(0) = \hat{c}_0 \\ \dot{\hat{T}} &= \theta(T_e - \hat{T}) - \eta(\hat{T} - T_c) + \beta r[\hat{c} - \kappa_r(\hat{T} - y), y, p_r] - \kappa_T(\hat{T} - y), \hat{T}(0) = \hat{T}_0,\end{aligned} \tag{3.10}$$

where κ_c (or κ_T) is the standard linear concentration (or temperature) gain, and κ_r is a constant gain for correction of the kinetics' argument.

Observe that: when $\kappa_r = 0$, a form of Luenbegrer observer with linear and constant gain pair (κ_T, κ_c) is obtained. Comparing with EKF [28], Luenbegrer [42], High-Gain [78] and Geometric [79] observers employed in previous chemical reactor studies, the proposed observer is simpler in the sense of constant (model independent) gains. As we shall see later, this simplicity and robustness oriented features will be exploited by combining transport and reaction dissipation mechanism features.

3.3.2 Estimation Error Dynamics

From the subtraction of (3.1) and (3.10) the stirred tank estimation error dynamics follow (with $\varepsilon_c \triangleq \hat{c} - c, \varepsilon_T \triangleq \hat{T} - T$)

$$\begin{aligned}\dot{\varepsilon}_c &= -\theta\varepsilon_c - \kappa_c\varepsilon_T - \rho(c, y; \varepsilon_c - \kappa_r\varepsilon_T), \\ \dot{\varepsilon_T} &= -(\theta + \eta + \kappa_T)\,\varepsilon_T + \beta\rho\,(c, y; \varepsilon_c - \kappa_r\varepsilon_T) \\ \rho\,(c, y; \varepsilon_c - \kappa_r\varepsilon_T) &\triangleq r\,(c + \varepsilon_c - \kappa_r\varepsilon_T, y, p_r) - r\,(c, y, p_r)\end{aligned} \tag{3.11}$$

These dynamics can be written as a two-subsystem interconnection in Lur'e-Popov form [73, 56] [2]

$$\begin{bmatrix} \dot{\varepsilon}_c(t) \\ \dot{\varepsilon}_T(t) \end{bmatrix} = \begin{bmatrix} -\theta(t) & -\kappa_c \\ 0 & -(\theta(t) + \eta + \kappa_T) \end{bmatrix} \begin{bmatrix} \varepsilon_c(t) \\ \varepsilon_T(t) \end{bmatrix} + \begin{bmatrix} 1 \\ -\beta \end{bmatrix} \nu \tag{3.12}$$

$$\zeta \triangleq \epsilon_c - \kappa_r\epsilon_T, \tag{3.13}$$

$$\nu = -\,\rho\,(c, y; \zeta)\,, \tag{3.14}$$

[2] For a possible physical interpretation of the output of the advective subsystem see [83] where it was argued that it can be viewed as an energy form: based on the definition of the adiabatic temperature rise β, the variable ζ is simply the enthalpy of the reacting mixture in dimensionless units and referred to the zero estimation error state $(\tilde{c}, \tilde{T})$.

where: (i) the advective subsystem (3.12)-(3.13) is linear and dynamic (with input ν and output ζ), and (ii) the kinetic subsystem (3.14), with the induced reaction rate error, is nonlinear and static.

3.3.3 Estimation Error Dissipation

In the light of the previous interpretation of the estimation error dynamics in terms of a two subsystem interconnection of (i) a linear dynamical transport subsystem, and (ii) a nonlinear static kinetic subsystem, the convergence assessment can be addressed within an energy-interchange framework, in the understanding that zero energy content corresponds to a zero estimation error. For this aim, a possible choice of a candidate Lyapunov energy function for the (closed) two-subsystem interconnection is given by the quadratic (potential squared error) energy function

$$E\left(\epsilon_T, \zeta\right) = \frac{1}{2}\left(\epsilon_T^2 + \zeta^2\right), \tag{3.15}$$

in terms of the temperature estimation error ϵ_T and the new variable ζ (which constitutes the output of the linear subsystem). In order to express the corresponding dissipation in terms of ϵ_T and ζ note that the dynamics of ζ is given by

$$\dot{\zeta} = \dot{\epsilon}_c - \kappa_r \dot{\epsilon}_T = -\theta\zeta - [\kappa_c - \kappa_r(\eta + \kappa_T)]\epsilon_T - [1 + \kappa_r\beta]\rho, \tag{3.16}$$

Accordingly, the estimation error dissipation is

$$\begin{aligned} \dot{E} &= \epsilon_T \dot{\epsilon}_T + \zeta\dot{\zeta} \\ &= \underbrace{-[\theta + \eta + \kappa_T]\epsilon_T^2 - [\kappa_c - \kappa_r(\eta + \kappa_T)]\epsilon_T\zeta - \theta\zeta^2}_{\triangleq \mathcal{D}_T} + \underbrace{[\beta\epsilon_T - (1 + \kappa_r\beta)\zeta]\rho}_{\triangleq \mathcal{D}_K} \end{aligned} \tag{3.17}$$

One clearly identifies two main elements of the dissipation corresponding to the dissipation of the linear dynamical transport subsystem $\mathcal{D}_T$ and to the nonlinear static kinetic's subsystem $\mathcal{D}_K$. The analysis of these two elements is addressed next. First of all, the influence of the nonlinear kinetic mechanism on the dissipation is analyzed, in the understanding that the bounds for the dissipation of the kinetic mechanism set the requirements for the dissipation of the linear transport mechanism.

Quadratic bounds for the nonlinear kinetics dissipation component $\mathcal{D}_K$

As the reaction rate r is continuously differentiable, the mean value theorem ensures the existence of a continuous secant function σ such that

$$\rho\left(c,y;\zeta\right)=\sigma\left(c,y;\zeta\right)\zeta=\sigma\left(c,y;\epsilon\right)\left[\epsilon_c-\kappa_r\epsilon_T\right], \tag{3.18}$$

which has conic bounds

$$\begin{aligned}
&s_l\leq\sigma\left(c,y;\zeta\right)\leq s_u\\
&s_l=\min_{X_p} r_c(c,y,p_e)<0\ ,\ \ s_u=\max_{X_p} r_c(c,y,p_r)>0\\
&X_p\subset X,\ \ \mathrm{rad}(X_p)=\epsilon_X,
\end{aligned} \tag{3.19}$$

where X_p is a concentration-temperature set of radius ϵ_X. Accordingly, the dissipation of the static-nonlinear subsystem (3.14) is fixed by the reaction rate's slope $\sigma=r_c$, and can be characterized by its restriction to the conic sector in the variable ζ [73, 6],

$$\mathcal{S}_\zeta\triangleq\left(s_u\zeta-\rho(c,T;\zeta)\right)\left(\rho(c,T;\zeta)-s_l\zeta\right)=\begin{bmatrix}\zeta\\ \rho\end{bmatrix}^T\begin{bmatrix}-s_us_l & \frac{s_u+s_l}{2}\\ \frac{s_u+s_l}{2} & -1\end{bmatrix}\begin{bmatrix}\zeta\\ \rho\end{bmatrix}\geq 0. \tag{3.20}$$

A geometrical interpretation of this condition is illustrated in Figure 3.4. Correspondingly, the nonlinear kinetic subsystem's dissipation component $\mathcal{D}_K$ can be bounded by a quadratic form

$$\begin{aligned}
\mathcal{D}_K&=[\beta\epsilon_T-(1+\kappa_r\beta)\zeta]\rho+\mathcal{S}_\zeta-\mathcal{S}_\zeta\\
&\leq\begin{bmatrix}\epsilon_T\\ \zeta\\ \rho\end{bmatrix}^T\begin{bmatrix}0 & 0 & \frac{\beta}{2}\\ 0 & -s_us_l & \frac{s_u+s_l-(1+\kappa_r\beta)}{2}\\ \frac{\beta}{2} & \frac{s_u+s_l-(1+\kappa_r\beta)}{2} & -1\end{bmatrix}\begin{bmatrix}\epsilon_T\\ \zeta\\ \rho\end{bmatrix},
\end{aligned} \tag{3.21}$$

and the observer design consists in finding output injection gains $\kappa_c,\kappa_T,\kappa_r$ for the linear subsystem (3.12,3.13) such that the two-system interconnection becomes internally exponentially stable, in the understanding that the sum of the dissipation of the linear transport and the nonlinear kinetic subsystem becomes strictly negative.

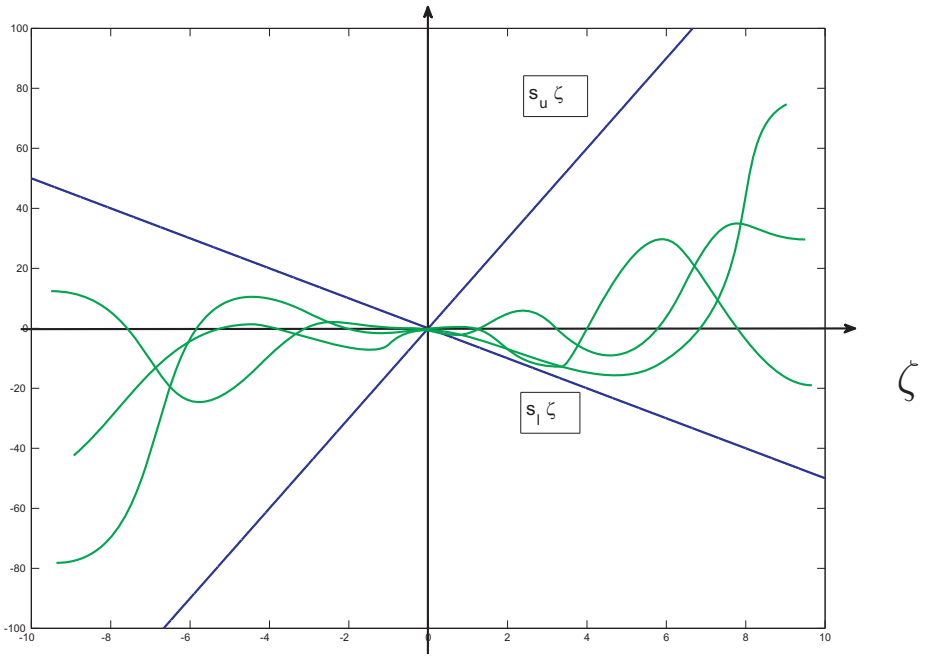

Figure 3.4: Geometric interpretation of the sector condition (3.20).

Quadratic bounds for the linear transport subsystem dissipation component $\mathcal{D}_T$

Note that corresponding to (3.17) the dissipation $\mathcal{D}_T$ of the linear transport subsystem can be expressed in the quadratic form

$$\mathcal{D}_T = -\begin{bmatrix} \epsilon_T \\ \zeta \end{bmatrix}^T \begin{bmatrix} [\theta + \eta + \kappa_T] & \frac{\kappa_c - \kappa_r(\eta+\kappa_T)}{2} \\ \frac{\kappa_c - \kappa_r(\eta+\kappa_T)}{2} & \theta \end{bmatrix} \begin{bmatrix} \epsilon_T \\ \zeta \end{bmatrix}. \tag{3.22}$$

This shows that the heat and mass transport dissipation mechanisms are improved in the understanding that (i) without correction terms ($\kappa_r = \kappa_c = \kappa_T = 0$) the corresponding components strictly dissipate energy (compare the preceding analysis of the natural dissipation by transport), and (ii) the heat transfer corresponding dissipation is improved by the gain κ_T, and an artificial coupling of the mass transfer with the heat transfer component is introduced.

Quadratic bounds for the estimation error dissipation

According to the preceding analysis, the overall dissipation can be bounded as follows:

$$\begin{aligned}\dot{E} &= \mathcal{D}_T + \mathcal{D}_K \\ &\leq -\begin{bmatrix} \epsilon_T \\ \zeta \\ \rho \end{bmatrix}^T \begin{bmatrix} \theta+\eta+\kappa_T & \frac{\kappa_c-\kappa_r(\eta+\kappa_T)}{2} & -\frac{\beta}{2} \\ \frac{\kappa_c-\kappa_r(\eta+\kappa_T)}{2} & \theta+s_u s_l & -\frac{s_u+s_l-1-\kappa_r\beta}{2} \\ -\frac{\beta}{2} & -\frac{s_u+s_l-1-\kappa_r\beta}{2} & 1 \end{bmatrix} \begin{bmatrix} \epsilon_T \\ \zeta \\ \rho \end{bmatrix}.\end{aligned} \tag{3.23}$$

This bound for the dissipation of the (potential squared error) energy (3.15) in quadratic form allows to analyze the complex inherent energy-interchange mechanisms in a simple and compact form. Based on this result, explicit convergence conditions can be drawn in terms of (i) system parameters and (ii) the observer correction gain triplet $(\kappa_c, \kappa_T, \kappa_r)$.

Convergence criteria

If one can show that the strict dissipativity condition $\dot{E} \leq -2\lambda E$ holds for some $\lambda > 0$, it follows by Lyapunov's direct method that the vector $[\epsilon_T, \zeta]^T$ converges exponentially to $\epsilon = [0,0]^T$ with rate λ, and amplitude $a = 1$ (see [73, 65] and compare Lemma 2.1). Thus it is sufficient to show that the quadratic form (3.23) is negative definite. This leads to the following result.

Proposition 3.1. *The observer (3.10), implemented in the presence of bounded model parameter, exogenous inputs, and measurement errors, with estimate $\varepsilon(t)$, converges exponentially to the motion $x(t)$ of the actual reactor (3.1) driven by a limited from below dilution rate input $\theta(t) \geq \theta^- > 0$ (3.26), with transient exponential response and bounded asymptotic error offset, depending on the disturbance sizes, if the estimator gain triplet $(\kappa_T, \kappa_c, \kappa_r)$ is chosen so that the following LMI is met (s_l, s_u being the minimum and maximum reaction rate's slope, corresponding to (3.19))*

$$\begin{bmatrix} \theta+\eta+\kappa_T & \frac{\kappa_c-\kappa_r(\eta+\kappa_T)}{2} & -\frac{\beta}{2} \\ \frac{\kappa_c-\kappa_r(\eta+\kappa_T)}{2} & \theta+s_u s_l & -\frac{s_u+s_l-1-\kappa_r\beta}{2} \\ -\frac{\beta}{2} & -\frac{s_u+s_l-1-\kappa_r\beta}{2} & 1 \end{bmatrix} > 0. \tag{3.24}$$

This LMI has a solution if and only if $\theta^- + s_u s_l > 0$.

(Proof in Appendix A.)

3.4 Discussion of the results

A short discussion of the particular features of the preceding observer design method is in order. As qualitative basis the basic structure of the dynamic interconnections characterizing the estimation error (3.12)-(3.14) is depicted in Figure 3.5 in block diagram form. The basic interplay of linear transport and nonlinear reac-

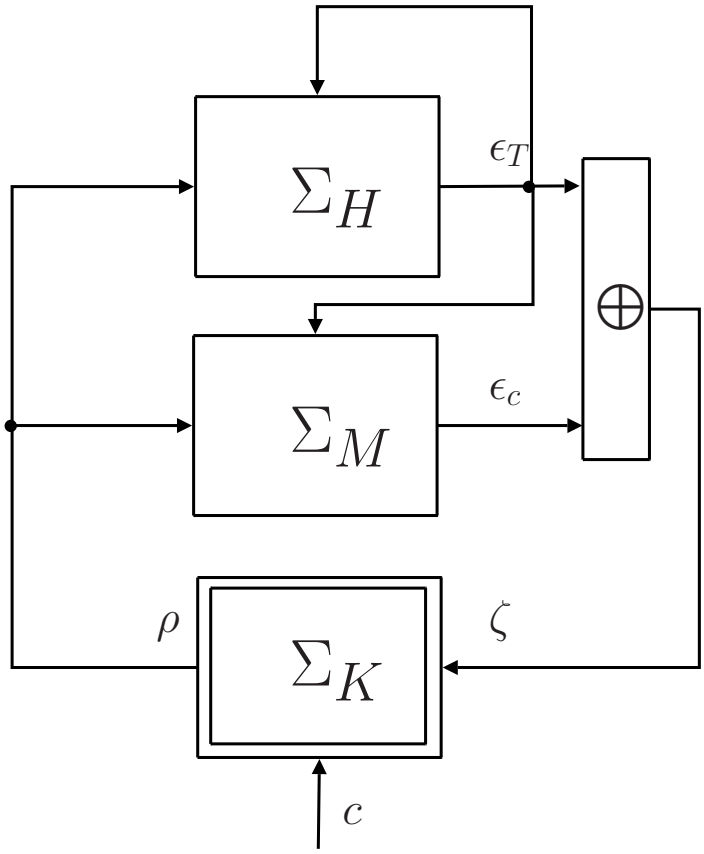

Figure 3.5: Basic interconnection structure of the error dynamics (3.12)-(3.14) corresponding to the stirred reactor dissipative observer (3.10), with
$\Sigma_H : \rho \mapsto \epsilon_T$, $\Sigma_M : (\rho, \epsilon_T) \mapsto \epsilon_c$, $\Sigma_K : (\epsilon_c, \epsilon_T, c) \mapsto \rho$.

tion, characterizing the reactor, observer, and estimation error dynamics, is exploited within an abstract energy interchange framework, in the sense that:

- the dissipation properties of the nonlinear kinetic subsystem have been bounded using a sector condition, representing a worst case scenario, in the understanding of maximal influence of the nonlinear kinetic subsystem on the energy

dissipation of the estimation error dynamics (3.12)-(3.14). It resulted that for non-monotonic kinetic rates, the kinetic dissipation component $\mathcal{D}_K$ has a destabilization potential, which has to be compensated.

- the basic energy dissipation mechanisms are identified, in the understanding that the transport mechanisms naturally dissipate the squared estimation error potential energy

- additional interconnection degrees of freedom have been introduced by the correction mechanism which allow to (i) improve the natural dissipation mechanisms by coupling them with the dissipation mechanism corresponding to physical heat transfer phenomena in the reactor itself, and (ii) compensate the convergence deficit of the nonlinear kinetic component.

In particular, note that the gain triplet $(\kappa_T, \kappa_c, \kappa_r)$ modifies the dissipation properties of the Lur'e-Popov's linear-dynamic subsystem (3.12)-(3.13), and of its interconnection with the nonlinear static subsystem (3.14), in the sense that: (i) (κ_c, κ_T) shapes the dissipation of the linear dynamical subsystem, while (ii) κ_r determines the interconnection form by correcting the output of the linear system. *The design procedure can thus be viewed as an optimization in the sense of best input-output structure and property assignment for the two-subsystem interconnection (3.12)-(3.14).*

Furthermore, it is noteworthy that for $\kappa_r = -1/\beta$ the dynamics of the variable ζ becomes a reaction invariant, i.e. a variable independent of the kinetic error function ρ. This choice of gain corresponds to the open-loop observer [47, 8] which converges robustly with rate fixed by the reactor residence time.

Additionally, there is a clear detectability-type (3.9) condition for the stability of the ζ-dynamics, namely

$$\theta + s_u s_l > 0, \quad s_l = \min r_c, s_u = \max r_c, \tag{3.25}$$

which reveals that a monotonic kinetics ($s_u s_l > 0$) improves the observer convergence, while for non-monotonic kinetics ($s_u s_l < 0$) the residence time has to be chosen in correspondence to (3.25). Comparing this detectability condition with (3.9), one notes that the present condition (3.25) specifies the lower bound q^- of the volumetric flowrate q in dependence of the kinetic properties of the chemical reaction rate.

Furthermore, note that the consideration of the sector condition in the convergence assessment allows to employ structural information about the nonlinearity in

the linearity-oriented approach using quadratic forms. It allows to obtain a simple LMI which is constant in the system nonlinearity gains s_l and s_u.

Finally, in the presence of bounded parameter, measurement and exogenous load errors and disturbances, respectively, the fulfillment of the LMI (3.24) in Proposition 3.1 ensures the estimation error convergence to a ball around the origin in the (ϵ_T, ζ)-plane with radius fixed by the error and disturbance sizes [83]. The corresponding LMI can be solved analytically or numerically and the corresponding solutions for the gains should be tested and adapted through numerical simulations, considering practically realistic disturbance sizes.

3.5 Application to Output-Feedback Control

In the sequel the problem of controlling a continuous exothermic (possibly open-loop unstable) reactor with non-monotonic kinetics, temperature measurements, joint manipulation of reactant and heat exchange rates, and operation at maximum production rate is considered. The respective work has been published in a series of conference articles [84, 85] and in the *Journal of Process Control* [83] proposing a solution within the robustness-oriented practical stability framework, drawing the identification of the underlying detectability and relative degree properties, and an interlaced passive controller-dissipative OF control design with emphasis on the derivation of: (i) solvability conditions with physical meaning, and (ii) a closed-loop stability criterion coupled with simple tuning guidelines.

3.5.1 Control Problem

In compact vector notation the *reactor model* (3.26) is written as follows

$$\dot{x} = f\left[x, d(t), u, p\right], \quad x(0) = x_0, \quad y = Cx, \quad z = x \tag{3.26}$$

where

$$x = [c, T]^T \in X = [0,1] \times (T^-, T^+) \subset \mathbb{R}^2, \quad p = (p_a^T, p_r^T)^T \quad f[\bar{x}, \bar{d}, \bar{u}, p] = 0$$
$$d = [c_e, T_e]', \quad T_e = y_e - \tilde{y}_e, \quad u = [\theta, T_c]^T, \quad C = [0,1], \quad p_a = (c_e, \beta, \eta)^T$$

x is the state, u (or d) is the control (or exogenous, possibly time-varying) input, p is the parameter vector of the nonlinear function f, and y (or z) is the measured (or

regulated) output. X is a concentration-temperature set with respect to which the reactor system (3.26) is positively invariant, meaning that all state motions starting in X stay in X [70].

The considered *control problem* consists in designing an observer-based dynamical *output-feedback (OF) controller*, on the basis of the reactor model (3.1) (with parameter approximation p). This problem formulation captures well the relevant features of industrial exothermic reactors with non-monotonic kinetics [19, 28, 7], in the sense that the attention is focused on the non-monotonicity, detectability, and open-loop instability features. The design of the complementary measurement-driven volume and cooling system control components can be performed in a straightforward manner [86, 87, 88].

From a robust control design perspective [89, 4] it is known that if a nonlinear (OF) controller does exist, it should be possible to implement it as the combination of a passive nonlinear state-feedback (SF) controller with a compatible nonlinear estimator, in the understanding that the interlaced estimator-control design is by no means trivial. Given that the reactant concentration and the reacting mixture temperature of an exothermic jacketed continuous reactor can be robustly controlled, regardless of the reaction kinetics, by manipulating the reactant dosage and the heat exchange rate according to a straightforward material-balance SF control scheme [87], the difficulty of the OF control problem with only temperature measurements resides in the two-valued nature of the non-monotonic kinetics rate function, which manifests itself as: (i) the lack of global complete observability, because the same reaction rate (quickly inferrable via temperature measurements and calorimetric estimation [86, 87, 22] corresponds to two different concentrations (see Figure 3.3), and (ii) the absence of local complete observability about the maximum reaction steady-state regime, because the reaction rate becomes insensitive to concentration changes. These considerations in conjunction with the peculiar observability/detectability feature of reactors with non-monotonic kinetics (see e.g. [19, 21]), motivate the present work with focus on the interplay between observer and control design, and emphasis on the identification of solvability conditions with physical meaning, and the characterization of a suitable tradeoff between reconstruction speed and robust (i.e. practical) convergence.

3.5.2 State-feedback (SF) control

In this section, a constructive control approach ([89, 3]) is applied to design a passive nonlinear SF controller, with emphasis on robustness and the identification of solvability conditions with physical meaning.

Accordingly, let $rd(u,z)$ denote the relative degree vector of the reactor with respect to the input-output pair (u,z), with $u^T=[\theta,T_j]$ and $z^T=[c,T]$, and draw the following conditions

$$\mathrm{rd}(u,z)=(1,1),\ z=x=[c,T]^T, u=[\theta,T_j]^T \ \Leftrightarrow c_e\neq c\ ,\ \eta\neq 0 \tag{3.27}$$

for the feedback equivalence of the reactor with respect to this input-output pair to a passive system [90].[3]

The nominal steady-state (of maximum production rate) of (3.26) is characterized by the nominal control input values, (i) the nominal residence time $\bar{\theta}$ and (ii) the nominal coolant jacket temperature $\bar{T}_j$, according to

$$\begin{aligned}&\bar{\theta}(\bar{c}_e-c^*)-r(c^*,T^*,p_r)=0,\\&\bar{\theta}(\bar{T}_e-T^*)-\eta(T^*-\bar{T}_j)+\beta r(c^*,T^*,p_r)=0.\end{aligned} \tag{3.28}$$

Based on these considerations, the corresponding linear-decentralized closed-loop output error dynamics (k_c and k_T are the adjustable control gains)

$$\dot{e}_c=-k_c e_c,\quad e_c=c-\bar{c};\quad \dot{e}_T=-k_T e_T,\quad e_T=T-\bar{T} \tag{3.29}$$

is enforced upon the reactor dynamics (3.1), to obtain the *nonlinear SF passive controller*

$$\begin{aligned}&\theta=[r(c,T)-k_c(c-\bar{c})]/(c_e-c),\\&T_j=T-[\beta r(c,T)+\theta(T_e-T)+k_T(T-\bar{T})]/\eta,\end{aligned}$$

or, in compact form,

$$u=\mu(x,d,p). \tag{3.30}$$

Consider the preceding state feedback controller with state (ϵ), parameter ($\tilde{p}_r$) and

[3]The zero dynamics of the system with control output z is trivial and thus naturally asymptotically stable, meaning that the reactor is minimum phase with respect to this input-output pair.

measurement ($\tilde{y}$) errors and load disturbances ($\tilde{d}$),

$$u = \mu(x + \tilde{x}, d + \tilde{d}, p + \tilde{p}), \tag{3.31}$$

apply it to the actual reactor system (2.14), and obtain the closed-loop dynamics (with $e = [e_c, e_T]^T = x - \bar{x}$, $\epsilon = [\epsilon_c, \epsilon_T]^T = \hat{x} - x$)

$$\dot{e} = -Ke + \tilde{f}\left[e; \epsilon, \tilde{d}(t), \tilde{p}\right], \quad e(0) = e_0, \quad K = \mathrm{diag}(k_c, k_T) \tag{3.32}$$

where

$$\tilde{f}\left(e; \epsilon, \tilde{d}, \tilde{p}\right) = f\left[\bar{x} + e, \bar{d} + \tilde{d}, \mu\left(x + \epsilon, \bar{d} + \tilde{d}, p + \tilde{p}\right), p + \tilde{p}\right] - f\left[\bar{x} + e, \bar{d}, \mu\left(x, \bar{d}, p\right), p\right],$$

e is the state regulation error, and $\tilde{f}(e; \epsilon, \tilde{d}, \tilde{p})$ means that $\tilde{f}$ vanishes with the arguments after its semicolon, i.e. $\tilde{f}\left(e; 0, 0, 0\right) = 0$. Given that the system has nominally trivially stable zero-dynamics $e = 0$, the (errorless) closed-loop is (nominally) stable. Thus, from the Lipschitz continuity of (f, μ) the practical-stability of the closed-loop system follows [71, 72, 3, 73], with a suitable tradeoff between the initial state (δ_0), parameter (δ_p), input (δ_d and $\delta_{\tilde{x}}$) and state excursion (ε_x) sizes, depending on the choice of the control gain pair (k_c, k_T) (compare Lemma 2.1). The P-stable reactor dynamics (3.32) represents: (i) *the behavior attainable with any robust controller*, and (ii) *the recovery target for the OF control design of the next section.*

For OF control design purposes, let us introduce the Lyapunov characterization of the closed-loop P-stability property (2.17) with the nonlinear passive SF control (3.31):

$$\begin{aligned} V &= \tfrac{1}{2}(e_c^2 + e_T^2), \\ \dot{V} &= -(k_c e_c^2 + k_T e_T^2) + e^T \tilde{f}\left[e; \epsilon, \tilde{d}, \tilde{p}\right] \\ &\leq -2\min\{k_c, k_T\} V + e^T \tilde{f}\left[e; \epsilon, \tilde{d}, \tilde{p}\right]. \end{aligned} \tag{3.33}$$

This characterization shows: (i) the unperturbed feedback (with $(\tilde{u}, \tilde{d}, \tilde{p}) = (0, 0, 0)$) is exponentially stable, and (ii) the closed loop system is ISS with respect to errors in estimation, parameter and exogenous input estimates. The task of the interlaced observer-controller tuning thus consists in providing conditions for which, in presence of state estimation errors, the closed-loop is not only ISS but is exponentially stable (in the absence of parameter and exogenous perturbations).

3.5.3 Output-feedback (OF) control

In this section, the closed-loop behavior of the exact model-based passive nonlinear SF controller (2.14) is recovered, up to the concentration estimation convergence rate fixed by the above discussed reactor detectability property, with: (i) an interlaced passive control-dissipative observer design, (ii) a closed-loop robust stability assessment coupled with simple tuning guidelines, and (iii) the identification of the underlying robustness versus response speed compromise in the light of the nonlocal practical stability framework.

Dynamic OF controller

The combination of the SF (3.30) passive nonlinear controller with the dissipative observer (3.10) yields the dynamic OF controller

$$\begin{aligned}
&\dot{\hat{c}} = -r[\hat{c} - \kappa_r(\hat{T} - y), y, p_r] + \theta(c_e - \hat{c}) - \kappa_c(y)(\hat{T} - y) \ , \quad \hat{c}(0) = \hat{c}_0 \\
&\dot{\hat{T}} = \beta r[\hat{c} - \kappa_r(\hat{T} - y), y, p_r] + \theta(T_e - \hat{T}) - \\
&\qquad\qquad -\eta(\hat{T} - T_c) - \kappa_T(y)(\hat{T} - y), \quad \hat{T}(0) = \hat{T}_0, \\
&\theta = [r(\hat{c} - \kappa_r(\hat{T} - y), y, p_r) - k_c(\hat{c} - \bar{c})]/(c_e - \hat{c}), \\
&T_c = \hat{T} - [\beta r(\hat{c} - \kappa_r(\hat{T} - y), y, p_r) + \theta(T_e + \hat{T}) + k_T(\hat{T} - \bar{T})]/\eta.
\end{aligned} \tag{3.34}$$

Closed-loop dynamics

The application of this controller to the actual reactor (2.14) yields the closed-loop dynamics (see Appendix B for its derivation)

$$\begin{aligned}
\dot{e}_c &= -k_c e_c + \frac{(\theta^* - k_c + \sigma)(c_e - c)}{c_e - \hat{c}}\epsilon_c - \kappa_r \sigma \frac{c_e - c}{c_e - \hat{c}}\epsilon_T \\
\dot{e}_T &= -k_T e_T - \beta\sigma\epsilon_c - (k_T - \eta - \theta_r - \kappa_r\beta\sigma)\,\epsilon_T \\
\dot{\epsilon}_c &= -[\theta_r + \sigma]\epsilon_c - [\kappa_c - \kappa_r\sigma]\,\epsilon_T \\
\dot{\epsilon}_T &= -[\theta_r + \eta + \kappa_T + \kappa_r\beta\sigma]\epsilon_T + \beta\sigma\epsilon_c,
\end{aligned} \tag{3.35}$$

where σ is the reaction rate's slope function according to (3.18).

Convergence criteria

The following specific stability conditions in terms of the five-gain set (k_c, k_T, κ_c, κ_r, κ_T) of the proposed passive-dissipative OF controller (3.34) can be established, which may serve as a basis for a gain-tuning scheme.

Proposition 3.2. *The actual reactor (2.14) with the proposed dynamic OF controller (3.34) yields a P-stable (2.16) closed loop system (3.35) if: the (reactor and estimator states, exogenous input, measurement and actuator) disturbance sizes* (δ, ϵ)*, and the control* (k_c, k_T) *and estimator* $(\kappa_c, \kappa_T, \kappa_r)$ *gains satisfy*

$$\begin{array}{ll} (i)\ \theta = \mu_\theta(k_c) > -k_1, & (ii)\ k_c > \iota_c(k_c) \\ (iii)\ k_T > \iota_T(k_c), & (iv)\ \kappa_T > \iota_\tau(k_c, k_T, \kappa_T, \kappa_c, \kappa_r), \end{array} \tag{3.36}$$

with μ_θ *given in (3.31) and* $\iota_c, \iota_T, \iota_\tau$ *defined as*

$$\begin{array}{l} \iota_c(k_c) = \dfrac{(\theta^* - [k_c - \sigma](c_e - c))^2}{4(c_e - \hat{c})(\theta_r + \sigma)}, \quad \iota_r(\kappa_r) = \mu + \eta + \kappa_r \beta \sigma, \\ \iota_T(k_c) = \dfrac{k_c \beta^2 \sigma^2}{4(\theta_r + \sigma)(k_c - \iota_c(k_c))} \quad \iota_1 = \dfrac{(k_T - \kappa_r \beta \sigma)^2}{4k_T} - \iota_r, \\ \iota_2 = \dfrac{\varpi(k_c, \kappa_c, \kappa_r)}{(\theta_r + \sigma)} - \iota_r, \quad \iota_\tau = \max\{\iota_1, \iota_2\}, \end{array} \tag{3.37}$$

and ϖ *is a bounded function of its arguments. Furthermore, if* $(\tilde{d}, \tilde{p}) = (0, 0)$*, the exponential convergence follows.*

(Proof in Appendix C).

Condition (i) is a closed-loop detectability requirement, Condition (ii) ensures the stability of the regulation-estimation concentration dynamics and imposes lower and upper limits ($k_c^- \approx \bar{\theta}, k_c^+ \approx 4\bar{\theta}$) on the composition control gain k_c ([87]), and Conditions (iii) and (iv) ensure the stability of the regulation-estimation temperature dynamics and of the complete interconnection. Thus, for $\kappa_r \approx 1/\beta, k_c \approx 3\bar{\theta}$, the preceding inequalities can be met by choosing: (i) k_T sufficiently large to dominate $\iota_T(k_c, \kappa_c, \kappa_r)$, and (ii) κ_T sufficiently large to dominate $\iota_\tau(k_c, k_T, \kappa_c, \kappa_r)$.

Tuning guidelines

From the preceding P-stability conditions the *conventional-like tuning guidelines* follow:

(i) set the gains conservatively at $(k_c, k_T) \approx (1, 3), (\kappa_r \approx 1/\beta,)\kappa_c \approx k_c, \kappa_T \approx 10\kappa_c$,

(ii) increase the T-estimation gain κ_T until oscillatory response is obtained at κ_T^+, back off and set $\kappa_T = \kappa_T^+/$(2-to-3),

(iii) in the same way set $k_T = k_T^+/$(2-to-3),

(iv) increase k_c (sufficiently below $k_c^+ \approx 4\bar{\theta}$) until there is no improvement, and adjust κ_r.

(v) If necessary, repeat steps (ii) to (iv).

3.5.4 Discussion of the results

The nominal closed loop stability (i.e. without parameter ($\tilde{p}$), exogenous input ($\tilde{d}$), and measurement ($\tilde{y}$) errors) can be established on the basis that the closed-loop dynamics can be viewed as a master-slave system interconnection, due to the single-way coupling (the control error dynamics depends on the estimation error, but not vice versa). This is reflected in the vector representation of the coupled control-estimation error dynamics

$$\begin{aligned}
\dot{e} &= \underbrace{\begin{bmatrix} -k_T & 0 \\ 0 & -k_c \end{bmatrix}}_{\triangleq A_e} e + \underbrace{\begin{bmatrix} \kappa_r\beta\sigma - k_T & -\beta\sigma \\ -\kappa_r\sigma\frac{c_e-c}{c_e-\hat{c}} & \frac{\theta^*-[k_c-\sigma](c_e-c)}{c_e-\hat{c}} \end{bmatrix}}_{\triangleq B_e} \epsilon \\
\dot{\epsilon} &= \underbrace{\begin{bmatrix} -\theta_r + \eta\kappa_T + \kappa_r\beta\sigma & \beta\sigma \\ \kappa_r\sigma - \kappa_c & -(\theta_r + \sigma) \end{bmatrix}}_{\triangleq A_\epsilon} \epsilon.
\end{aligned} \tag{3.38}$$

Correspondingly: the master system is exponentially stable (ϵ converges exponentially to zero in the errorless case), and the slave is input-to-state stable (ISS) with respect to the master system's state, i.e. the estimation error (the connection matrix B_e has bounded norm $||B_e||$ for bounded gains and $\hat{c} \neq c_e$), and, for $\epsilon = 0$, the e-dynamics is exponentially stable. The closed-loop dynamic's asymptotic stability follows (cp. [84]).

On the other hand, *the need of a more constructive stability criterion in the sense of practical applicability for gain tuning and behavior assessment purposes motivates the formulation of explicit stability conditions in terms of the system parameters and the estimator-controller five gain set* $k_c, k_T, \kappa_c, \kappa_r, \kappa_T$. As the temperature is measured, the temperature estimation is a rather simple task, and the estimation problem resides in the concentration ambivalence caused by the non-monotonicity feature of the reaction rate. This ambivalence issue causes the discussed lack of observability, and limits the global estimation speed in correspondence to the inverse residence time θ, characterizing the detectability condition (3.9). Furthermore, the

temperature control is also simple, as it is directly measured, while the concentration is difficult to control, because of the mentioned estimation ambivalence feature. Thus, the main problem resides in the inherent structural restrictions for the concentration estimation and control.

The solvability of the robust OF reactor control problem is a consequence of: (i) the solvability of the OF control (3.27) and dissipative closed-loop observer (condition (i) in Proposition 3.2) problems, and (ii) the adequate choice of gains according to Proposition 3.2.

3.5.5 Application Example

To subject the proposed OF controller to a severe test, let us consider an extreme case of an industrial situation: the operation of the continuous reactor (2.14) with the Langmuir-Hinshelwood (LH) kinetics model [18, 19]

$$\begin{aligned} r(c,T,\pi) &= \frac{cke^{-\left(\frac{\gamma}{T}\right)}}{(1+\sigma c)^2} \\ r_c &= (c^*,T,\pi) = 0, c^* = 1/\sigma \end{aligned} \tag{3.39}$$

adapted from a previous (partial open-loop or asymptotic and full measurement injection) estimation study with EKF and experimental data for the catalytic carbon monoxide oxidation reaction ([28]), with c being the dimensionless concentration of carbon monoxide. Figure 3.6 shows how this kinetics depends on the inhibition parameter σ. With the following nominal parameters and inputs

$$\begin{aligned} \bar{d}^T &= (\bar{c}_e, \bar{T}_e) = (1, 370K), \bar{u}^T = (\bar{\theta}, \bar{T}_c) = (1, 370K), \\ p &= (p_a^T, p_r^T)^T, p_a = (\beta, \eta)^T = (200, 1), \\ p_r^T &= (k, \gamma, \sigma) = (e^{25}, 10000, 3), c^* = 1/3 \end{aligned}$$

the reactor has three open-loop steady-states [22], with two of them corresponding to extinction and ignition stable regimes, and one of them being unstable with maximum concentration rate $r^* \approx 0.6614$ at concentration $\bar{c} = c^* = 1/3$ and temperature $\bar{T} = 430K$.

Tuning of the control and estimator gains in accordance to the conditions (3.36)

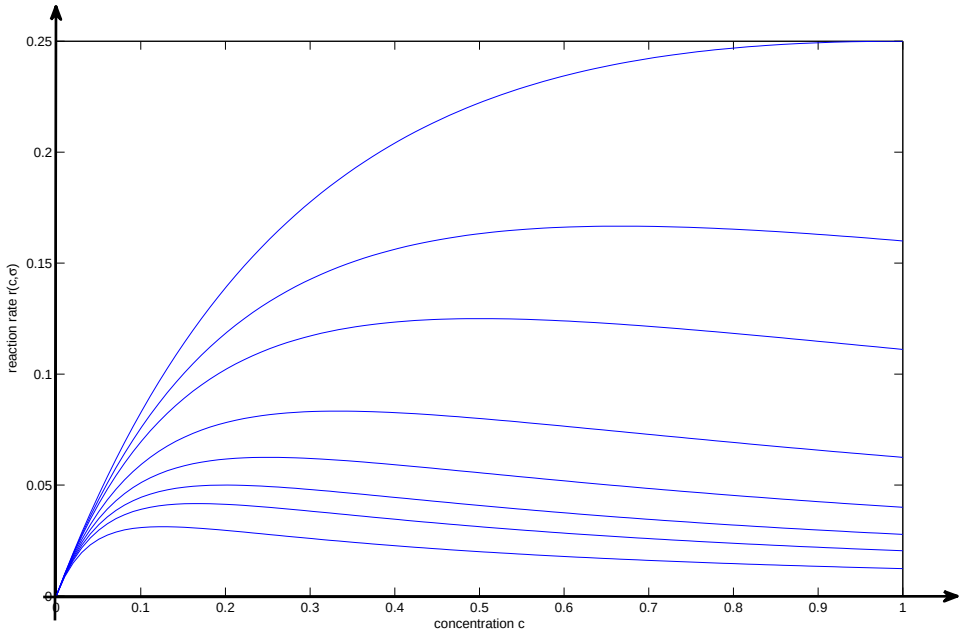

Figure 3.6: Dependence of the Langmuir-Hinshelwood kinetics (3.39) on the inhibition parameter σ: Monotonic behavior for $\sigma \leq 1$ (and $c \in [0, 1]$) and non-monotonic behavior (with maximum in $c^* = 1/\sigma$ for $\sigma > 1$).

yielded the following gain values:

$$\kappa_c = 0.62,\ \kappa_T = 30,\ \kappa_r = \frac{1}{50},\ k_c = 2,\ k_T = 3.$$

The reactor (x_0) and estimator ($\hat{x}_0$) initial conditions were set about the unstable steady-state:

$$x_0 = [0.28, 430]^T, \qquad \hat{x}_0 = [0.35, 425]^T$$

In the spirit of the nonlocal P-stability framework employed in the control design developments, the reactor closed-loop system with nominal SF (without modeling and measurement errors), nominal OF and perturbed OF will be subjected to initial state, input (persistent model parameter and sinusoidal exogenous input) disturbances, and the kind of transient, asymptotic and combined transient-asymptotic responses will be analyzed. For the nominal maximum rate-unstable steady-state regime, the relative degree (3.27) and global detectability [83] conditions are adequately met, according to the following quantitative values:

$$c_e - \bar{c} = 2/3 > 0, \eta = 1 > 0, 1/3 = \theta^- \leq \theta \leq \theta^+ = 3/2$$

Behavior with SF control without modeling and measurement errors and disturbances

For methodological development and comparison purposes, the closed-loop reactor behavior with exact model-based nonlinear passive SF controller (3.30) with errorless model, and initial state deviations is presented in Figure 3.7. As expected from the control gain values the concentration (or temperature) response is about one half (or quarter) settling residence time ($4/\theta = 4$), with smooth and coordinated dilution rate and coolant temperature control actions, safely away from saturation. This is in agreement with the optimality-based non-wasteful feature of the SF controllers discussed in [83].

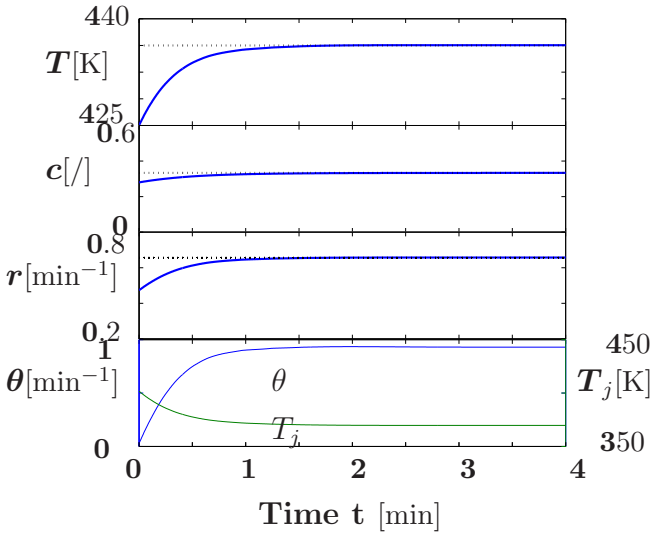

Figure 3.7: Reactor closed-loop nominal behavior with nonlinear SF controller: input and response (—) , estimate (− −), and set point ($\cdots$).

Behavior with OF control without modeling and measurement errors and load disturbances

Initially, the reactor was in the above stated deviated initial conditions, and subjected to the known constant feed concentration and temperature inputs $c_e = 1$ and $T_e = 370K$, respectively. The resulting behavior with errorless model-based OF control (3.34) is presented in Figure 3.8, showing that: (i) the concentration and temperature responses are quite similar to the ones of the nonlinear SF controller

(Figure 3.7), in spite of a sluggish concentration estimate response (about 3/4th of the natural settling time), and (iii) the control actions occur in a smooth and efficient manner, reasonably away from saturation. This test verifies the ISS property of the closed-loop reactor system with the proposed OF dynamic control, with asymptotic convergence to the prescribed steady-state.

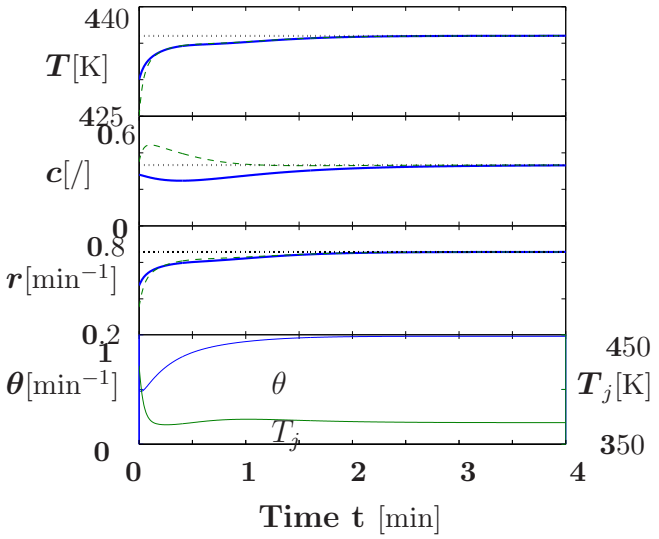

Figure 3.8: Reactor closed-loop nominal behavior with nonlinear OF controller: input and response (—) , estimate (− −), and set point ($\cdots$).

Behavior with OF control subject to modeling and measurement errors and load disturbances

To test the robustness of the proposed OF controller, the reactor and the estimator initial states were deviated from the nominal open-loop unstable and maximum reaction rate steady-state, the closed loop system was subjected to oscillatory feed concentration and temperature

$$c_e = 0.99 + 0.01\cos(4\pi t), \quad T_e = 370 + 2\sin(4\pi t)$$

and the estimation model had the following errors: (i) the feed concentration was set at the mean value $\hat{c}_e(t) = 0.991$ of the actual periodic input signal, (ii) the measured feed and reactor temperatures had rather drastic periodic errors $\hat{T}_e(t) - T_e(t) = y(t) - T(t) = 2\cos(40\pi t)$ (four degrees amplitude band and frequency close to

natural resonance mechanism), as well as (iii) a -1.5, -10, and $+3$ % errors in the activation energy (γ), heat transfer coefficient (η), and adiabatic temperature rise (β), respectively. It must be pointed out that the combination of these measurement and modelling errors represents a worst-case situation meant to subject the proposed OF controller to a rather severe robustness test. The resulting robust closed-loop behavior is presented in Figure 3.9, showing that: (i) the closed loop system is adequately P-stable with transient response trend that basically coincides with the one of the errorless model case (see Figure 3.8), (ii) as expected from the severe modelling errors, the unmeasured concentration exhibits a significant ($\approx -30\%$) asymptotic offset, some reaction rate offset ($\approx -20\%$) and the temperature estimate generated by the linear-dynamical advective (that is mass-energy balance based) component of the dissipative estimator displays an offset-less trend response, and (iii) given the flatness feature of the reaction kinetics in the isotonic branch of the reaction rate function, in spite of the -30% concentration trend offset, the reaction rate trend is only a -20% of its maximum set point value. In principle , the optimal reaction rate offset can be arbitrarily reduced by performing online kinetic parameter model calibration on the basis of the occasional or periodic concentration measurements that are usually taken in industrial settings for product quality and process efficiency assessment purposes.

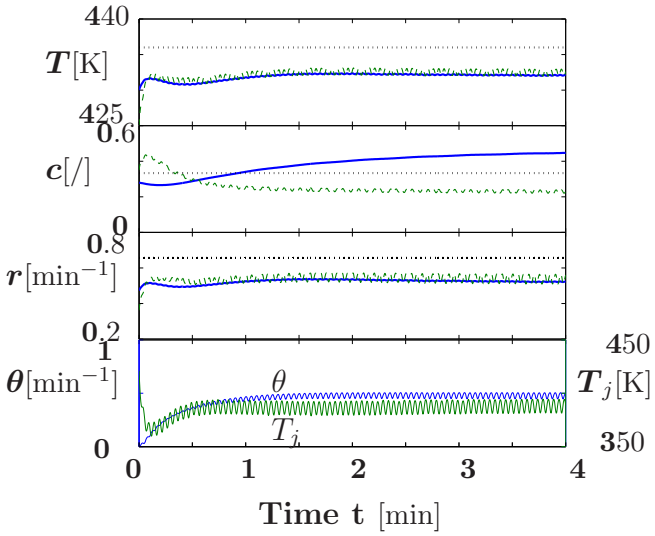

Figure 3.9: Reactor closed-loop robust behavior with nonlinear OF controller: input and response (—) , estimate ($--$), and set point ($\cdots$).

3.5.6 Concluding Remarks

The preceding responses to initial state deviations, exogenous input disturbances, and model parameter errors verify that, in agreement with the methodological developments, the proposed passive-dissipative OF controller: (i) recovers rather well the behavior of its exact model-based nonlinear passive SF counterpart, with optimality-based robustness and non-wastefulness, and (ii) exhibits P-(robust and non local) stability with respect to model, and measurement errors. The closed-loop behavior assessment through simulations made quantitative the P-stability features, like transient response speed, overshoot, and high frequencies oscillatory components, as well as asymptotic response offsets, and verifies the effectiveness of the tuning guidelines in the light of the P-stability characterization.

3.6 Summary

In this chapter, the problem of concentration and temperature estimation for a non-isothermal CSTR with temperature measurement was addressed.

Motivated by the process inherent transport and reaction mechanisms, as well as the underlying detectability properties of the CSTR, a dissipative observer was designed which allowed to

- identify the basic dissipation mechanisms of the estimation error dynamics, corresponding to linear transport and nonlinear reaction
- improve their corresponding dissipation features by appropriately choosing the energy interchange structure between both mechanisms in function of the correction gains
- identify an approach to employ bounds for the nonlinear subsystem's dissipation in the sense of a quadratic form by means of conic sector conditions for the (induced) nonlinear reaction rate error
- obtain explicit solvability conditions in terms of detectability-type conditions, and low dimensional matrix inequalities

In comparison to previous results the presented dissipative observer unifies the basic requirements of (i) systematic design, (ii) mathematically rigorous and physically

meaningful convergence conditions, (iii) simple implementation, and (iv) convergence improvement.

Furthermore, the dissipative observer was combined with a passive nonlinear SF controller to obtain a dynamic OF controller for the stabilization of the SS of the reactor with maximum production rate. This particular application study enables to identify the structural features corresponding to the employment of a dissipative observer, in the understanding that the structure-oriented design approach of the dissipative observer permits to treat the complex nonlinear closed-loop stability problem by means of explicit matrix inequalities. This issue allows to overcome the corresponding difficulties of the closed-loop stability assessment and yields explicit simple convergence criteria with physical meaning based on which explicit and mathematically rigorous tuning guidelines are identified.

In comparison with previous studies on this subject, the presented dissipative-passive OF controller offers (i) systematic design, (ii) mathematically rigor with physical meaning, (iii) implications for process design parameters, (iv) identification of capabilities and limitations, (v) recovery of the ideal SF controller.

The non-isothermal stirred tank represents the limit case of the non-isothermal tubular reactor and thus constitutes an important particular sub-problem which had to be addressed before treating the tubular reactor case because it enables to

- identify the main structural features of a unifying chemical reactor observer design methodology has to include in virtue of exploiting the process inherent structural properties

- set the methodological starting point of an energy-based Lyapunov-type design approach for a entire class of chemical reactors

- identify a mathematically rigorous way of analyzing the influence on the dissipation of the nonlinear kinetic mechanisms (employing sector conditions)

In the spirit of a methodological inductive step towards the distributed tubular reactor counterpart, next, the isothermal tubular reactor with concentration measurements is considered, because it allows to

- extend the analysis of the lumped transport characteristic dissipativity properties to the case of diffusive-convective distributed transport

- identify a way of analyzing the spatially distributed influence of the nonlinear kinetic mechanism on the dissipation, extending the sector-condition approach employed in this chapter to the distributed case.

Chapter 4

The Isothermal Tubular Reactor

Having as point of departure the stirred tank reactor dissipative observer, in terms of a dissipation mechanism with linear-dynamical transport and nonlinear-static reaction components, in this section the basic ideas of the dissipative approach are extended to the distributed case associated with the isothermal tubular reactor with boundary and/ or domain point concentration measurements. The consideration of this problem represents an important intermediate step towards the consideration of the non-isothermal tubular reactor with temperature measurements, because it allows to identify a methodological framework for the treatment of (i) the distributed diffusive-convective transport, and (ii) the distributed nonlinear reaction.

Accordingly, functional analysis and Lyapunov-type energy methods for distributed parameter systems are employed to draw the corresponding version of the convergence criteria and the tuning guidelines.

In comparison with previous studies reported in the literature the designed observer presents (i) a systematic design approach, (ii) mathematically rigorous convergence conditions with physical meaning, (iii) convergence improvement, and (iv) explicit implications of the isotonicity features of the reaction kinetic rate on the attainable observer performance.

The extension of the employment of the sector condition to the context of the distributed system enables the weighting of regions of maximal versus those of minimal convergence, what represents a first step towards the complex problem of transferring convergence intensity superhavit to regions with a slower convergence, in accordance with the diffusive-convective transport physical mechanisms.

The results are illustrated through numerical simulations including cases of low and high Peclet-numbers.

4.1 Introduction

This chapter deals with the extension of the dissipative observer design employed in the preceding chapter for the non-isothermal CSTR with temperature measurement, to the isothermal tubular reactor with boundary and/ or domain point concentration measurements. The isothermal tubular reactor model is given by (see (2.11) in Section 2.3)

$$\frac{\partial c(x,t)}{\partial t} = \frac{1}{P_{ec}}\frac{\partial^2 c}{\partial x^2} - \frac{\partial c}{\partial x} - D_a r(c(x,t), T(x,t)) \tag{4.1}$$

for $t > 0, \quad x \in (0,1)$, with corresponding Danckwerts' boundary conditions

$$x = 0 : \frac{1}{P_{ec}}\frac{\partial c(0,t)}{\partial x} = (c(0,t) - c_{in}(t)), \quad x = 1 : \frac{1}{P_{ec}}\frac{\partial c(1,t)}{\partial x} = 0, \tag{4.2}$$

for all $t \geq 0$, initial profile $c(x,0) = c_0(x)$, and measurement vector

$$y(t) = [c(0,t),\, c(\xi,t),\, c(1,t)]^T. \tag{4.3}$$

The related estimation problem represents an important intermediate step towards the consideration of the non-isothermal tubular reactor with temperature measurements, in the understanding that the main mechanisms of distributed nature of the process can already be characterized for the isothermal case. These are

- diffusive-convective transport,
- nonlinear distributed chemical reaction,
- locally discrete measurements.

For this purpose, the previously identified energy-function Lyapunov-type dissipative observer design is extended to address the design of a locally distributed data-assimilation scheme for the profile estimation of the concentration, based on point concentration measurements on the boundary and/ or in the domain.

For the analysis of the distributed transport and the innovation mechanisms, linear functional analysis tools are employed, as there are: (i) spectral theory based on Fourier series synthesis, and (ii) basic ideas from variational calculus (energy method).

4.2 Dissipative Observer

4.2.1 Observer Construction

As a generalization of the structure of the dissipative observer (3.10)[1], employed in the CSTR case study, a linear gain Luenberger-type observer is set ($y = [c(0,t),\, c(\xi,t),\, c(1,t)]^T$):

$$\frac{\partial \hat{c}(x,t)}{\partial t} = \frac{1}{P_{ec}}\frac{\partial^2 \hat{c}}{\partial x^2} - \frac{\partial \hat{c}}{\partial x} - D_a r(\hat{c}(x,t), \bar{T}) - l_\xi(\hat{c}(\xi,t) - y_2(t)) \tag{4.4}$$

for $t > 0, x \in (0,1)$, with boundary conditions

$$\begin{aligned} x = 0: \ & \frac{1}{P_{ec}}\frac{\partial \hat{c}(0,t)}{\partial x} = \hat{c}(0,t) - c_{in}(t) - l_0(\hat{c}(0,t) - y_1(t)) \\ x = 1: \ & \frac{1}{P_{ec}}\frac{\partial \hat{c}(1,t)}{\partial x} = -l_0(\hat{c}(0,t) - y_3(t)), \end{aligned} \tag{4.5}$$

for $t \geq 0$, and initial condition $\hat{c}(x,0) = \hat{c}_0(x), \quad x \in [0,1]$. The data-assimilation-scheme (4.4)-(4.5) depends on: (i) the observer gains l_0, l_1 at the boundary, (ii) the location $\xi \in (0,1)$ of the measurement y_2 in the domain, and (iii) the spatial distribution $l_\xi(x)$ of the corresponding injection mechanism, which represents an important design degree of freedom whose influence will become clear later.

4.2.2 Estimation Error Dynamics

For the assessment of explicit convergence conditions the estimation error dynamics, given by the difference of (4.4)-(4.5) and (4.1)-(4.2) is considered

$$\frac{\partial e}{\partial t} = \frac{1}{P_{ec}}\frac{\partial^2 e}{\partial x^2} - \frac{\partial e}{\partial x} - D_a\left[r(c+e) - r(c)\right] - l_\xi(x)e(\xi,t) \tag{4.6}$$

for $x \in (0,1), t > 0$, with boundary conditions

$$x = 0: \ \frac{1}{P_{ec}}\frac{\partial e}{\partial x}(0,t) - e(0,t) = -l_0 e(0,t), \quad x = 1: \ \frac{1}{P_{ec}}\frac{\partial \hat{c}}{\partial x}(1,t) = -l_1 e(1,t) \tag{4.7}$$

for $t \geq 0$, and initial conditions $e(x,0) = e_0(x), \quad x \in [0,1], \quad e_0(x) = \hat{c}_0(x) - c_0(x)$.

[1]Note that in the distributed case examples no correction mechanism is introduced for the reaction rate's argument. Such a mechanism can be considered but in the present work the main attention is focussed on the design of a conventional-like observer of simple structure, in order to focuss the attention on the main issues which have to be taken into account for the design.

In a way that is analogous to the treatment of the stirred tank reactor (Section 3.3), the estimation error dynamics for the isothermal tubular reactor case is represented as an interconnection of two subsystems, one associated with the distributed convective-diffusive mass transport (compare (3.12)-(3.13)), and one with the nonlinear kinetics (compare(3.14))

$$\frac{de}{dt} = A_c e + D_a \nu, \tag{4.8}$$

$$\nu = -\rho(c; e), \tag{4.9}$$

for $e \in \mathrm{Dom}(A_c)$, where A_c is the linear transport operator given by

$$A_c = \frac{1}{P_{ec}} \frac{\partial^2}{\partial x^2} - \frac{\partial}{\partial x} \tag{4.10}$$

which acts on its domain of definition $\mathrm{Dom}(A_c)$, characterized basically by the boundary conditions (4.7)

$$\mathrm{Dom}(A_c) = \left\{ h(x) \in L^2([0,1], \Xi \subset \mathbb{R}) : h(x), \frac{dh}{dx}(x) \text{ a.c.}, \right. \\ \left. \text{and (4.7) holds} \right\}, \tag{4.11}$$

and $\rho(c; e)$ is the nonlinear function which represents the induced reaction rate error

$$\rho(c; e) \triangleq r(c + e) - r(c), \quad \rho(c; 0) = 0, \tag{4.12}$$

in dependence of the (space and time) varying actual concentration. From Figure 4.1 one can appreciate that the basic structure is the same as in the case of the stirred tank (compare Figure 3.5), in the understanding that in the limiting case of high dispersion, the isothermal reactor (4.1)-(4.3) becomes the isothermal version of the lumped non-isothermal reactor (3.1) [9] with concentration measurement (compare Figure 3.2 without Σ_H).

In order to analyze the dissipation properties of the given estimation error dynamics in dependence on the system parameters and correction gain structure, in the spirit of the stirred tank study (Chapter 3), an energy-based Lyapunov-type method is employed, which exploits the process inherent interplay of transport and reaction mechanisms.

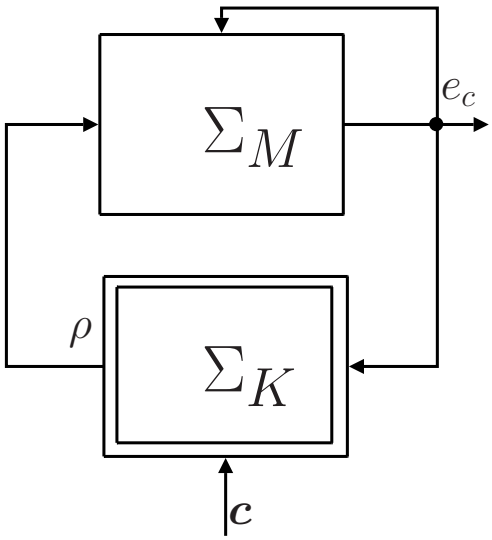

Figure 4.1: Basic interconnection structure of the mass transport and the kinetic subsystems in the estimation error dynamics (4.8)-(4.9), with
$\Sigma_M : \rho \mapsto \epsilon_c$, $\Sigma_K : (\epsilon_c, c) \mapsto \rho$.

4.2.3 Estimation Error Dissipation

Here, in the spirit of the Lyapunov approach for distributed parameter systems (see e.g. [63, 65]) the underlying energy dissipation mechanism is identified in the light of the above discussed mass transport plus kinetics system partition, in order to identify explicit bounds for the dissipation which serve as a basis for the convergence assessment.

For this aim, the influences of the nonlinear kinetic and the linear transport subsystems are identified, and subsequently bounds for the corresponding dissipations are drawn. For the nonlinear kinetic subsystem an explicit bound is obtained by employing the sector condition (3.20) previously identified for the lumped continuous stirred reactor, and for the linear transport subsystem two different approaches are employed to find explicit bounds for the dissipation: (i) in terms of the dominant eigenvalues via a spectral decomposition approach (cp. [35, 38, 37, 39, 26]), and (ii) a direct, functional-analytic approach (cp. [34, 91, 65, 66]).

For this aim, introduce the potential (weighted squared error) energy in $Z = L^2([0,1], \Xi = [0,1] \subset \mathbb{R})$

$$E(e) = \int_0^1 w(x) e^2(x,t) dx = \langle e, we \rangle_Z \,, \tag{4.13}$$

where $w(x) > 0$ is the continuous positive definite weighting function, which is viewed as an important design degree of freedom, and which later will be related to the particular data-assimilation structure chosen for the correction mechanism in the domain.

The dissipation corresponding to (4.13) is given by

$$\frac{dE(e)}{dt} = \mathcal{D}_K + \mathcal{D}_T \tag{4.14}$$

$$\mathcal{D}_K = -2\int_0^1 w(x)e(x,t)D_a\left\{r[c(x,t)+e(x,t)] - r[c(x,t)]\right\}dx \tag{4.15}$$

$$\mathcal{D}_T = -2\int_0^1 w(x)e(x,t)\left\{-\frac{1}{P_{ec}}\frac{\partial^2 e(x,t)}{\partial x^2} + \frac{\partial e(x,t)}{\partial x} + l_\xi(x)e(\xi,t)\right\}dx, \tag{4.16}$$

where $\mathcal{D}_K$ is the dissipation corresponding to the kinetic component (4.9) of the estimation error dynamics, and $\mathcal{D}_T$ is the linear transport dissipation component, corresponding to the linear dynamical subsystem (4.8) of the estimation error dynamics.

In accordance to the preceding CSTR estimation study, the subsequent analysis is performed for the dissipation of the nonlinear static kinetic subsystem $\mathcal{D}_K$, and of the linear dynamic transport subsystem $\mathcal{D}_T$. The degree of freedom $w(x) > 0$ will be exploited in the analysis of the linear dynamical transport subsystem dissipation component, which will turn out to depend explicitly on the particular structure of the correction mechanism $l_\xi(x)$ which is employed.

4.2.4 Quadratic bounds for the nonlinear kinetic subsystem dissipation $\mathcal{D}_K$

Next, the dissipation of the nonlinear kinetic subsystem Σ_K (4.9), corresponding to the nonlinear kinetic function $\rho(c;e)$, is bounded employing the sector condition (3.20), used in the preceding CSTR study, in a version extended for the consideration of the spatially distributed case.

Remember that, due to the continuous differentiability of the rate function $r(c,T)$, in any point $x \in [0,1]$, and for any value $c(x,t)$, the nonlinear function $\rho(c(x,t);e(x,t))$ is included in the sector $[s_l, s_u]$, where $s_l = \min \dfrac{\partial r}{\partial c}$ and $s_u = \max \dfrac{\partial r}{\partial c}$,

i.e.

$$(s_u e - \rho(c;e))\,(\rho(c;e) - s_l e) \geq 0, \tag{4.17}$$

and, accordingly, one can bound the influence of the kinetic mechanism on the dissipation (4.14) in any $x \in [0,1]$ using quadratic forms. Note that, in consequence, for all (at least continuous) positive definite functions $h(x)$ it holds that for all $x \in [0,1]$

$$h(x)\,(s_u e - \rho(c;e))\,(\rho(c;e) - s_l e) \geq 0,$$

and thus one finds the integrally weighted sector condition

$$\mathcal{S}_h \triangleq \int_0^1 h(x)\,(s_u e - \rho(c;e))\,(\rho(c;e) - s_l e)\,dx \geq 0. \tag{4.18}$$

Consequently, an explicit bound for the kinetic subsystem dissipation component is given by

$$\begin{aligned}\mathcal{D}_K &= -2\int_0^1 w(x)e(x,t)D_a\rho(c;e)dx + \mathcal{S}_h - \mathcal{S}_h \\ &\leq -\int_0^1 \begin{bmatrix} e \\ \rho \end{bmatrix}^T \begin{bmatrix} h(x)s_u s_l & \frac{2D_a w(x) - [s_u + s_l]h(x)}{2} \\ \frac{2D_a w(x) - [s_u + s_l]h(x)}{2} & h(x) \end{bmatrix} \begin{bmatrix} e \\ \rho \end{bmatrix} dx.\end{aligned} \tag{4.19}$$

This bound characterizes the first dissipation component $\mathcal{D}_K$ of the estimation error dynamics dissipation (4.14) corresponding to the weighted squared energy (4.13). Note, that an additional degree of freedom $h(x) > 0$ has been introduced, which later on will result to allow the derivation of explicit convergence conditions by combining the given bound (4.19) for the dissipation $\mathcal{D}_K$ of the kinetic subsystem (4.9) with a bound for the linear transport subsystem dissipation component $\mathcal{D}_T$ (4.16) which is identified next *for two different types of injection mechanisms* (*treated accordingly in two different theoretical frameworks*).

4.2.5 Quadratic bounds for the linear transport subsystem dissipation $\mathcal{D}_T$

Bounds for the linear innovated transport subsystem (4.8) will clearly depend on the particular correction mechanism $l_\xi(x)$ employed. As mentioned in Section 1.3 for linear systems different estimation and control design techniques have been reported and different approaches to the analysis of the related stability issues have been employed. In the sequel, two main approaches, reported in the DPS literature, are employed for the design of the correction mechanism for the linear dynamic distributed parameter transport subsystems (4.8), to draw explicit quadratic bounds for the corresponding dissipation component $\mathcal{D}_T$ (4.16). These approaches are:

(A) Modal injection, within a Fourier frequency, spectral decomposition approach [34, 35, 36, 38, 37, 91, 39].

(B) Point injection within a direct, functional-analytic approach (energy method)[34, 91, 65, 33, 59].

(A) Spectral Approach

In the spirit of modal innovation mechanisms recorded in the literature for applications in control and observation of linear DPS (see e.g. [34, 35, 36, 38, 37, 91, 39, 26]), a finite-dimensional modal correction mechanism can be employed to reassign the first N dominant eigenvalues of the linear transport subsystem. For this purpose consider a Fourier series expansion of the estimation error function $e(x,t)$ in the bi-orthogonal eigenfunction basis (Φ_k, Ψ_k) of the eigenfunctions Φ_k of the mass transport operator A_c and the adjoint ones Ψ_k (see Appendix D for more details)

$$e(x,t) = \sum_{k=1}^{\infty} \underbrace{\int_0^1 w(x)e(x,t)\Psi_k(x)dx}_{\triangleq\, e_k(t)} \Phi_k(x), \tag{4.20}$$

with the weighting function $w(x)$ of the energy definition (4.13), which will be defined next. Correspondingly, *the $e_k(t)$ are the modes of the linear dynamical transport subsystem* $\Sigma(A_c, D_a)$. The weighting function $w(x)$ is chosen such that the eigenfunctions are pairwise orthogonal, i.e. (cp. e.g. [92, 93, 94, 95])

$$w(x) = e^{-P_{ec}x/2}. \tag{4.21}$$

Corresponding to the eigenfunction property $A_c\Phi_k = \lambda_k\Phi_k$, with λ_k being the k-th eigenvalue of the operator A_c, the action of the operator A_c can be expressed as

$$A_c e(x,t) = \sum_{k=1}^{\infty} \lambda_k e_k(t)\Phi_k(x). \tag{4.22}$$

Note, that the negative of the operator A_c is a Sturm-Liouville (SL) operator. In virtue of this SL property, it is known [96] that **all eigenvalues λ_k, $k \in \mathbb{N}$ of the operator A_c are real, negative, and form a discrete series which monotonically decreases to minus infinity**. Consequently, for each negative number $-\delta < 0$, there is a finite number of eigenvalues which are greater or equal to it, i.e. the set

$$\{\lambda_k : \quad \lambda_k \geq -\delta\}$$

is finite. This means that there exists a number $N \in \mathbb{N}$ so that

$$\lambda_k < -\delta, \quad \forall k > N. \tag{4.23}$$

Consequently, one can separate the modes $e_k(t)$ in those which are fast or slow with respect to $-\delta$. Accordingly, and in virtue of the representation (4.22) of the action of the operator A_c, one can formulate the dynamics of the linear dynamical transport subsystem $\Sigma(A_c, D_a)$ in form of a modal decomposition according to

$$\frac{d}{dt}\begin{bmatrix} e_k^s \\ e_k^f \end{bmatrix} = \begin{bmatrix} A_c^s & 0 \\ 0 & A_c^f \end{bmatrix}\begin{bmatrix} e_k^s \\ e_k^f \end{bmatrix} \tag{4.24}$$

(see e.g. [38, 37, 92, 39] for more details), where the vector e_k^s has dimension N (4.23), and the corresponding $N \times N$ matrix A_c^s is diagonal

$$A_c^s = \mathrm{diag}(\lambda_1, \ldots, \lambda_N). \tag{4.25}$$

Based on this modal representation of the dynamics of the linear transport subsystem, it is natural to consider a N-dimensional modal innovation mechanism to improve the dissipation properties of the linear dynamical transport subsystem. There-

fore consider the innovation mechanism

$$l_\xi(\hat{c}(\xi,t)-y_2(t))=\sum_{k=1}^{N} l_{\xi,k}\Phi_k(x)(\hat{c}(\xi,t)-y_2(t)). \tag{4.26}$$

Furthermore, the estimation error corresponding to the point $x=\xi$ where the measurement y_2 is obtained at, can be expressed analogously as

$$e(\xi,t)=\hat{c}(\xi,t)-y_2(t)=\sum_{k=1}^{\infty} e_k(t)\Phi_k(\xi), \tag{4.27}$$

and, consequently, the action of the operator A_c (4.22) together with the modal correction mechanism l_ξ (4.26) obtains the following form

$$A_c e(x,t)-l_\xi(x)e(\xi,t)=\sum_{k=1}^{\infty}\lambda_k e_k(t)\Phi_k(x)-\sum_{k=1}^{N} l_{\xi,k}\Phi_k(x)\left(\sum_{l=1}^{\infty} e_l(t)\Phi_l(\xi)\right).$$

Introducing the modal gain vector

$$L_N=\begin{bmatrix} l_{\xi,1} \\ \vdots \\ l_{\xi,N} \end{bmatrix}, \tag{4.28}$$

and the restriction of the corresponding measurement operator to the N-dimensional space of slow modes Z^s, i.e.

$$C^s=\begin{bmatrix} \Phi_1(\xi), & \cdots, & \Phi_N(\xi) \end{bmatrix}, \tag{4.29}$$

and the corresponding restriction to the (infinite-dimensional) modal subspace of fast modes Z^f according to

$$C^f e(\xi,t)=\sum_{k=N+1}^{\infty} e_k(t)\Phi_k(\xi), \tag{4.30}$$

one obtains the modal representation of the innovated linear transport subsystem's dynamics

$$\frac{d}{dt}\begin{bmatrix} e_k^s \\ e_k^f \end{bmatrix} = \begin{bmatrix} A_c^s - L_N C^s & L_N C^f \\ 0 & A_c^f \end{bmatrix} \begin{bmatrix} e_k^s \\ e_k^f \end{bmatrix}. \tag{4.31}$$

Accordingly, a necessary and sufficient condition for the assignability of the dominant slow eigenvalues $\lambda_1, \ldots, \lambda_N$ is given by Kalmann's observability condition for the pair (A_c^s, C^s) [38, 37, 39], i.e. the full rank condition of the observability matrix

$$\mathcal{O}^s = \left[C^s | A^s C^s | \ldots | (A_c^s)^{N-1} C^s\right]. \tag{4.32}$$

This obviously sets a condition on the sensor location $\xi \in [0,1]$ in the light of the structure of the measurement matrix C^s (4.29). More precisely, this condition requires that **the sensor location $\xi \in [0,1]$ does not correspond to any root of the first N eigenfunctions $\Phi_k(x)$, $k = 1, \ldots, N$** [37].

Based on these considerations, one can find explicit bounds on the dissipation $\mathcal{D}_T$, a function of the innovated linear transport operator action, in terms of the reassigned eigenvalues of the slow, dominant modal dynamics, and the fast modal dynamics corresponding to the linear transport operator A_c.

Lemma 4.1. *Under the consideration of the modal correction mechanism (4.26), the dissipation $\mathcal{D}_T$ of the linear dynamic transport subsystem is bounded in the following way*

$$\mathcal{D}_T \leq 2\max\{\Re(\lambda^*), \lambda_{N+1}\}E, \tag{4.33}$$

where $\Re(\lambda^*)$ denotes the real part of the maximal eigenvalues of the $N \times N$ matrix

$$A_L^s \triangleq A_c^s - L_N C^s = \begin{bmatrix} \lambda_1 - l_{\xi,1}\Phi_1(\xi) & -l_{\xi,1}\Phi_2(\xi) & \cdots & -l_{\xi,1}\Phi_N(\xi) \\ -l_{\xi,2}\Phi_1(\xi) & \lambda_2 - l_{\xi,2}\Phi_2(\xi) & \cdots & -l_{\xi,2}\Phi_N(\xi) \\ \vdots & & \ddots & \vdots \\ -l_{\xi,N}\Phi_1(\xi) & -l_{\xi,N}\Phi_2(\xi) & \cdots & \lambda_N - l_{\xi,N}\Phi_N(\xi) \end{bmatrix}, \tag{4.34}$$

λ_{N+1} is the $N+1$-th eigenvalue of the linear transport operator A_c (4.10) and

$E = \int_0^1 w(x)e^2(x,t)dx$ *(4.13) is the weighted squared estimation error energy, with weighting function* $w(x)$ *given by (4.21).*

(*Proof in Appendix E.*)

This finishes the bounding of the linear transport dissipation component $\mathcal{D}_T$ (4.16) using a modal injection mechanism. For later comparison, an alternative bound, using a point injection mechanism is drawn next within a direct, functional analytic framework.

(B) Variational Approach

Next, an alternative bound for the linear transport dissipation component $\mathcal{D}_T$ (4.16) is drawn, based on the employment of a point injection mechanism in place of the modal injection mechanism. For this aim, a direct, functional analytic approach [33, 34, 91, 65, 59] (in mathematical theory called energy method, see e.g. [59]) is employed to obtain quadratic bounds for the dissipation component $\mathcal{D}_T$. Considering a point-injection in the domain, i.e. setting the data-assimilation scheme in the following way,

$$l_\xi = l_\xi^0 \delta(x - \xi), \tag{4.35}$$

integrating by parts the expression for $\mathcal{D}_T$ (4.16), and employing Wirtinger's inequality (e.g. [97, 98, 66]) to bound the integral over the squared estimation error gradient by an integral over the squared estimation error profile, one obtains the following bound for the dissipation component $\mathcal{D}_T$ of the linear dynamical transport subsystem (4.8) of the estimation error dynamics.

Lemma 4.2. *Under the consideration of the correction mechanism given in (4.35), the dissipation of the linear dynamical transport subsystem is bounded in the following*

way

$$\mathcal{D}_T \leq -\int_0^1 \zeta^T \bar{Q} \zeta dx \tag{4.36}$$

$$\zeta \triangleq [e(x,t), \quad e(0,t), \quad e(\xi,t), \quad e(1,t)]^T$$

$$\bar{Q} \triangleq \begin{bmatrix} D[w] & \frac{w_{\min}\pi}{2} & 0 & 0 \\ \frac{w_{\min}\pi}{2} & \mathcal{R}_0 & 0 & 0 \\ 0 & 0 & l_\xi^0 w(\xi) & 0 \\ 0 & 0 & 0 & \mathcal{R}_1 \end{bmatrix}$$

$$D[w] = -\frac{d^2 w}{dx^2} + P_e \frac{dw}{dx} + \frac{w_{\min}\pi}{2P_{ec}}$$

$$\mathcal{R}_0 = -\frac{dw}{dx}(0) - l_0 w(0) + \frac{w_{\min}\pi}{2P_{ec}} \tag{4.37}$$

$$\mathcal{R}_1 = \frac{dw}{dx}(1) + [P_e + l_1] w(1). \tag{4.38}$$

(*Proof in Appendix F*).

This bound, based on a point injection mechanism, varies from the bound (4.33) in the following sense: (i) the weighing function $w(x) > 0$ is not fixed by methodological requirements, (ii) the values of the estimation error on the boundary appear directly, and not in form of the underlying eigenvalues, and (iii) the collocated measurement injection in $x = \xi$ appears as a separate component in the dissipation bound (4.36) for $\mathcal{D}_T$.

The particular differences implied by the presented data assimilation schemes are discussed later, on the basis of the corresponding convergence criteria, obtained next by combining the previously identified bounds for the nonlinear kinetic dissipation component $\mathcal{D}_K$ (4.19), with the bounds (4.33) and (4.36) of the linear transport dissipation component $\mathcal{D}_T$.

4.2.6 Convergence Assessment

According to the two different injection mechanisms employed in the above analysis, (A) a finite-dimensional modal injection, and (B) a point injection, two different sets of convergence criteria and conditions are obtained.

(A) Modal injection - spectral decomposition approach

First, convergence criteria are drawn for the case of a modal injection mechanism, using the corresponding bound (4.33) for the linear transport dissipation component $\mathcal{D}_T$ together with the bound $\mathcal{D}_K$ of the nonlinear kinetic dissipation component.

Therefor, recall the dissipation (4.14) with the corresponding components $\mathcal{D}_T$ (4.16) of the linear dynamical subsystem (4.8), with the finite-dimensional measurement injection mechanism (4.26), and $\mathcal{D}_K$ (4.15) of the nonlinear static (feedback) subsystem (4.9) as given in (4.33) and (4.19), and write the corresponding estimation error dissipation with respect to the energy (4.13)

$$\begin{aligned}
&\frac{dE(e)}{dt} = \mathcal{D}_T + \mathcal{D}_K \\
&\quad \leq -\int_0^1 \begin{bmatrix} e \\ \rho \end{bmatrix}^T \begin{bmatrix} -2\gamma w(x) + h(x) s_u s_l & \dfrac{2D_a w(x) - [s_u + s_l]h(x)}{2} \\ \dfrac{2D_a w(x) - [s_u + s_l]h(x)}{2} & h(x) \end{bmatrix} \begin{bmatrix} e \\ \rho \end{bmatrix} dx. \\
&\gamma = \max\{\lambda^*, \lambda_{N+1}\}
\end{aligned} \tag{4.39}$$

In the light of the Lyapunov-like approach (cp. Lemma 2.1), the aim of the observer design consists in ensuring that the dissipation (4.39) becomes strictly negative, in the understanding that it fulfills an inequality of the type

$$\frac{dE(e)}{dt} \leq -2\lambda E(e), \quad \lambda > 0. \tag{4.40}$$

These considerations motivate the following result, stating explicit conditions for the exponential stability of the estimation error dynamics in terms of (i) sensor location, (ii) system parameters, and (iii) modal observer gains.

Recall, that the weighting function $w(x)$ is given by (4.21), so that the main degrees of freedom are (i) the innovation dimension N, (ii) the weighting function for the nonlinear kinetic dissipation bounds $h(x) > 0$, (iii) the sensor location $\xi \in [0, 1]$, and (iv) the modal gains $l_{\xi,k}$. For the particular choice of the sector weighting function $h(x) = w(x) = e^{-P_{ec}x}$, it is furthermore possible to find explicit conditions which allow to draw simple conditions on the observer gains and the system parameters.

Theorem 4.1. *Consider the isothermal tubular reactor (4.1)-(4.2), together with the dissipative observer (4.4)-(4.5), with $l_0 = l_1 = 0$ and modal measurement injection*

$l_\xi(x)$ corresponding to (4.26). Let $s_l = \min \dfrac{\partial r}{\partial c}$, and $s_u = \max \dfrac{\partial r}{\partial c}$ be the minimal and the maximal slope of the reaction rate r, respectively, and $h(x) = w(x) = e^{-P_{ec}x}$. The estimation error $e = \hat{c} - c$ converges exponentially to zero with rate $\lambda > 0$ and amplitude $a = e^{P_{ec}/2}$, i.e.

$$||e(x,t)|| \leq a\,||e_0(x)||\,e^{-\lambda t}, \tag{4.41}$$

if the following conditions are met

(i) the modal innovation dimension N is chosen so that

$$\forall x \in [0,1]: \quad -2\lambda_{N+1} > \frac{(2D_a - [s_u + s_l])^2}{4} - s_u s_l + 2\lambda, \tag{4.42}$$

(ii) the sensor location $x = \xi$ does not correspond to any root of the first N eigenfunctions $\Phi_k, k = 1, \ldots, N$ of A_c, and

(iii) the modal gains $l_{\xi,k}, k = 1, \ldots, N$ are chosen so that

$$\lambda^* \leq \lambda_{N+1} \tag{4.43}$$

where λ^* is the maximal eigenvalue of the matrix $A_L^s = A_c^s - L_N C^s$ (4.34).

(*Proof in Appendix G.*)

Before this result is discussed, its counterpart corresponding to the pointwise injection mechanism (4.35) is presented.

(B) Point injection - variational approach

Next, the convergence criteria are drawn which correspond to the bound (4.36) for the dissipation component $\mathcal{D}_T$ corresponding to the linear dynamical subsystem (4.8) with the point injection structure (4.35).

In virtue of the expression (4.36) and (4.19) for the dissipation component $\mathcal{D}_T$ of the linear transport subsystem subject to to the point correction mechanism (4.35), and the dissipation $\mathcal{D}_K$ of the nonlinear static kinetic subsystem, respectively, the dissipation according to the energy (4.13) can be written as an integral quadratic

form

$$\frac{dE}{dt} \leq -\int_0^1 \varpi^T Q \varpi dx, \tag{4.44}$$

with the vector

$$\varpi = [e(x,t),\, e(0,t),\, \rho(c;e),\, e(\xi,t),\, e(1,t)]^T \tag{4.45}$$

and the matrix valued function

$$\begin{aligned}
\bar{Q} &\triangleq \begin{bmatrix} D[w] & \frac{w_{\min}\pi}{2P_{ec}} & 0 & 0 \\ \frac{w_{\min}\pi}{2P_{ec}} & \mathcal{R}_0 & 0 & 0 \\ 0 & 0 & \mathcal{R}_1 & 0 \\ 0 & 0 & 0 & l_\xi^0 w(\xi) \end{bmatrix} \\
D[w] &= -\frac{d^2w}{dx^2} - P_e\frac{dw}{dx} + \frac{w_{\min}\pi}{2P_{ec}} \\
\mathcal{R}_0 &= \frac{1}{P_{ec}}\frac{dw}{dx}(0) + \frac{2-2l_0-P_{ec}}{P_{ec}}w(0) + \frac{w_{\min}\pi}{2P_{ec}} \\
\mathcal{R}_1 &= \frac{1}{P_{ec}}\frac{dw}{dx}(1) + \frac{2l_1+P_{ec}}{P_{ec}}w(1).
\end{aligned} \tag{4.46}$$

Correspondingly, if one can ensure the strict dissipation (4.40) based on the given bound (4.44) for the dissipation component $\mathcal{D}_T$ corresponding to the proposed data-assimilation scheme, one can ensure the exponential stability of the estimation error zero solution $e(x,t) = 0$ in terms of the systems transport and kinetic parameters and the observer injection gains.

Theorem 4.2. *Consider the isothermal tubular reactor (4.1)-(4.2), together with the dissipative observer (4.4)-(4.5), with point correction injection $l_\xi = \delta(x-\xi)l_\xi^0$ corresponding to (4.35). Let $s_l = \min \dfrac{\partial r}{\partial c}$, and $s_u = \max \dfrac{\partial r}{\partial c}$ be the minimal and the maximal slope of the reaction rate r, respectively, and let $\lambda > 0$ be a constant. If there exists a ($\mathcal{C}^2$) function $w(x) > 0$, a function $h(x) > 0$, and gains l_0, l_ξ^2, l_1 such that it holds*

$$Q > diag(2\lambda w, 0, 0, 0, 0), \tag{4.47}$$

where Q is the matrix-valued function given in (4.46), then the estimation error zero

solution $e(x,t) = 0$ *is g.e.s., i.e.*

$$||e(x,t)|| \leq a\,||e_0(x)||\,e^{-\lambda t}, \tag{4.48}$$

with $a = \sqrt{w^*/w_*}$, $w^* = \max_{x\in[0,1]} w(x)$ *and* $w_* = \min_{x\in[0,1]} w(x)$.

(*Proof in Appendix H.*)

Note that, choosing a particular function $w(x)$, the condition (4.47) corresponds to a LMI for each point $x \in [0,1]$. Thus, finding a $w(x) >$ so that $D[w] > 2\lambda w$, one obtains the following explicit solvability conditions in terms of the system parameters and the correction gains.

Proposition 4.1. *The estimation error dynamics (4.6) has g.e.s. zero solution* $e(x,t) = 0$*, if the following conditions on the system parameters and the measurement injection gains are satisfied:*

$$\begin{array}{l}(i)\, P_{ec} \geq \iota_1(s_u, s_l, D_a, \lambda), \quad (ii)\, l_0 < \iota_2(P_{ec}, s_u, s_l, D_a, \lambda) \\ (iii)\, l_\xi^0 > 0, \quad (iv)\, l_1 > \iota_3(P_{ec}, s_u, s_l, D_a, \lambda),\end{array} \tag{4.49}$$

with $w(x)$ *being the weighting function given by*

$$w(x) = w_0 e^{-P_{ec}x/2} cosh\left(\sqrt{\frac{P_e^2}{4} - P_e\left(2\lambda - s_l s_u + \frac{(2D_a - [s_l + s_u])^2}{4}\right)}x\right), \tag{4.50}$$

$w_* = \min_{x\in[0,1]} w(x)$*, and* $\iota_1, \ldots, \iota_3$ *bounded functions of its arguments according to*

$$\begin{aligned}\iota_1 &\triangleq 8\lambda - 4s_l s_u + (2D_a - [s_l + s_u])^2 \\ \iota_2 &\triangleq \frac{2w_* - \dfrac{dw}{dx}(0)}{w(0)} \\ \iota_3 &\triangleq -w(1)\frac{dw}{dx}(1) - P_{ec}.\end{aligned}$$

(*Proof in Appendix I.*)

Corresponding to the differences identified for the bounds (4.33) and (4.36) for the linear transport dissipation component $\mathcal{D}_T$, the obtained convergence criteria present similar differences. A short discussion of this issue is given in the next section.

4.3 Discussion of the results

4.3.1 General Considerations

Using the modal and point injection mechanisms it has been shown, that one can find explicit conditions which ensure the exponential convergence with rate λ in dependence on (i) the system transport and kinetic parameters, (ii) the sensor location, and (iii) the observer gains.

In comparison to a natural dissipation mechanism (corresponding to the case that all gains are set to zero), one can see that the dissipation and thus the convergence can be improved by choosing the corresponding observer gains according to the presented conditions. According to the preceding studies on this subject, reported in the literature, the presented results yield interesting contributions.

It turned out, that the convergence conditions can be represented in form of space-dependent LMIs. This issue allows a systematic approach to the solution of the design problem, but it should be mentioned here, that the solution of general space-dependent LMIs is a non-trivial task, in the understanding that the classical problem does not consider this case [99]. In particular, if there are several state variables, the corresponding LMIs become difficult to solve. For instance, one can approach the solution of the integral LMIs (4.33) and (4.36) by maximization algorithms in the understanding of a variational calculus, seeking to find an optimal weighting function $h(x) > 0$, but this is an issue which should be addressed in future studies.

For the particular result based on the modal injection (4.26), the injection gains in the boundary were set to zero. This condition is not necessary, but allows to focuss the main attention on the action of the distributed modal innovation mechanism. Effectively, the boundary injection gains can be shown to enable a dominant eigenvalue shift of about $-3\pi^2/4$. Therefore, the consideration of boundary injection gains for the eigenvalue-reassignment allows an interesting degree of freedom, in particular for processes which are diffusion dominated (low Peclet numbers). For a convection dominated process, it results that the eigenvalues are thus negative, that shifting them about $\pi/2$ does not provoke an important change from a frequency analysis point of view [26, 100]. On the other hand, from the variational approach it results that the effect of the boundary injection gains may cause additional improvement which is not directly reflected in the linear eigenvalue decomposition approach.

The modal injection is particularly useful if the Peclet-number is small, be-

cause, as mentioned above, the eigenvalue distribution of the corresponding linear diffusive-convective transport operator with Danckwert's boundary conditions can be improved using low gain correction injections. This becomes clear when considering that the eigenvalues λ_n of A_c correspond to the relation

$$\lambda_n = -\frac{P_{ec}^2 + 4\omega_n^2}{4P_{ec}}, \tag{4.51}$$

and the corresponding eigenfrequencies ω_n satisfy bounds of the following type (see Appendix J for a derivation)

$$\begin{aligned} 0 \leq &\omega_1 \leq \pi \\ (n-1)\pi \leq &\omega_n \leq n\pi. \end{aligned} \tag{4.52}$$

Accordingly, the difference between the eigenvalues is basically bounded by the number π, while the location of the eigenvalues is determined by the square of the Peclet number. This implies that for high Peclet numbers the innovation gains would have to be great in order to perform a significant change in the convergence behavior.

In the light of this basic restriction, the point injection in the domain allows for a performance improvement even in the case of convection-dominated scenarios (high Peclet-numbers), in particular when considering several measurements in the domain, as will become clear in the numerical application study at the end of this chapter.

From the variational approach it follows in particular, that there is an intrinsic interplay of the injection mechanism at the inlet ($e(0,t)$) with the behavior of the dissipation in the estimation error profile ($e(x,t)$) and the reaction rate estimation error (ρ).

The weighting function (4.50) differs from the conventional exponential weighting (4.21) for pure transport dynamics. This difference consists in the reaction rate-dependent term connecting the transport with the reaction specific time measures, and further the sector bounds of the nonlinearity. The consideration of this weighting function thus permits to identify the regions with strong influence on the over all dissipation, and those with less influence. This particular issue should be studied in future work with more detail, in the light of a possible transfer of convergence intensity superhavit to regions with convergence deficit.

The region characterized by condition (i) in (4.49) can be graphically represented

in the (P_e, D_a)-plane. The basic interrelation of these two parameters according to the given condition is presented in Figure 4.2 for the case that the sum $s_l + s_u$

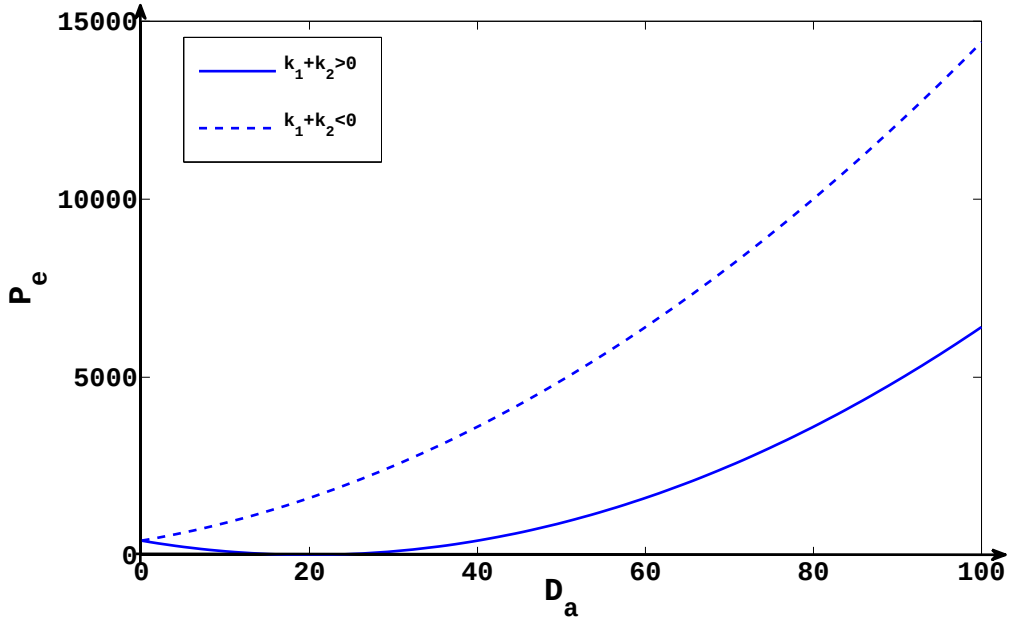

Figure 4.2: Feasibility regions according to condition (I.4). The possible constellations correspond to points above the drawn lines. $--$ (solid line) $s_l + s_u > 0$, $- -$ (dashed line) $s_l + s_u < 0$.

is (i) positive (solid line), corresponding to a monotonic or a weakly non-isotonic kinetics (the negative gain is less than the positive one), and (ii) negative (dashed line), corresponding to strongly non-isotonic kinetics (the negative slope is greater than the positive one). One appreciates, that for a monotonic kinetics ($s_u s_l > 0$) the condition on the required Peclet-number (proportional to the fluid velocity v and inversely proportional to the diffusion coefficient D) is weaker than for the non-monotonic case. This observation corresponds to the fact that the non-monotonicity feature of the reaction rate introduces destabilizing effects to the estimation error dynamics, and consequently, the dissipation of the linear mass transport subsystem Σ_M has to be stronger, in order to compensate the dissipation deficit of the nonlinear kinetic subsystem Σ_K

It is important to remark that the present assumption of isothermal reaction can be relaxed by assuming the temperature profile to be known. This assumption can be found frequently in the literature on tubular reactor observers [42, 46, 47, 49], where it is based on the application of many temperature sensors between which the

profile is interpolated. A more physical cause for a completely known temperature profile is given for the case of high thermal conductivity in the reaction mixture and short reactor extensions, yielding an almost homogeneous spatial temperature profile. Accordingly, measuring the temperature at any point of the reactor extension yields the same temperature trajectory. In either of these cases the reaction proportionality factor will be (possibly) space-dependent. This change has no major implications on the design methodology proposed here, because the nonlinear reaction rate error function is bounded via the employment of the spatially weighted sector condition (4.18).

4.3.2 Behavior with modelling and measurement errors

It is widely known, that for real-world applications, and in particular for those in chemical, biological, and biochemical engineering, one has to expect errors and disturbances in: (i) the system parameters, and in particular in the reaction rate parameters p_r, i.e. $\tilde{p}_r$, (ii) the measurement $\tilde{y}$, due to noise and a standard (about 1-2%) uncertainty, and (iii) exogenous load (feed) disturbances due to temporal variations and uncertainties in the feed concentration $\tilde{c}_{in}(t)$. It is straight-forward to consider parameter ($\tilde{p}_r$) and measurement ($\tilde{y}$) errors in the above framework, and this issue is analyzed in this section. The consideration of feed (exogenous load) disturbances can be modelled in the present case in form of a time-varying disturbance ($\tilde{c}_{in}$) acting only in the inlet $x = 0$. Accordingly, assuming the above nominal (i.e. errorless) strict dissipation $\dot{E} \leq -\lambda E$ for some $\lambda > 0$, the consideration of the mentioned errors yields the corresponding dissipation of the estimation error

$$\frac{dE}{dt} \leq -\lambda E + \int_0^1 w(x) \left[l_\xi \tilde{y} - D_a e(x,t) \tilde{r}(c(x,t); \tilde{p}_r) \right] dx + e(0,t) w(0) \tilde{c}_{in}(t). \quad (4.53)$$

Correspondingly, one notices that: (i) the estimation error dynamics is ISS [72, 73] with respect to these parameter errors (in the sense of norm-convergence), (ii) the measurement noise is injected proportionally, according to the chosen correction mechanism, (iii) the reaction parameter offset $\tilde{p}_r$ yields a spatio-temporally varying linear offset function, and (iv) the time-varying exogenous load (feed) disturbance of the inlet concentration $\tilde{c}_{in}$ yields a time-varying offset. These disturbances imply the following:

- if the innovation gain is chosen too large, the amplified measurement noise may

destroy the convergence properties.

- the reaction parameter error yields a spatio-temporally varying linear gain (k_p) disturbance which implies the existence of a ball around the origin (with radius proportional to the linear gain k_p), to which the estimation error will converge, but which is impossible to be penetrated.

- the time-varying exogenous load (feed concentration) error yields an offset, which can not be removed by the considered estimation scheme. This means that the convergence in norm will nether reach the origin completely.

From these basic considerations, the following requirements are deduced for an application in a realistic scenario: (i) the innovation structure and the corresponding gains, and, in particular, the sensor location, play a key role in the possible performance attainable with the observer, (ii) the reaction approximation should be iteratively improved by repeated product quality monitoring, so that the constant parameter offset reduces, and furthermore, the sensor location should be chosen so that the region of maximal reaction rate error can be dominated, and (iii) the load disturbance size has to be normally sufficiently small, so that the time-varying offset will not destroy the performance.

These considerations suggest that a practical convergence can be obtained by adequately choosing: (i) the innovation structure in dependence on system parameters (over all the (Peclet,Damköhler)-number pair (P_e, D_a)), (ii) the sensor location $\xi \in (0, 1)$ according to simulation studies with considerable modeling and measurement errors, and (iii) gain tuning in the light of a suitable compromise between convergence speed and robustness.

4.4 Application Example

In order to illustrate the convergence behavior of the dissipative observer for a critical case, a non-monotonic (non-isotonic) Langmuir-Hinshelwood (LH) type kinetics [18, 19] is considered, in the understanding that: (i) non-isotonical kinetics imply a difficult observation problem because of the presence of destabilizing regions corresponding to certain estimation error regimes, (i) the non-monotonicity feature is characterized by different signs of the reaction rate slope and accordingly the dissipation expression proportional to $s_l s_u$ represents an inherent burden in the strict

dissipation assessment, and (iii) it permits to understand the principal mechanism for monotonic kinetics too, as they present, particular limit cases of the non-monotonic ones.

The LH (in a biological context also known as Haldane) kinetics is analytically given by [18, 19] (compare Section 3.5.5)

$$r(c,\sigma) = \frac{c}{(1+\sigma c)^2}, \tag{4.54}$$

where σ is the inhibition coefficient. A local (pointwise) sector for this kinetics, which can be determined by application of the mean value theorem, is given by

$$\int_0^1 h(x)\left(s_u e_c - \rho(c;e_c)\right)\left(\rho(c;e_c) - s_l e_c\right) dx \geq 0, \tag{4.55}$$

where $s_l = \min r_c = -\dfrac{1}{27}$ and $s_u = \max r_c = 1$. The negative lower bound characterizes the non-monotonicity feature of the reaction kinetics $r(c,\sigma)$ (4.54). Simulation studies for the proposed observer with this reaction rate expression have been carried out considering different regimes of parameters: (i) a diffusion dominated behavior (packed-bed) corresponding to $(P_e,\sigma,D_a) = (10,3,10)$ and (ii) a more convection dominated (open-tube) corresponding to $(P_e,\sigma,D_a) = (100,3,10)$. For either of these cases the nominal (errorless) and robust (considering errors $\tilde{\sigma},\tilde{y}$ and exogenous disturbances $\tilde{c}_{in}$) convergence behavior is tested for initial conditions around the concentration with maximal reaction rate, one in the increasing and one in the decreasing branch of the reaction kinetics.

4.4.1 Dissipative observer with modal injection

The effect of distributed modal injection with one single point measurement in the domain $\xi \in (0,1)$ is compared with the behavior of a simple system copy (natural error dissipation) to see the convergence improvement. Furthermore the robust convergence behavior is tested, considering parameter $(\tilde{k},\tilde{\sigma})$, and measurement $\tilde{y}$ errors and exogenous disturbances $\tilde{c}_{in}$, which have to be expected in practical applications. Based on the consideration of such errors the sensor location has been varied in various simulations and the best obtained results are presented suggesting the localization of the sensor in the first third of the reactor extension (compare e.g. the suggestion in [46]).

Convergence without modelling and measurement errors

Simulation results for the case that the process is diffusion-dominated $(P_e, \sigma, D_a) = (10, 3, 10)$, with initial conditions $[c_0(x),\ \hat{c}(0)(x)] = [0.2,\ 0.7]$ are presented in Figure 4.3. The simulation at the top corresponds to a pure system response (i.e. the observer gains are all set to zero). In the graphics at the bottom one appreciated the behavior corresponding to a modal injection of the measurement located in $\xi = 0.3$. Considering that the corresponding eigenvalues λ_k are given in correspondence to the expression (4.56) in dependence on the eigenfrequencies ω_k (4.57)

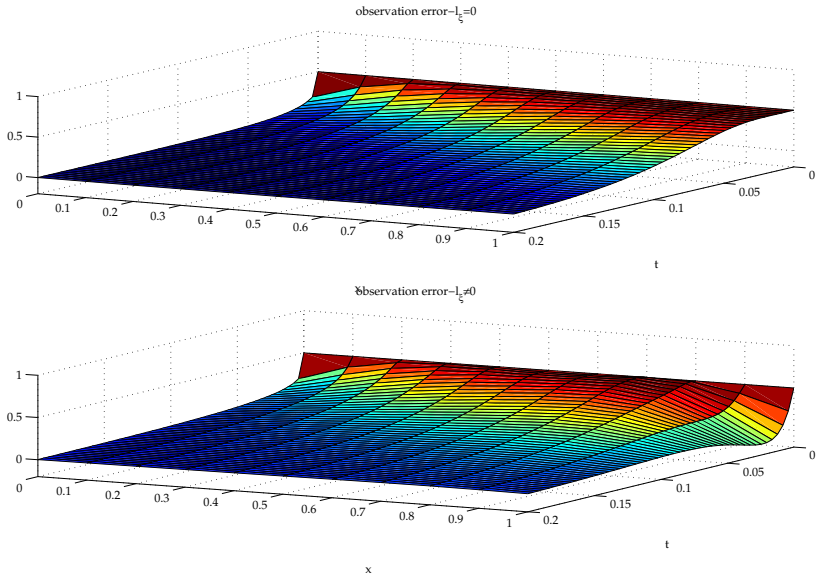

Figure 4.3: Estimation error behavior with exact (errorless) model for diffusion-dominated scenario $(P_e, \sigma, D_a) = (10, 3, 10)$ and [top] $l_\xi = 0$ (natural system response), and [bottom] measurement (in $\xi = 0.3$) injection over the first four eigenmodes with corresponding modal injection gains $l_{\xi,k} = 75, k = 1, \ldots, 4$.

$$\lambda_k = -\frac{P_e^2}{4} - \omega_k^2 \tag{4.56}$$

$$\cot(\omega_k) = \frac{4\omega_k^2 - P_e^2}{4P_e\omega_k}, \tag{4.57}$$

(see Appendix J), one can see that it is sufficient to innovated over the first $N = 4$ modes. The corresponding modal gains have been chosen all equal to $l_{\xi,k} = 75$. Analyzing the presented behavior one notices that: (i) the convergence is wave-like, from the inlet towards the outlet of the reactor, and (ii) the innovated convergence

behavior shortens the convergence time of about two times. The sensor location was determined through numerical simulations to obtain the best convergence behavior.

For high Peclet-numbers $P_e \geq 20$, the eigenvalues are very great $\lambda_1 \approx 20^2/4 = 100$, in correspondence to (4.56), and the natural solution accordingly decreases exponentially with rate about λ_1. Consequently, an important improvement is only possible using very high injection gains, what on the other hand implies a lost of robustness issues with respect to realistic measurement errors (the error $\tilde{y}$ is amplified proportional to the injection gain).

Convergence with modelling and measurement errors

In order to expose the observer behavior to a sever test, parameter errors in the reaction rate are considered about $(\Delta k, \Delta\sigma) = (+20\%, -30\%)$ and measurement errors with superposed noise are imposed, considering $\Delta y = 2\%$ and noise frequencies simulated by a high-frequency sinus (periodicity of $\pi/50$).

Figure 4.4 shows the corresponding simulation results for the case that the process is diffusion dominated $(P_e, \sigma, D_a) = (10, 3, 10)$, with initial conditions $[c_0, \hat{c}(0)] = [0.31, 0.35]$ (i.e. around the concentration of maximum rate). One can see that the asymptotic offset of the natural system response is clearly diminished (about two times) and that the convergence speed-up is maintained. As mentioned above, for high Peclet-numbers $P_e \geq 20$, due to the corresponding eigenvalues $\lambda_1 < -100$, there is no realistic improvement possible, unless the employed gains are chosen thus high, that the considered realistic measurement uncertainty becomes amplified to much.

4.4.2 Dissipative observer with point injections

The corresponding results for point injections as proposed by the variational approach considering measurements at the boundary and in some point of the domain, is compared with the behavior of a simple system copy (natural error dissipation) to see the convergence improvement. Furthermore it is straight-forward to consider in the presented methodological framework more than one measurement and injection in the domain. The consideration of three such collocated measurement injections is presented for the analyzed cases in order to show how the performance can be further improved. Based on the consideration of modeling and measurement errors the sensor location has been varied in various simulations and the best obtained results are presented.

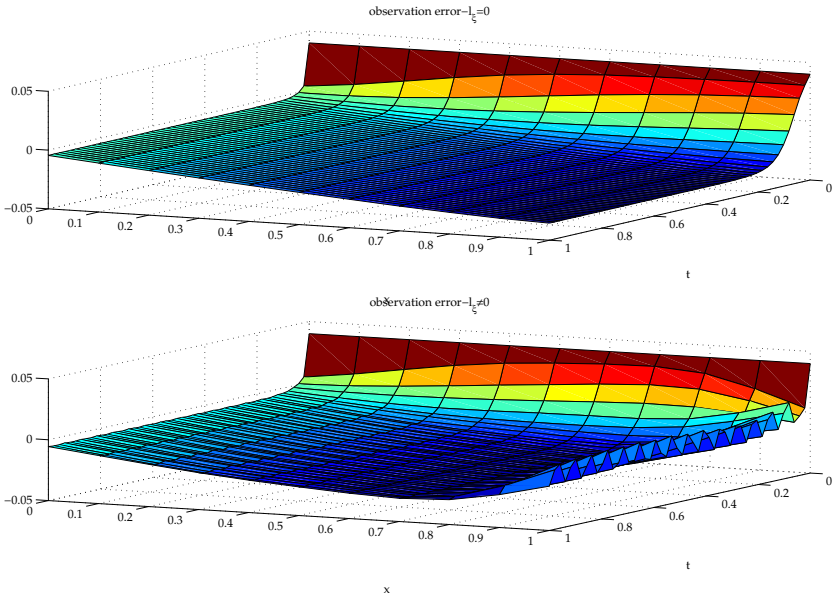

Figure 4.4: Estimation error behavior with kinetic parameter errors $(\Delta k, \Delta\sigma) = (+20\%, -30\%)$ and high-frequency measurement noise. Simulation results for diffusion-dominated scenario $(P_e, \sigma, D_a) = (10, 3, 10)$ and [top] $l_\xi = 0$ (natural system response), and [bottom] measurement (in $\xi = 0.3$) injection over the first four eigenmodes with corresponding modal injection gains $l_{\xi,k} = 75, k = 1, \ldots, 4$.

Convergence without modeling and measurement errors

Simulation results for the case that the process is diffusion-dominated $(P_e, \sigma, D_a) = (10, 3, 10)$, with initial conditions $[c_0(x),\ \hat{c}(0)(x)] = [0.2,\ 0.7]$ are presented in Figure 4.5. The graphic at the top shows the response considering a pure system copy (all observer gains are set to zero). In the center one appreciates the consideration of measurement injection at the boundaries $x = 0, 1$ and in the domain $(\xi = 0.35)$. The corresponding gain triplet used for this simulation is given by $(k_0, k_\xi, s_l) = (0.1, -50, -10)$. Analyzing the presented behavior one notices that: (i) the natural convergence is wave-like, from the inlet towards the outlet of the reactor, (ii) the innovated convergence behavior shortens the convergence time of about two times by shortening the distance which the information has to pass. The graphic at the bottom represents the consideration of three collocated measurement point injections in the domain whose location was determined through numerical simulations. One notices a clear convergence speed-up of about two times compared with the consideration of one single point measurement injection in the domain.

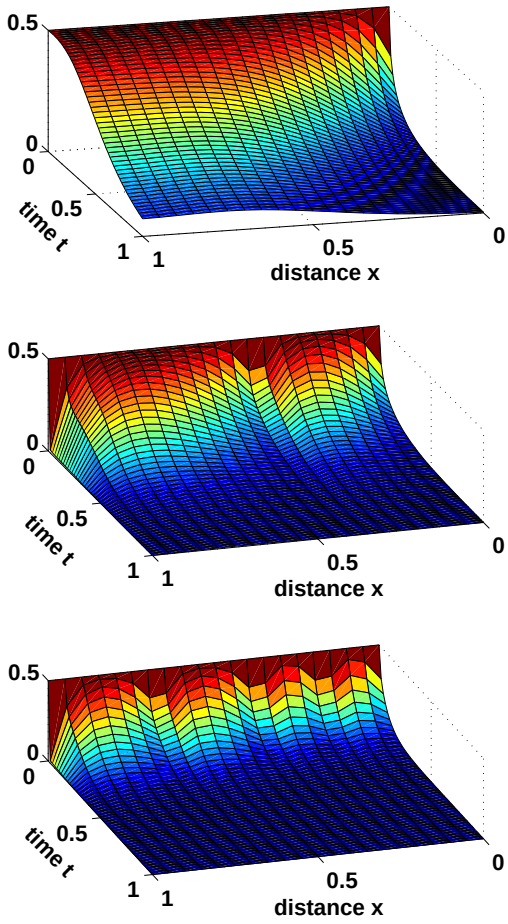

Figure 4.5: Estimation error behavior with exact model for diffusion-dominated scenario $(P_e, \sigma, D_a) = (10, 3, 10)$ and [top] $(k_0, k_\xi, k_1) = (0, 0, 0)$ (natural system response), [center] measurement injection at the boundaries and in $\xi = 0.35$ with $(k_0, k_\xi, k_1) = (0.1, -50, 10)$, [bottom] measurement injection at the boundaries and in three points in the domain $\xi_1 = 0.15, \xi_2 = 0.35, \xi_3 = 0.65$ and corresponding gains $(k_0, k_{\xi 1}, k_{\xi 2}, k_{\xi 3}, k_1) = (0.1, -50, -50, -50, -10)$.

A convection-dominated scenario with $(P_e, \sigma, D_a) = (100, 3, 10)$ is analyzed in comparison and the results are presented in Figure 4.6. In the graphic at the top, one can appreciate a more shock-wave-like convergence propagation from the inlet towards the outlet of the reactor. As can be noticed in the graphic in the center, the convergence is speed up about two times by shortening the wave-expansion time considering a measurement injection in $\xi = 0.35$. The location of the sensor is chosen

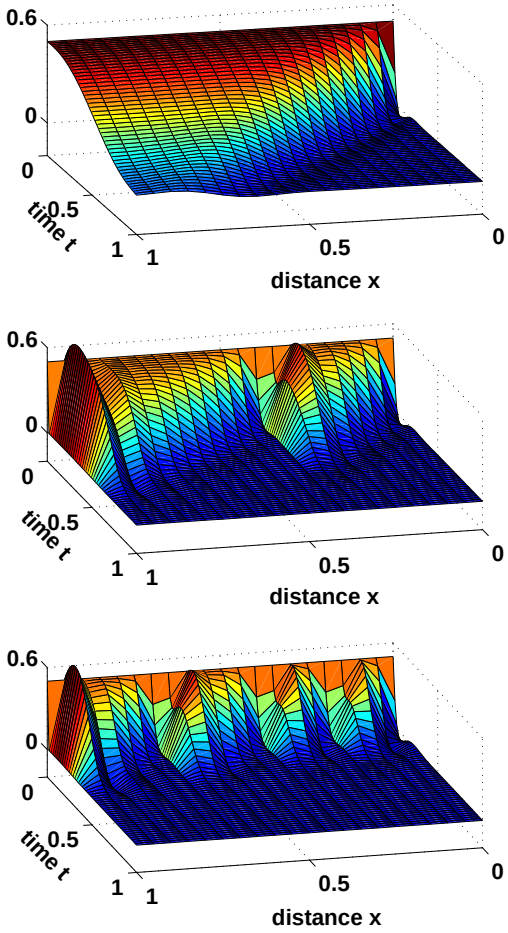

Figure 4.6: Estimation error behavior with exact model for convection-dominated scenario $(P_e, \sigma, D_a) = (100, 3, 10)$ and [top] $(k_0, k_\xi, k_1) = (0, 0, 0)$ (natural system response), [center] measurement injection at the boundaries and in $\xi = 0.35$ with $(k_0, k_\xi, k_1) = (0.1, -50, 10)$, [bottom] measurement injection at the boundaries and in three points in the domain $\xi_1 = 0.15, \xi_2 = 0.35, \xi_3 = 0.65$ and corresponding gains $(k_0, k_{\xi 1}, k_{\xi 2}, k_{\xi 3}, k_1) = (0.1, -50, -50, -50, -10)$.

through numerical simulations such that the propagation time from the injection towards the outlet of the reactor is already identical to the propagation time from the inlet towards the injection. This ensures the present convergence speed-up. Considering more than one measurement injection these propagation times can be shorten and the convergence can be speed up even more, as can be appreciated in the graphic at the bottom of Figure 4.6. The gain tuning has been carried out in correspondence

to the consideration of severe errors in the kinetics parameters, what is presented next.

Convergence with modeling and measurement errors

In order to expose the observer behavior to a sever test, parameter errors in the reaction rate are considered about $(\Delta k, \Delta\sigma) = (+20\%, -30\%)$ and measurement errors with superposed noise are imposed, considering $\Delta y = 2$ and different noise frequencies in each measurement following Table 4.1

measurement location	amplitude	frequency-expression
x=0	2%	$\cos(25t)$
x=0.15	2%	$\cos(30t)$
x=0.35	2%	$\sin(35t)$
x=0.65	2%	$\sin(35t)$
x=1	2%	$\sin(35t)$

Table 4.1: Considered amplitude and frequency for noise simulation at the different measurement points.

Figure 4.7 shows the corresponding simulation results for the case that the process is diffusion dominated $(P_e, k, \sigma) = (10, 3, 10)$, with initial conditions $[c_0(x), \hat{c}(0)(x)] = [0.31, 0.35]$ (i.e. around the concentration of maximum rate). One can see that the asymptotic offset of the natural system response is clearly diminished (about two times) and the consideration of more measurement injections reduces this offset even more.

Figure 4.8 shows the corresponding simulation results for the case that the process is convection dominated $(P_e, k, \sigma) = (100, 3, 10)$. It can be noticed that the improvement of the robust convergence behavior remains like in the diffusion dominated case. In comparison with the diffusion dominated behavior the strong convective phenomena sharpen the profile near the peaks due to the strong shock-wave-like convergence distribution from the inlet towards the outlet superposed with the reactive error propagation.

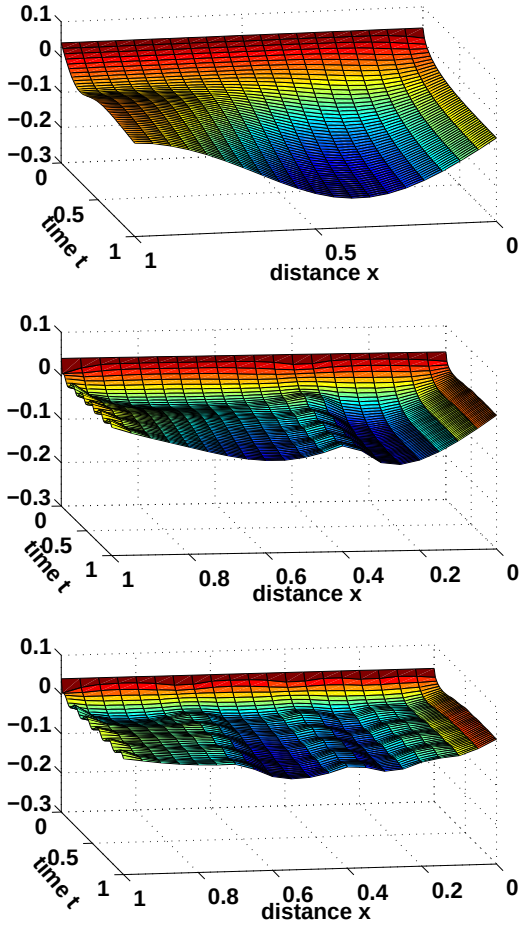

Figure 4.7: Estimation error behavior with kinetic parameter errors $(\Delta k, \Delta\sigma) = (+20\%, -30\%)$ and measurement noise according to Table 4.1. Simulation results for diffusion-dominated scenario $(P_e, \sigma, D_a) = (10, 3, 10)$ and [top] $(k_0, k_\xi, k_1) = (0, 0, 0)$ (natural system response), [center] measurement injection at the boundaries and in $\xi = 0.35$ with $(k_0, k_\xi, k_1) = (0.1, -50, 10)$, [bottom] measurement injection at the boundaries and in three points in the domain $\xi_1 = 0.15, \xi_2 = 0.35, \xi_3 = 0.65$ and corresponding gains $(k_0, k_{\xi 1}, k_{\xi 2}, k_{\xi 3}, k_1) = (0.1, -50, -50, -50, -10)$..

Concluding remarks

The presented simulation studies show that (i) for small Peclet-numbers, say $P_e \leq 20$, the domain injection improves the convergence behavior and (ii) there is a clear wave-like convergence propagation (information propagates up- and downstream), (iii) for both, low and high Peclet-numbers, the point correction mechanism

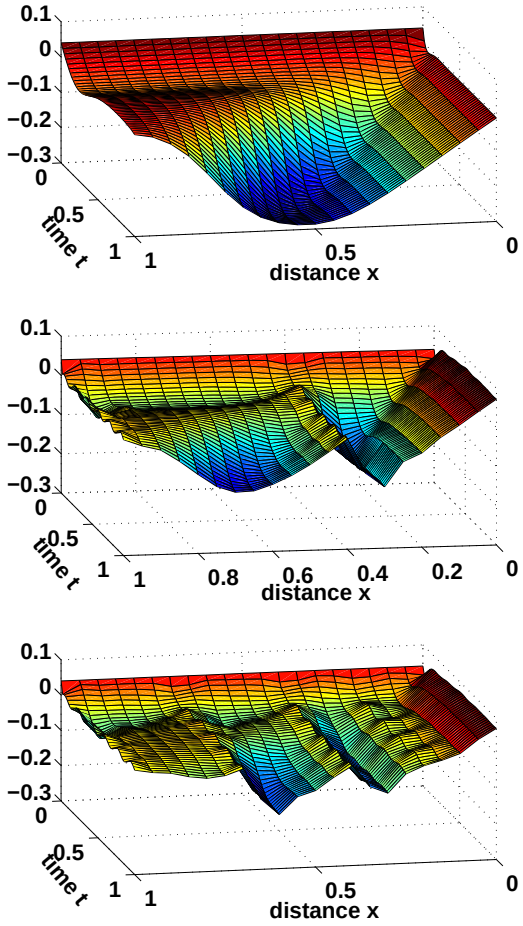

Figure 4.8: Estimation error behavior with kinetic parameter errors $(\Delta k, \Delta\sigma) = (+20\%, -30\%)$ and measurement noise according to Table 4.1. Simulation results for convection-dominated scenario $(P_e, \sigma, D_a) = (100, 3, 10)$ and [top] $(k_0, k_\xi, k_1) = (0, 0, 0)$ (natural system response), [center] measurement injection at the boundaries and in $\xi = 0.35$ with $(k_0, k_\xi, k_1) = (0.1, -50, 10)$, [bottom] measurement injection at the boundaries and in three points in the domain $\xi_1 = 0.15, \xi_2 = 0.35, \xi_3 = 0.65$ and corresponding gains $(k_0, k_{\xi 1}, k_{\xi 2}, k_{\xi 3}, k_1) = (0.1, -50, -50, -50, -10)$..

acts as a dissipating element in the specific injection point, and thus should be located, in accordance to numerical simulations, in the region of greatest dissipation deficit (according to the simulation studies this is in the first third of the reactor extension), (iv) for Peclet-numbers corresponding to convection-dominated transport behavior ($P_e > 20$) the domain point injection effectively allows to shorten the shock-

wave like convergence propagation and thus to significantly increment the convergence time. This motivates the employment of various measurements and injections in the domain, to improve the convergence behavior under realistic conditions.

4.5 Summary

In this chapter, the dissipative observer design methodology introduced for the non-isothermal CSTR with temperature measurement has been extended to the isothermal tubular reactor with point concentration measurements at the boundary and/ or in the domain. In comparison with previous studies on the estimation problem with similar dynamics (i) the presented observer allows for consideration of non-monotonic kinetic rates, (ii) enables a convergence improvement due to the distributed domain injection mechanism, and (iii) the methodological framework yields mathematical rigor and insight into the underlying interplay between kinetics, transport and injection as well as the influence of isotonicity features on the convergence properties.

Furthermore, the consideration of this problem allowed to address two particular issues:

- the extension of the analysis for the lumped transport mechanisms energy interchange properties to the case of diffusive-convective distributed transport
- the consideration of the influence of a distributed nonlinear reaction kinetic mechanism on the energy interchange behavior of the related estimation error dynamics.

These issues have been analyzed in detail and three main approaches have emerged from this study: two different data-assimilation structures and an innovating approach for the analysis of the distributed influence of the kinetic mechanism on the convergence behavior.

- A modal innovation mechanism has been designed which allowed to shape the dissipation of the squared estimation error energy corresponding to the dominant modes of the linear diffusive-convective transport.
- A point correction injection mechanism has been employed which, in dependence of the sensor location introduces a point-wise innovation to the estimation

error dynamics and showed to improve the convergence in a significant manner in numerical simulations.

- The employment of a spatially weighted integral sector condition together with the spatial weighting of the transport mechanism, show a structural requirement of geometrical character, which may allow to approach the complicated question of compensating regional differences of dissipation superhavit and deficit, in order to obtain an over-all, improved strict dissipation.

The results of this chapter, together with those of the preceding CSTR estimation study, form the basis for the following consideration of the estimation problem for the non-isothermal tubular reactor with point temperature measurements at the boundary and/ or in the domain.

Chapter 5

The Non-Isothermal Tubular Reactor

Based on the preceding non-isothermal continuous stirred and isothermal tubular reactor studies, in this chapter the dissipative observer design approach is extended to the non-isothermal tubular reactor with boundary and/ or domain point temperature measurements. Having as point of departure the preceding extension of the design methodology to the consideration of distributed transport and reaction mechanisms, the present study has to address two main issues:

- the analysis and exploitation of the underlying mechanisms in the light of regional convergence sources and sinks, for a possible compensation of regional convergence deficit by means of linear coupling with the mechanisms of convergence superhavit, i.e. the heat and mass transfer mechanisms

- the extension of the analysis framework used for the bounding of the dissipation of the nonlinear kinetic subsystem, to the consideration of nonlinear coupling of temperature and concentration dynamics through the kinetic mechanism.

For this aim, both approaches introduced for the isothermal tubular reactor with concentration measurements (spectral, and variational) are applied to obtain bounds for the dissipation corresponding to the linear transport mechanisms, and a Lipschitz-type sector condition is employed to bound the dissipation of the nonlinear kinetics mechanism.

In comparison to previous studies recorded in the literature, the resulting dissipative observer allows for considering monotonic or non-monotonic reaction kinetic

rates, requires only few temperature sensors, and satisfies basic design requirements with respect to (i) mathematical rigor, (ii) simple implementation, and (ii) convergence improvement.

The obtained dissipative observer is tested numerically considering a non-monotonic strongly exothermic Langmuir-Hinshelwood kinetics for different data-assimilation structures (modal, distributed and point injections), and parameter constellations covering strongly diffusive and strongly convective flow scenarios.

5.1 Introduction

In this chapter, the dissipative observer for the isothermal tubular reactor with boundary and/ or domain point concentration measurements is extended to the consideration of the non-isothermal tubular reactor with boundary and/ or domain point temperature measurements. Based on the preceding non-isothermal continuous stirred and isothermal tubular reactor, this extension has to consider two main issues:

- exploitation of the underlying mechanisms for compensation of regional convergence deficit by means of linear coupling of the temperature and concentration dynamics through the correction mechanism
- extending the analysis for the consideration of nonlinear coupling of the temperature and concentration dynamics through the kinetic mechanism.[1]

The dynamics of the non-isothermal tubular reactor with boundary and/ or domain point temperature measurements are governed by

$$\begin{array}{l} \dfrac{\partial c}{\partial t} = \dfrac{1}{P_{ec}}\dfrac{\partial^2 c}{\partial x^2} - \dfrac{\partial c}{\partial x} - D_a r(c,T) \\ \dfrac{\partial T}{\partial t} = \dfrac{L_e}{P_{eT}}\dfrac{\partial^2 T}{\partial x^2} - L_e\dfrac{\partial T}{\partial x} - \eta(T_j - T) + \beta D_a r(c,T) \end{array}, \tag{5.1}$$

for $x \in (0,1)$, $t > 0$, with boundary conditions

$$x = 0 : \frac{1}{P_{ec}}\frac{\partial c}{\partial \xi} = c - c_{\in}, \quad \frac{1}{P_{eT}}\frac{\partial T}{\partial \xi} = T - T_{\in} \tag{5.2}$$

$$x = 1 : \frac{\partial c}{\partial x} = 0, \quad \frac{\partial T}{\partial x} = 0, \tag{5.3}$$

for $t \geq 0$, initial conditions $x \in [0, L] : c(x,0) = c_0(x), \quad T(x,0) = T_0(x)$, and measurement vector

$$y = [T(0,t),\, T(\xi,t),\, T(1,t)]^T, \quad \xi \in (0,1). \tag{5.4}$$

For this reactor a dissipative observer is designed in the sequel.

[1] Remember that in the previous studies, the sector conditions employed for bounding the dissipation of the nonlinear kinetic subsystem did only depend on the concentration and not on temperature.

5.2 Dissipative Observer

In this section, a dissipative observer is designed for the estimation of the concentration and temperature profile for the non-isothermal tubular reactor (5.1)-(5.4) with boundary and/ or domain point temperature measurements.

5.2.1 Observer Construction

In the previous isothermal tubular reactor study it turned out that the domain correction mechanism represents an important design degree of freedom. For this reason, the dissipative observer is set with simple and constant, linear gains for the boundary correction mechanisms and a general injection mechanism for the concentration and temperature correction in the domain. Correspondingly, the dissipative observer is given by

$$\begin{aligned} \frac{\partial \hat{c}}{\partial t} &= \frac{1}{P_{ec}}\frac{\partial^2 \hat{c}}{\partial x^2} - \frac{\partial \hat{c}}{\partial x} - D_a r(\hat{c},\hat{T}) - l_{c,\xi}(\hat{T}(\xi,t) - y_2(t)) \\ \frac{\partial \hat{T}}{\partial t} &= \frac{L_e}{P_{eT}}\frac{\partial^2 \hat{T}}{\partial x^2} - L_e\frac{\partial \hat{T}}{\partial x} - \eta(T_j - \hat{T}) + \beta D_a r(\hat{c},\hat{T}) - l_{T,\xi}(\hat{T}(\xi,t) - y_2(t)) \end{aligned}, \quad (5.5)$$

for $x \in (0,1)$, $t > 0$, with boundary conditions

$$\begin{aligned} x = 0: \quad & \frac{1}{P_{ec}}\frac{\partial \hat{c}}{\partial x} = \hat{c} - c_{\in} - l_{c,0}(\hat{T}(0,t) - y_1(t)) \\ & \frac{1}{P_{eT}}\frac{\partial \hat{T}}{\partial x} = \hat{T} - T_{\in} - l_{T,0}(\hat{T}(0,t) - y_1(t)), \\ x = 1: \quad & \frac{\partial \hat{c}}{\partial x} = -l_{c,1}(\hat{T}(1,t) - y_3(t)) \\ & \frac{\partial \hat{T}}{\partial x} = -l_{T,1}(\hat{T}(1,t) - y_3(t)), \end{aligned} \quad (5.6)$$

for $t \geq 0$, and initial conditions $x \in [0,L]: \hat{c}(x,0) = \hat{c}_0(x), \quad \hat{T}(x,0) = \hat{T}_0(x)$.

Correspondingly, the design degrees of freedom for the dissipative non-isothermal tubular reactor observer are (i) the gains $l_{c0}, l_{c1}, l_{T0}, l_{T1}$ of the boundary injections, (ii) the sensor location $\xi \in (0,1)$ for the temperature measurement y_2 in the domain, and (iii) the structure $l_{c,xi}, l_{T,\xi}$ used for the data-assimilation of the measurement in the domain.

5.2.2 Estimation Error Dynamics

The estimation error dynamics for the dissipative non-isothermal tubular reactor observer (5.5)-(5.6) is obtained from the subtraction of (5.1)-(5.2) from (5.5)-(5.6) ($e_c \triangleq \hat{c} - c$, $e_T \triangleq \hat{T} - T$)

$$\begin{array}{l} \dfrac{\partial e_c}{\partial t} = \dfrac{1}{P_{ec}}\dfrac{\partial^2 e_c}{\partial x^2} - \dfrac{\partial e_c}{\partial x} - D_a\left[r(\hat{c},\hat{T}) - r(c,T)\right] - l_{c,\xi}(\hat{T}(\xi,t) - y_2(t)) \\ \dfrac{\partial e_T}{\partial t} = \dfrac{L_e}{P_{eT}}\dfrac{\partial^2 e_T}{\partial x^2} - L_e\dfrac{\partial e_T}{\partial x} - \eta e_T + \beta D_a\left[r(\hat{c},\hat{T}) - r(c,T)\right] - l_{T,\xi}(\hat{T}(\xi,t) - y_2(t)) \end{array}, \tag{5.7}$$

for $x \in (0,1)$, $t > 0$, with boundary conditions

$$\begin{array}{lll} x = 0, & t \geq 0: & \dfrac{1}{P_{ec}}\dfrac{\partial e_c}{\partial x} = e_c - l_{c,0}(\hat{T}(0,t) - y_1(t)) \\ & & \dfrac{1}{P_{eT}}\dfrac{\partial e_T}{\partial x} = e_T - l_{T,0}(\hat{T}(0,t) - y_1(t)), \\ x = 1, & t \geq 0: & \dfrac{\partial e_c}{\partial x} = -l_{c,1}(\hat{T}(1,t) - y_3(t)) \\ & & \dfrac{\partial e_T}{\partial x} = -l_{T,1}(\hat{T}(1,t) - y_3(t)), \end{array} \tag{5.8}$$

and initial condition $x \in [0,L]: \; e_c(x,0) = e_{c,0}(x), \quad e_T(x,0) = e_{T,0}(x)$.

In the spirit of the estimation studies of the preceding chapters, two main components of the estimation error dynamics (5.7)-(5.8) are identified: (i) a linear dynamical subsystem representing the transport of heat and mass through the reactor, and (ii) a nonlinear static subsystem corresponding to the kinetic mechanism at play. Accordingly, the estimation error dynamics (5.7)-(5.8) can be expressed in Popov-Lur'e form for the vector profile $e = [e_c, \, e_T]^T$,

$$\frac{\partial e}{\partial t} = Ae + G\nu \tag{5.9}$$

$$\nu = -\rho(c,T;e), \tag{5.10}$$

for $e \in \mathrm{Dom}(A)$. Here, the linear transport operator A is given by

$$A = \begin{bmatrix} A_c & 0 \\ 0 & A_T \end{bmatrix} = \begin{bmatrix} \dfrac{1}{P_{e,c}}\dfrac{\partial^2}{\partial x^2} - \dfrac{\partial}{\partial x} & 0 \\ 0 & \dfrac{L_e}{P_{e,c}}\dfrac{\partial^2}{\partial x^2} - L_e\dfrac{\partial}{\partial x} - \eta \end{bmatrix}, \tag{5.11}$$

with domain of definition corresponding to the boundary conditions

$$\mathrm{Dom}(A) = \left\{ e = \begin{bmatrix} e_c \\ e_T \end{bmatrix} \in L^2([0,1], \Xi \subset \mathbb{R}^2) : e, \frac{\partial e}{\partial x} \text{ a.c., and (5.8) hold} \right\}, \quad (5.12)$$

kinetic gain vector

$$G = \begin{bmatrix} -D_a \\ \beta D_a \end{bmatrix}, \quad (5.13)$$

and nonlinear reaction rate error

$$\rho(c, T; e) \triangleq r(c + e_c, T + e_T) - r(c, T). \quad (5.14)$$

This dynamic interconnection is represented in form of a block diagram in Figure 5.1. One can see that the underlying interchange structure between the heat and mass transfer subsystem, and the nonlinear kinetic subsystem is basically the same as for the non-isothermal continuous stirred reactor (compare Figure 3.5). This results natural, taking into account that the non-isothermal continuous stirred reactor is the lumped counterpart of the non-isothermal tubular reactor [9].

5.2.3 Error Dissipation

Following the ideas of the preceding isothermal tubular reactor study, a Lyapunov-like approach (cp. [63, 65]) is employed for the exponential stability assessment. First, the dissipation components of the estimation error dynamics (5.7)-(5.8) are identified, then the corresponding dissipation expressions are bounded, and explicit convergence criteria are drawn.

Therefor, the potential (weighted squared error) energy

$$E(e) = \int_0^1 \left\{ w_1(x) e_c^2(x,t) + w_2 e_T^2(x,t) \right\} dx, \quad (5.15)$$

is introduced, where $w_1, w_2 > 0$ are positive definite continuously differentiable weighting functions, which represent important design degrees of freedom, as has turned out in the isothermal tubular reactor estimation study. Recall that, according to this previous study, these weighting functions should to be chosen in correspondence to the employed data-assimilation structure. The dissipation associated with

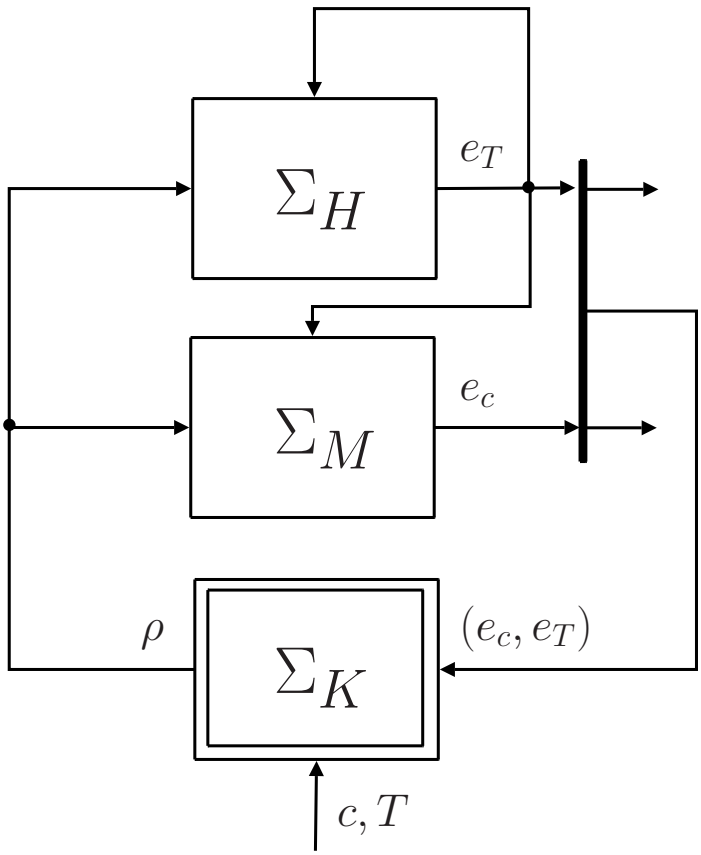

Figure 5.1: Basic dynamic interconnection of the estimation error dynamics (5.9), with
$\Sigma_H : \rho \mapsto \epsilon_T$, $\Sigma_M : (\rho, \epsilon_T) \mapsto \epsilon_c$, $\Sigma_K : (\epsilon_c, \epsilon_T, c, T) \mapsto \rho$..

(5.15) is given by the sum of the dissipation components $\mathcal{D}_K$, and $\mathcal{D}_T$, of the nonlinear kinetic subsystem and the linear dynamical transport subsystem, respectively, i.e.

$$\begin{aligned}
&\frac{dE(e)}{dt} = \mathcal{D}_K + \mathcal{D}_T \\
&\mathcal{D}_K = -2\int_0^1 \left\{-e(x,t)^T W G\rho(c,T;e)\right\} dx, \quad W = \mathrm{diag}(w_1, w_2), \\
&\mathcal{D}_T = -2\int_0^1 \left\{ \left[-\frac{1}{P_{ec}}\frac{\partial^2 e_c}{\partial x^2} + \frac{\partial e_c}{\partial x} + l_{\xi,c} e_T(\xi,t)\right] w_1 e_c + \right. \\
&\qquad \left. + \left[-\frac{L_e}{P_{eT}}\frac{\partial^2 e_T}{\partial x^2} + L_e\frac{\partial e_T}{\partial x} + \eta e_T + l_{\xi,T} e_T(\xi,t)\right] w_2 e_T \right\} dx.
\end{aligned} \tag{5.16}$$

In the sequel, quadratic bounds for these two components are drawn, extending the approach previously presented for the isothermal tubular reactor: (i) the nonlinear kinetic dissipation component $\mathcal{D}_K$ is bounded via employing a sector condition,

and (ii) the linear transport dissipation component $\mathcal{D}_T$ is bounded in dependence of the employed data-assimilation scheme. In the spirit of the preceding isothermal tubular reactor study, two different kinds of correction mechanisms are used: (A) a modal injection mechanism, analyzed correspondingly using a spectral decomposition, and (B) a coupled point and distributed injection mechanism, analyzed using direct functional analytic integral transformations.

Finally, combining the bounds for the nonlinear ($\mathcal{D}_K$) and linear transport ($\mathcal{D}_T$) dissipation components, conditions will be drawn which ensure the strict dissipation of the energy $E(e)$ (5.15), and therefore the exponential stability.

5.2.4 Quadratic bounds for the nonlinear kinetic dissipation component $\mathcal{D}_K$

The nonlinear kinetic dissipation component $\mathcal{D}_K$ is bounded using a Lipschitz sector condition for the nonlinear function ρ (5.14).

Note that the sector condition employed in the previous studies for the continuous stirred and the isothermal tubular reactor, can not be used here, because the nonlinear function ρ depends on two arguments, e_c and e_T. Therefore, a Lipschitz sector condition is employed, in the understanding that, due to the Lipschitz continuity of the reaction rate $r(c,T)$, with Lipschitz constant L_ρ, it follows directly that for all $x \in [0,1]$

$$\rho(z;e) \leq |\rho(z;e)| = |r(z+e) - r(z)| \leq L_\rho \, ||e|| \,, \tag{5.17}$$

and consequently the sector-type condition

$$(L_\rho \, ||e|| - \rho(z;e))(\rho(z;e) + L_\rho \, ||e||) \geq 0, \quad \forall x \in [0,1], \tag{5.18}$$

holds. This condition remains valid if one multiplies it in every point with a positive definite function $h(x) > 0$, i.e.

$$h(x)(L_\rho \, ||e|| - \rho(z;e))(\rho(z;e) + L_\rho \, ||e||) \geq 0, \quad \forall x \in [0,1],$$

and integrates over the spatial domain, yielding

$$\begin{aligned}\mathbb{S}_{h,L} &\triangleq \int_0^1 h(x)(L_\rho\,||e(x,t)|| - \rho(z(x,t);e(x,t)))(\rho(z(x,t);e(x,t)) + L_\rho\,||e(x,t)||)dx \\ &= \int_0^1 \begin{bmatrix} e(x,t) \\ \rho(z;e) \end{bmatrix}^T \begin{bmatrix} L_\rho^2 h(x) I_2 & 0 \\ 0 & -h(x) \end{bmatrix} \begin{bmatrix} e(x,t) \\ \rho(z;e) \end{bmatrix} dx \geq 0.\end{aligned} \tag{5.19}$$

Based on this structural property of the nonlinear kinetic function ρ, the following bound is obtained for the dissipation of the nonlinear kinetic mechanism

$$\mathcal{D}_K \leq -\int_0^1 \begin{bmatrix} e(x,t) \\ \rho(z;e) \end{bmatrix}^T \begin{bmatrix} -L_\rho^2 h(x) I_2 & -WG \\ -G^T W & h(x) \end{bmatrix} \begin{bmatrix} e(x,t) \\ \rho(z;e) \end{bmatrix} dx \tag{5.20}$$

These quadratic bounds allow to delimit the maximal destabilizing influence of the nonlinear kinetic mechanism, and, consequently, establishes the basis for the design of the dissipative observer, in the understanding that the functioning of the dissipative observer is motivated by on the transfer of convergence intensity superhavit to mechanisms and regions of convergence deficit. For this purpose, the next step to be addressed is given by the bounding of the linear innovated transport dynamic dissipation component of the estimation error dynamics.

5.2.5 Quadratic bounds for the linear transport dynamic dissipation component $\mathcal{D}_T$

Next, the linear dissipation component $\mathcal{D}_T$ is bounded. Recall that in the preceding study on the isothermal tubular reactor, the respective bound depended on the particular data-assimilation scheme employed in the correction mechanism in the domain. There, (A) a modal innovation and (B) a point innovation has been employed, and correspondingly different bounds for the linear dissipation have been found. Accordingly, the analysis presented here follows the same approach.

Note that the basic mass transport mechanism has already been analyzed previously in the isothermal tubular reactor estimation study. Furthermore, the structure of the linear heat transport subsystem, without the heat exchange component, is basically the same as the one of the mass transport analyzed in the previous chapter. The only difference thus resides in the heat exchange mechanism, but this

has been already analyzed in the CSTR estimation study of Chapter 3. In particular this implies that the spectral and variational approaches used to bound the dissipation component $\mathcal{D}_T$ in the preceding isothermal tubular reactor study, can be directly extended to the present case. The particular form, the linear dynamic transport dissipation component $\mathcal{D}_T$ attains, in correspondence to the choice of the data-assimilation structure, is presented in the following.

(A) Spectral Approach

On the basis of an eigenfunction-eigenvalue Fourier expansion of the linear transport subsystem of the estimation error dynamics (5.9), considering a modal innovation over the first N dominant modes of the temperature and concentration dynamics

$$\begin{aligned} l_\xi^c\left(\hat{T}(\xi,t)-y(t)\right) &= \sum_{k=1}^{\infty} l_{\xi,k}^c \varphi_{k,1}\left(\hat{T}(\xi,t)-y(t)\right) \\ l_\xi^T\left(\hat{T}(\xi,t)-y(t)\right) &= \sum_{k=1}^{\infty} l_{\xi,k}^T \varphi_{k,2}\left(\hat{T}(\xi,t)-y(t)\right), \end{aligned} \tag{5.21}$$

and setting the weighting function so that the linear heat and mass transport eigenfunctions are pairwise orthogonal (with respect to the corresponding weighted inner product) [92, 93, 95, 94], i.e.

$$w_1 = e^{-P_{e,c}x}, \quad w_2 = e^{-P_{e,T}x}, \tag{5.22}$$

one obtains the following bound for the dissipation of the linear subsystem.

Lemma 5.1. *For the modal injections (5.21), and weighting functions (5.22), the dissipation $\mathcal{D}_T$ of the linear transport subsystem $\Sigma_T(A,G)$ in (5.9) can be bounded as follows:*

$$\mathcal{D}_T \leq \max\{\lambda_{LN}^*,\, \lambda_{N+1,1},\, \lambda_{N+1,2}\}E, \tag{5.23}$$

where λ_{LN}^* is the maximal eigenvalue of the $2N \times 2N$ (constant coefficient) matrix

$\mathcal{M}_L^u$ *given by*

$$\mathcal{M}_L^u = \begin{bmatrix} M_{11} & M_{12} & \dots & M_{1N} \\ \star & M_{22} & \dots & M_{2N} \\ \vdots & \vdots & \ddots & \vdots \\ \star & \star & \star & M_{NN} \end{bmatrix} \tag{5.24}$$

$$\begin{aligned} M_{kk} &= \begin{bmatrix} 2\lambda_{k,1} & -l_{\xi,k}^c \varphi_{k,2}(\xi) \\ \star & 2\lambda_{k,2} - l_{\xi,k}^T \varphi_{k,2}(\xi) \end{bmatrix} \\ M_{kj} &= \begin{bmatrix} 0 & -l_{\xi,k}^c \varphi_{j,2}(\xi) \\ -l_{\xi,j}^c \varphi_{k,2}(\xi) & -l_{\xi,k}^T \varphi_{j,2}(\xi) - l_{\xi,j}^T \varphi_{k,2}(\xi) \end{bmatrix} \end{aligned} \tag{5.25}$$

and $\lambda_{N+1,i}$, $i = 1, 2$ *is the* N*-th eigenvalue of the linear concentration and temperature transport operator* A_c *and* A_T*, respectively, and* $\varphi_{k,2}$, $k = 1, \dots, N$ *is the* k*-th eigenfunction of the temperature transport operator* A_T*.*

(*Proof in Appendix 5.1.*)

This quadratic bound for the linear dissipation component $\mathcal{D}_T$ will later be combined with the bound for the nonlinear component $\mathcal{D}_K$ in order to obtain a quadratic bound for the complete dissipation (5.16) and corresponding convergence criteria on the basis of a strict dissipation condition. But before this final step is addressed, an alternative data-assimilation scheme is employed and another bound for the linear dissipation component $\mathcal{D}_T$ is obtained, in order to allow for later comparison of the corresponding convergence results.

(B) Variational Approach

In correspondence to the analysis for the isothermal tubular reactor, due to the measurement of the temperature in the point $x = \xi$, a point injection can be used in the temperature dynamics to improve the convergence behavior. On the other hand, as the concentration is not measured, a general distributed injection is considered for the correction mechanism in the concentration dynamics based on temperature measurement injection. This leads to the following injection mechanism

$$l_{\xi,c} = l_{\xi,c}(x), \quad l_{\xi,T} = l_{\xi,T}^0 \delta(x - \xi). \tag{5.26}$$

Following the variational approach employed in the isothermal tubular reactor study, integration by parts of the differential terms in the dissipation expression $\mathcal{D}_T$ and

application of Wirtinger's Lemma [97, 98, 66], allows to bound $\mathcal{D}_T$ by an integral quadratic form.

Lemma 5.2. *The dissipation of the linear transport subsystem $\Sigma(A, G)$ is bounded in the following way*

$$
\begin{aligned}
&\mathcal{D}_T \leq -\int_0^1 \bar{\varpi}^T Q' \bar{\varpi} dx, \\
&\bar{\varpi} = [e_c(x,t),\, e_T(x,t),\, e_c(0,t),\, e_T(0,t),\, e_T(\xi,t),\, e_c(1,t),\, e_T(1,t)]^T \\
&Q' = \begin{bmatrix}
D_c[w_1] & 0 & -\frac{w_{1,\min}\pi}{2P_{e,c}} & 0 & l_{\xi,c}\frac{w_1}{2} & 0 & 0 \\
\star & D_T[w_2] & 0 & \frac{L_e w_{2,\min}\pi}{2P_{e,T}} & 0 & 0 & 0 \\
\star & \star & \mathcal{R}_{c,0} & l_{c,0}w_1(0) & 0 & 0 & 0 \\
\star & \star & \star & \mathcal{R}_{T,0} & 0 & 0 & 0 \\
\star & \star & \star & \star & l^0_{\xi,T} w_w(\xi) & 0 & 0 \\
\star & \star & \star & \star & \star & \mathcal{R}_{c,1} & l_{c,1}\frac{w_1(1)}{P_{e,c}} \\
\star & \star & \star & \star & \star & \star & \mathcal{R}_{T,1}
\end{bmatrix}, \\
&D_c[w_1] = -\frac{1}{P_{e1}}\frac{d^2 w_1}{dx^2} - \frac{dw_1}{dx} + \frac{w_{1,*}\pi}{2P_{e,c}} \qquad (5.27) \\
&D_T[w_2] = -\frac{L_e}{P_{e2}}\frac{d^2 w_2}{dx^2} - \frac{dw_2}{dx} + \eta w_2 + \frac{L_e w_{2,*}\pi}{2P_{e,T}} \\
&\mathcal{R}_{c,0} = \frac{w_{1,*}\pi}{2P_{e,c}} + \frac{1}{P_{e,c}}\frac{\partial w_1}{\partial x}(0) + \frac{P_{ec}-2}{P_{ec}} w_1(0) \\
&\mathcal{R}_{T,0} = \frac{w_{2,*}\pi}{2P_{e,T}} + \frac{L_e}{P_{e,T}}\frac{\partial w_2}{\partial x}(0) + \frac{P_{eT} + 2l_{T0} - 2L_e}{P_{eT}} w_2(0) \\
&\mathcal{R}_{c,1} = \frac{1}{P_{e,c}}\frac{\partial w_1}{\partial x}(1) + w_1(1) \\
&\mathcal{R}_{T,1} = \frac{L_e}{P_{e,T}}\frac{\partial w_2}{\partial x}(1) + L e w_2(1)\frac{2l_{T1+P_{eT}}}{P_{e,T}}
\end{aligned}
$$

(*Proof in Appendix L.*)

This quadratic bound for the linear dissipation $\mathcal{D}_T$, and the one previously determined for a modal correction mechanism will be used in the sequel to draw explicit convergence criteria.

5.2.6 Convergence Assessment

Having as point of departure the previously drawn quadratic bounds for the nonlinear ($\mathcal{D}_K$) and linear transport ($\mathcal{D}_T$) dissipation components, next, conditions for strict dissipation are identified by combining both components, and employing

the Lyapunov-like convergence result presented in Lemma 2.1.

Recall that the proposed modal correction mechanism (5.21) and the coupled point and distributed injection mechanism (5.26) yield different bounds for the dissipation of the linear transport subsystem. Therefore the following convergence analysis is carried out in dependence of the corresponding case.

(A) Modal Injection - Spectral Approach

Based on (i) the bound (5.20) for the dissipation of the nonlinear kinetic subsystem, (ii) the modal injection mechanism (5.21), and (iii) the corresponding bound (5.23) for the dissipation of the linear transport subsystem, both in integral quadratic form, the estimation error dissipation is bounded as follows

$$\begin{aligned}
&\frac{dE(e(x,t))}{dt} \leq -\int_0^1 \begin{bmatrix} e(x,t) \\ \rho(z;e) \end{bmatrix}^T \begin{bmatrix} -2\lambda^* W - L_\rho^2 h(x) I_2 & -WG \\ -G^T W & h(x) \end{bmatrix} \begin{bmatrix} e(x,t) \\ \rho(z;e) \end{bmatrix} dx, \\
&\lambda^* = \max\{\lambda_{LN}^*, \lambda_{N+1,1}, \lambda_{N+1,2}\}, \\
&W = \mathrm{diag}(w_1, w_2), \quad w_1 = e^{-P_{ec}x},\ w_2 = e^{-P_{eT}x}.
\end{aligned} \tag{5.28}$$

Accordingly, the exponential stability can be concluded if a strict dissipation property of the form $\dot{E}(e) \leq -2\lambda E(e)$ is fulfilled. This requirement yields the following criteria for exponential convergence.

Theorem 5.1. *Consider the tubular reactor (5.1)-(5.2) together with the linear distributed gain Luenberger-type observer (5.5)-(5.6), with modal injection according to (5.21), and modal gains $l_{\xi,k}^c$ and $l_{\xi,k}^T$. Let L_ρ be the Lipschitz constant of the reaction rate expression $r(c,T)$, $\lambda_{k,1}$ (or $\lambda_{k,2}$) be the eigenvalues of the linear concentration (or temperature) transport operator, $\varphi_{k,1}$ (or $\varphi_{k,2}$) the corresponding eigenfunctions, and N a finite number so that for a given $\lambda > 0$*

$$\forall x \in [0,1]: \quad -2\max\{\lambda_{N+1,1}, \lambda_{N+1,2}\} I_2 > L_\rho^2 h W^{-1} + 2\lambda + \frac{GG^T W}{h(x)} \tag{5.29}$$

is satisfied for some continuous positive definite function $h(x)$, and $w_i(x)$, $i = 1,2$ given by (5.22). If: (i) the sensor location $x = \xi \in [0,1]$ does not correspond to any of the roots of the first N temperature eigenfunctions, i.e. $\varphi_{k,2}(\xi) \neq 0$, $k = 1,\ldots,N$, and (ii) the modal gains $l_{\xi,k}^c, l_{\xi,k}^T$, $k = 1,\ldots,N$ are chosen such that the maximal

eigenvalue λ^*_{LN} *of the* $N \times N$ *matrix* $\mathcal{M}^u_L$ *given in (5.24) satisfies*

$$\forall x \in [0,1]: \quad -2\lambda^*_{LN} > L^2_\rho + 2\lambda + \frac{D_a^2(w_1^2 + \beta^2 w_2^2)}{h(x)}, \tag{5.30}$$

then, the estimation error zero solution $e(x,t) = 0$ *is g.e.s. with convergence rate* $\lambda > 0$ *and amplitude* $a = \sqrt{w^*/w_*}$, $w^* = \max_{x\in[0,1],i=1,2} w_i(x)$, $w_* = \min_{x\in[0,1],i=1,2} w_i(x)$.

(*Proof in Appendix M.*)

Note that this result invokes decisions on the weighting function $h(x) > 0$, the innovation dimension N, the sensor location $\xi \in [0,1]$ and the modal observer gains $l^j_{\xi,i}$, $i = 1,\ldots,N$, $j = c,T$.

Before this result is discussed, its counterpart corresponding to the injection mechanism (5.26) is presented.

(B) Point and Distributed Injection - Variational Approach

Recall the quadratic bounds for (i) the dissipation component $\mathcal{D}_K$ of the nonlinear kinetic subsystem (5.20), and (ii) (5.27) for the dissipation component $\mathcal{D}_T$ of the linear transport subsystem. Correspondingly, the complete dissipation is bounded

as follows

$$\dot{E}(e) \leq -\int_0^1 \zeta Q \zeta dx,$$
$$\zeta = [e_c(x,t),\, e_T(x,t),\, \rho(z;e),\, e_c(0,t),\, e_T(0,t),\, e_T(\xi,t),\, e_c(1,t),\, e_T(1,t)]^T,$$

$$Q = \left[\begin{array}{ccccc|ccc}
D_c[w_1] - 2\lambda w_1 & 0 & D_a w_1 & -\frac{w_{1,\min}\pi}{2P_{e,c}} & 0 & & & \\
\star & D_T[w_2] - 2\lambda w_2 & -\beta D_a w_2 & 0 & \frac{L_e w_{2,\min}\pi}{2P_{e,T}} & & & \\
\star & \star & h & 0 & 0 & & & \\
\star & \star & \star & \mathcal{R}_{c,0} & l_{c,0} w_1(0) & & & \\
\star & \star & \star & \star & \mathcal{R}_{T,0} & & & \\
\star & \star & \star & \star & \star & & & \\
\star & \star & \star & \star & \star & & & \\
\star & \star & \star & \star & \star & & & \\
\hline
 & & & & & l_{\xi,c}\frac{w_1}{2} & 0 & 0 \\
 & & & & & 0 & 0 & 0 \\
 & & & & & 0 & 0 & 0 \\
 & & & & & 0 & 0 & 0 \\
 & & & & & 0 & 0 & 0 \\
 & & & & & l^0_{\xi,T} w_w(\xi) & 0 & 0 \\
 & & & & & \star & \mathcal{R}_{c,1} & l_{c,1}\frac{w_1(1)}{P_{e,c}} \\
 & & & & & \star & \star & \mathcal{R}_{T,1}
\end{array}\right], \tag{5.31}$$

with $D_c, D_T, \mathcal{R}_{i,j}, i = c, T, j = 0, 1$ given in (5.27). Requiring a strict dissipation property of the form $\dot{E}(e) \leq -2\lambda E(e)$, the following criteria for exponential convergence are obtained.

Theorem 5.2. *Consider the non-isothermal tubular reactor (5.1)-(5.2) with the dissipative observer (5.5)-(5.6), and the injection gain structure given by (5.26). The estimated profile converges exponentially to the actual profile with rate $\lambda > 0$ and amplitude $a = \sqrt{w^*/w_*}$, $w^* = \max_{x\in[0,1], i=1,2} w_i(x)$, $w_* = \min_{x\in[0,1], i=1,2} w_i(x)$, i.e.*

$$||e(x,t)|| \leq a\, ||e_0(x)||\, e^{-\lambda t}, \tag{5.32}$$

if for all $x \in [0,1]$ the following LMI holds

$$Q \geq diag(2\lambda w_1, 2\lambda w_2, 0, 0, 0, 0, 0, 0) \tag{5.33}$$

with Q given in (5.31).

Proof. If the above condition is satisfied it follows $\frac{dE}{dt}+2\lambda E \leq 0$ and the exponential stability results from Lemma 2.1. □

Based on this general result, particular solvability conditions for the process parameters can be found for the exponential convergence.

Proposition 5.1. *The observer gains can be chosen such that the LMI (5.33) is fulfilled, if the transport ($P_{e,c}$, $P_{e,T}$, L_e) and reaction (D_a, β) parameters and the required dissipation $\lambda > 0$ satisfy the following set of inequalities*

$$\begin{aligned} P_{e,c} &> \iota_{c1}(P_{ec}, \lambda, L_\rho, D_a) \\ P_{e,T} &> \iota_{T1}(P_{eT}, \lambda, L_\rho, D_a, \beta, \eta), \end{aligned} \tag{5.34}$$

and the weighting functions are chosen as

$$\begin{aligned} w_1(x) = h(x) = e^{P_{e,c}x} cosh(\varpi_c x),\ \varpi_c &= \frac{P_{e,c}^2}{4} - P_{e,c}\left(2\lambda + L_\rho^2 + m_1\right) \\ w_2(x) = e^{P_{e,T}x} cosh(\varpi_T x),\ \varpi_T &= \frac{P_{e,T}^2}{4} + P_{e,T}\left(\eta - 2\lambda - \beta^2 D_a^2 - m_2\right), \end{aligned}$$

and the functions ι_{ij}, $i = c, T, j = 1, 2, 3$ are bounded functions of their arguments according to

$$\begin{aligned} \iota_{c1} &\triangleq 4\left(2\lambda + L_\rho^2 + \frac{D_a^4\beta^2}{L_\rho\sqrt{(D_a^2\beta^2 - 1)}}\right) \\ \iota_{T1} &\triangleq 4\left(2\lambda + \beta^2 D_a^2 + L_\rho\sqrt{(D_a^2\beta^2 - 1) - \eta}\right). \end{aligned}$$

(*Proof in Appendix N.*)

A short comparison between this and the previous (modal injection) convergence criteria is given in the following discussions of the results.

5.3 Discussion of the results

5.3.1 General Considerations

Note that for the modal injection, the requirement on the innovation dimension N depends on (i) the desired convergence velocity λ, (ii) the transport characteristic Peclet-numbers $P_{e,i}$, $i = c, T$ (i.e. the diffusion-to-convection characteristic time quotient), as can be seen from (4.51)-(4.52), and (iii) the reaction characteristic

Lipschitz constant L_ρ, the Damköhler number D_a (i.e. the convection-to-reaction characteristic time quotient), and the adiabatic temperature rise β (i.e. the heat production-to-capacity ratio). The gain condition on the other hand is less clear because it involves the determination of the eigenvalues of the matrix $\mathcal{M}_L^u$ (5.24).

The possibilities to assign the eigenvalues of the temperature dynamics depend on the location $\xi \in [0, 1]$ of the temperature sensor, while the eigenvalues of the linear concentration dynamics cannot be assigned arbitrarily, due to the diagonal structure of the transport operator. The question on how the eigenvalue coupling is influenced by the kinetic coupling of temperature and concentration, has to be addressed in future studies.

The conditions (5.34) on the Peclet numbers P_{ei}, $i = c, T$ basically require that the stability issues induced by hydrodynamical transport are strong enough to dominate the destabilization potential of the nonlinear reaction rate estimation error, characterized by the adiabatic temperature rise β, the reaction-to-convection characteristic time quotient D_a, and the corresponding Lipschitz constant L_ρ of the reaction rate expression r, characterizing the maximal (minimal) slope of the reaction rate.

The conditions have to be viewed in the light of a worst case scenario, in the understanding that it is supposed that the reaction rate error attains its maximal value in all points along the reactor. Therefore the drawn conditions are conservative, but reflect the principal requirements for all tubular reactors and their interpretation nicely corresponds to the argumentation in the stability assessment of open-loop observers (compare [47, 49]), based on hydrodynamically induced stability.

It should be mentioned here that, for a practical scenario, the slope bounds have to be considered in a certain region about a given nominal (SS) profile which is determined according to some product quality criteria and, accordingly, the process design parameters.

For the analyzed particular structures of the correction mechanism, it turned out that, the greater Péclet's characteristic transport parameters $P_{e,i}$, $i = c, T$, i.e. the more convection dominated the transport, the corresponding stabilization effects of the heat and mass transfer corresponding mechanisms are very strong. On the other hand, the smaller the Peclet-numbers are, i.e. the more diffusion-dominated is the transport behavior, the stabilizing effect of the transport mechanism becomes weaker. In the limit $P_{e,i} \to 0$, $i = c, T$, the phenomenological behavior is equivalent to the

CSTR [9], and as shown in Chapter 3, the corresponding solvability conditions require a minimum volumetric flow rate q, in order to permit a solution. Without going into more detail, a clear parallel exists between this condition for the observer existence in the case of the CSTR and the conditions for the tubular reactor observer existence, because the flow rate q determines the Peclet-numbers $P_{e,i} = \frac{Lv}{D_i} = \frac{Lq}{D_i A}$, $D_i = \alpha, D$.

The consideration of modeling and measurement errors corresponds to the reasoning presented in the last chapter (see Section 4.3.2). Accordingly, the reactor estimation error dynamics is input-to-state stable with respect to bounded, exogenous errors, but does not compensate them completely. This subject should be analyzed with more detail in future studies.

5.4 Application Example

The observer convergence behavior is tested by consideration of the critical case example used in the previous studies: the non-monotonic exothermic Langmuir-Hinshelwood type reaction kinetics. This choice is based on the facts that: (i) non-isotonical kinetics imply a difficult observation problem because of the presence of destabilizing regions corresponding to certain estimation error regimes, and impossibility to directly infer the concentration profile from temperature measurements, (ii) a strongly exothermic reaction requires strongly stabilizing features of the corresponding transport mechanisms (cp. the discussion in Section 3.2.3), and (iii) it permits to understand the principal mechanism for monotonic kinetics too, in the understanding that monotonic kinetics present, from a local point of view, particular limit cases of non-monotonic ones.

The Langmuir-Hinshelwood (in a biological context also known as Haldane) kinetics is analytically expressed as [18, 19]

$$r(c, \sigma) = \frac{c}{(1 + \sigma c)^2} e^{-\gamma/T}, \tag{5.35}$$

where σ is the inhibition coefficient, and $\gamma = E_A/R$ is the Arrhenius quotient of the activation energy E_A and the gas constant R. A possible Lipschitz constant L_ρ for this nonlinearity can be derived using the mean-value theorem ($\Xi = [0, 1] \times$

$[T^-, T^+] \subset \mathbb{R}^2$ is the region where the reactor states attain their values):

$$\begin{aligned}
&\sup_{\Xi} ||r(c+e_c, T+e_T) - r(c,T)|| \\
&= \sup_{\Xi} \left|\left| \nabla r(\xi,\tau) \begin{bmatrix} e_c \\ e_T \end{bmatrix} \right|\right| \\
&\leq \sup_{\Xi} ||\nabla r(\xi,\tau)|| \left|\left| \begin{bmatrix} e_c \\ e_T \end{bmatrix} \right|\right| \\
&= \sup_{\Xi} \sqrt{\left(\frac{\partial r}{\partial c}(\xi,\tau)\right)^2 + \left(\frac{\partial r}{\partial T}(\xi,\tau)\right)^2} \left|\left| \begin{bmatrix} e_c \\ e_T \end{bmatrix} \right|\right|,
\end{aligned}$$

and correspondingly one identifies

$$L_\rho \geq \sup_{\Xi} \sqrt{\left(\frac{\partial r}{\partial c}(\xi,\tau)\right)^2 + \left(\frac{\partial r}{\partial T}(\xi,\tau)\right)^2}. \tag{5.36}$$

Note further that

$$\sqrt{\left(\frac{\partial r}{\partial c}(\xi,\tau)\right)^2 + \left(\frac{\partial r}{\partial T}(\xi,\tau)\right)^2} = e^{-\gamma/\tau} \sqrt{\frac{1-\sigma^2\xi^2 + \xi^2\frac{\gamma^2}{\tau^4}}{(1+\sigma\xi)^4}} \leq e^{-\gamma/T^{+4}} \sqrt{1+\frac{\gamma^2}{T^{-4}}},$$

so that a Lipschitz constant is given by

$$L_\rho = e^{-\gamma/T^{+4}} \sqrt{1+\frac{\gamma^2}{T^{-4}}}. \tag{5.37}$$

Consequently the estimation nonlinearity $\rho(z;e) = r(z+e) - r(z)$ satisfies the sector condition (5.19) with L_ρ given by (5.37).

Simulation studies of the proposed observer with the non-monotonic reaction rate expression (5.35) have been carried out considering different regimes of parameters: (i) a diffusion dominated behavior (packed-bed) exothermic one, corresponding to $(P_{e,c}, P_{e,T}, D_a, \sigma, \beta, \gamma) = (10, 10, 3\cdot 10^4, 200, 3, 10^4)$ and (ii) a more convection dominated (open-tube) exothermic one, corresponding to $(P_{e,c}, P_{e,T}, D_a, \sigma, \beta, \gamma) = (100, 100, 3\cdot 10^4, 200, 3, 10^4)$. For either of these cases the nominal (errorless) and robust (considering errors $\tilde{\sigma}, \tilde{y}$ and exogenous disturbances $\tilde{c}_{in}$, $\tilde{T}_{in}$) convergence behavior is tested for initial conditions corresponding to trajectories around the concentration with maximal reaction rate, one in the increasing and one in the decreasing kinetic branch.

5.4.1 Modal Correction Mechanism

In order to test the modal injection mechanism (5.21), the reactor model (5.1) was equipped with parameters corresponding to (i) a diffusion dominated scenario $P_e = \mathcal{O}(10)$, and (ii) a convection dominated scenario $P_e = \mathcal{O}(10^2)$. The convergence behavior has been tested (i) for the nominal case (no errors in parameters and measurement), and (ii) for the case that the dynamics are subject to errors in the reaction parameters and the measurement.

As pointed out in the isothermal tubular reactor study, for Peclet P_e numbers higher than approximately 20, the convergence speed induced by the transport process is so fast, that a modal improvement would require very high gains and innovation dimensions, which on the other hand imply a loss of robustness with respect to measurement error amplification. Therefore, only the diffusion dominated case is analyzed for the application of the spectral modal innovation approach.

Convergence without modeling and measurement errors

In order to test the convergence behavior of the observer (5.5) with modal measurement injection mechanism (5.21), the reactor was equipped with the parameter set $(P_{e,1}, P_{e,2}, D_a, \gamma, \sigma, \beta) = (10, 10, 3 \cdot 10^4, 10^4, 3, 200)$. The measurement location has been determined through numerical simulation in the light of reaction parameter offsets and measurement errors (see the next section), which yield best behavior for $\xi = 0.3$. The initial conditions have been set to $z_0 = [375, 0.2]^T$, $\hat{z}_0 = [380, 0.4]^T$. The modal innovation dimension has been chosen as $N = 4$, and the corresponding modal gains, obtained from tuning in the sense of convergence speed up and robustness improvement (see the next section) are given by

$$(l^T_{\xi,1}, l^T_{\xi,2}, l^T_{\xi,3}, l^T_{\xi,4}, l^c_{\xi,1}, l^c_{\xi,2}, l^c_{\xi,3}, l^c_{\xi,4}) = (20, 25, 50, 10, -0.5, -1, -1.5, -0.5). \quad (5.38)$$

The corresponding result is presented in Figure 5.2. One appreciates that (i) the convergence behavior is wave like, from the inlet towards the outlet (up-stream), (ii) the correction mechanism in the temperature dynamics behaves like a secondary wave, imposed in correspondence to the shape of the first 4 eigenfunctions (compare Figure J.2) and in particular improving the convergence around the outlet $x = 1$, (iii) the convergence is sped up in the temperature estimation error about 70 %, and (iv) the convergence speed of the concentration estimation is about the one of the

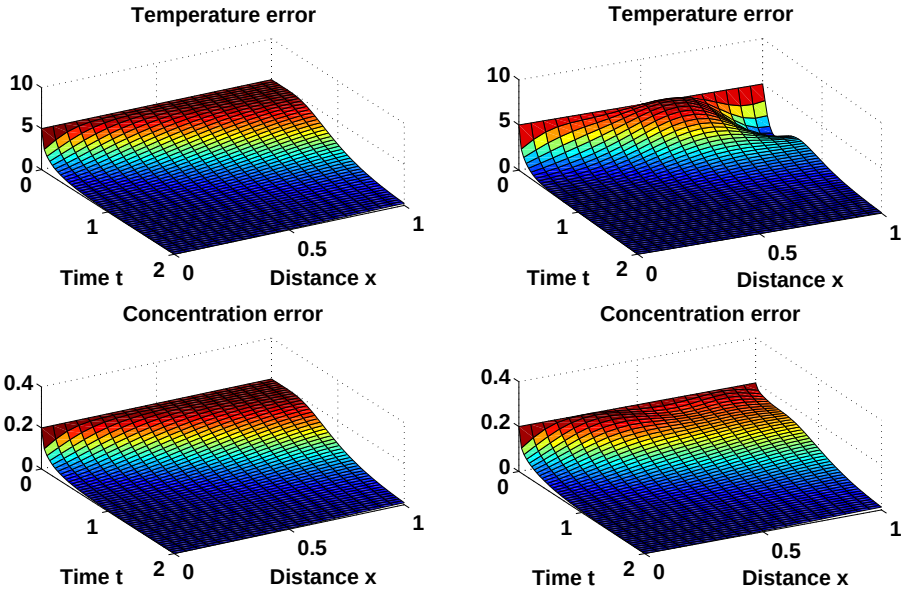

Figure 5.2: Convergence behavior for diffusion dominated process corresponding to parameters $(P_{e1}, P_{e2}, D_a, \beta, \sigma, \gamma) = (10, 10, 3 \cdot 10^4, 200, 3, 10^4)$, and constant initial profiles $z_0 = [375, 0.2]^T$, $\hat{z}_0 = [380, 0.4]^T$. On the left: natural convergence behavior. On the right: improved convergence behavior corresponding to the observer (5.5) with gains according to (5.39). Top: Temperature estimation error, bottom: concentration estimation error.

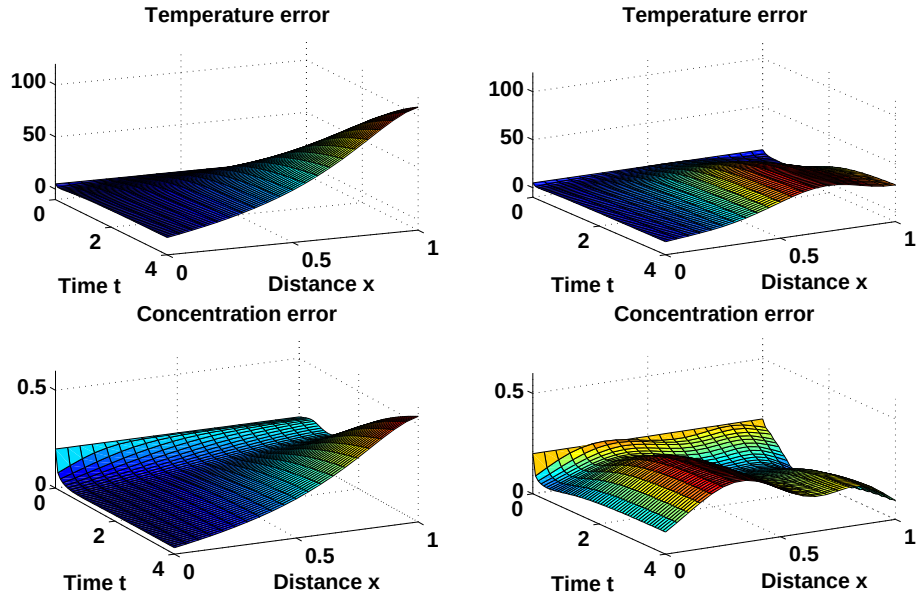

Figure 5.3: Robust convergence behavior for diffusion dominated process corresponding to parameters $(P_{e1}, P_{e2}, D_a, \beta, \sigma, \gamma) = (100, 100, 3 \cdot 10^4, 200, 3, 10^4)$, and constant initial profiles $z_0 = [375, 0.2]^T$, $\hat{z}_0 = [380, 0.4]^T$. The process is subject to reaction parameter errors of -60 % in σ, γ, and D_a, and measurement noise of 2 K amplitude and 50 Hz frequency. On the left: natural convergence behavior. On the right: improved convergence behavior corresponding to the observer (5.5) with gains according to (5.39). Top: Temperature estimation error, bottom: concentration estimation error.

natural convergence speed.

Convergence with modeling and measurement errors

In order to test the designed observer in the presence of reaction parameter errors of -60 % of the nominal parameters $(\sigma, \gamma, D_a) = (3, 10^4, 3 \cdot 10^4)$, and measurement uncertainty of 2 K and noise, simulated by sinusoidal signals with frequency 50 Hz. The modal gains used for simulation are given by (5.38). The corresponding simulation result is presented in Figure 5.3. One appreciates that the natural asymptotic offset is reduced: (i) in the temperature estimation about 70 %, and (ii) the maximal concentration offset is reduced about 50 %.

5.4.2 Coupled point and distributed injection

The performance of the observer convergence has been tested in terms of improvement in comparison to natural convergence behavior through numerical simulations. For these simulations, a simple method of lines algorithm has been used. First, assuming errorless parameter estimates, measurements and perfect knowledge of exogenous feed concentration and temperature, two cases are analyzed: (i) a diffusion dominated scenario, and (ii) a convection dominated one, in order to identify the corresponding effects of the process transport mechanism. Then, considering offsets in the reaction parameters (k, σ, γ), the robust convergence behavior is considered for both cases.

Convergence without modeling and measurement errors

As stated in the analysis of the dissipation behavior, the transport characteristic Peclet-numbers P_{ei}, $i = c, T$ can be used to characterize the stability property of the estimation error dynamics. For low Peclet numbers ($P_e \leq 20$) the process is diffusion dominated and in the limit case corresponding to $P_e = 0$, the spatial profile is homogenous. The case of very low Peclet numbers thus corresponds to the consideration of continuous stirred reactors and has been analyzed in Chapter 3 (for a more analytic comparison of the tubular reactor and the stirred tank see e.g. [9]). On the other hand, the destabilization potential due to the reaction grows if (i) the reaction frequency k is augmented and correspondingly the reaction time becomes shorter, and / or (ii) the reaction enthalpy $-\Delta H$ grows and correspondingly the ratio of stored heat becomes greater. In the light of this interplay of stabilizing transport and potentially destabilizing reaction, the particular reactor parameters of the subsequent simulation studies have been chosen, in order to provide a challenging reactor observation problem.

Considering a diffusion dominated scenario with fast and strongly exothermic reaction, the reactor parameters are set to $(P_{e1}, P_{e2}, D_a, \beta, \sigma, \gamma) = (10, 10, 3 \cdot 10^4, 200, 3, 10^4)$. The convergence improvement is studied in comparison to the natural convergence behavior. The corresponding simulation results corresponding to spatially constant initial profiles $z_0 = [375, 0.2]^T$, $\hat{z}_0 = [380, 0.4]^T$ are presented in Figure 5.4. The natural convergence behavior is shown on the left side of the figure,

and the improved convergence behavior on the right side, corresponding to gains

$$(l_{T0}, l_{T\xi}, l_{T1}, l_{c0}, l_{c\xi}, l_{c1}) = (-10, 30, 20, 0.75, 0.1, -0.25). \tag{5.39}$$

At the top of the figure one can appreciate the convergence of the temperature estimation errors and at the bottom of the concentration estimation errors, respectively. The sensor location in the domain has been chosen as $\xi = 0.4$ through numerical simulation studies considering the parameter offsets and measurement errors (see next section). One notices that: (i) for all errors the basic convergence is wave-like from the inlet $x = 0$ towards the outlet $x = 1$, (ii) the innovated temperature error converges about 30 % faster than the natural one, (iii) the corresponding convergence is wave-like from the injection points up- and downstream, and (iv) the concentration error convergence is speed-up about 10 %. One notices that the basic convergence behavior of the concentration is quite different in comparison to the natural one. This is due to the distributed measurement injection throughout the extension with constant gain $l_{c,\xi} = 0.1$. The injection at the boundaries $x = 0, 1$ is proportional to the temperature estimation error offset at these points.

In order to consider a convection-dominated transport the parameter set is chosen as $(P_{e1}, P_{e2}, D_a, \beta, \sigma, \gamma) = (100, 100, 3 \cdot 10^4, 200, 3, 10^4)$, the gains are chosen equal (5.39), and the initial conditions are set as constant profiles $z_0 = [375, 0.2]^T$, $\hat{z}_0 = [380, 0.4]^T$. The corresponding simulation results are presented in Figure 5.5. In comparison with the diffusion-dominated transport, one appreciates that: (i) the natural convergence is quite faster, (ii) the convergence speed up in the concentration estimation error is less visible (unless still about 10 %), (iii) the corresponding temperature estimation error convergence also maintains the corresponding improvement about 30 %, (iv) the basic convergence behavior becomes sharper, in the sense that one notices a shock-wave-like distribution over the reactor extension, and (v) the temperature estimation error convergence is unidirectional (down-stream) from the corresponding measurement injection points.

Convergence with modeling and measurement errors

In order to test the designed observer in a more realistic scenario, the above simulation studies have been repeated considering (i) constant reaction parameter offsets in σ, γ, k of -60%, and (ii) temperature measurement errors with amplitude 2 K and overlaid sinusoidal oscillation with frequency of 50 Hz, and phase offset

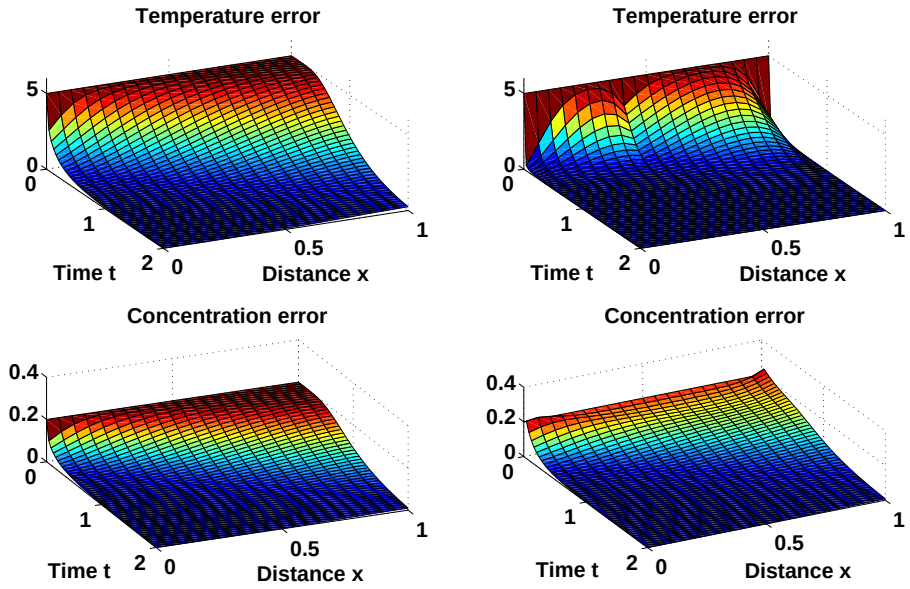

Figure 5.4: Convergence behavior for diffusion dominated process corresponding to parameters $(P_{e1}, P_{e2}, D_a, \beta, \sigma, \gamma) = (10, 10, 3 \cdot 10^4, 200, 3, 10^4)$, and constant initial profiles $z_0 = [375, 0.2]^T$, $\hat{z}_0 = [380, 0.4]^T$. On the left: natural convergence behavior. On the right: improved convergence behavior corresponding to the observer (5.5) with gains according to (5.39). Top: Temperature estimation error, bottom: concentration estimation error.

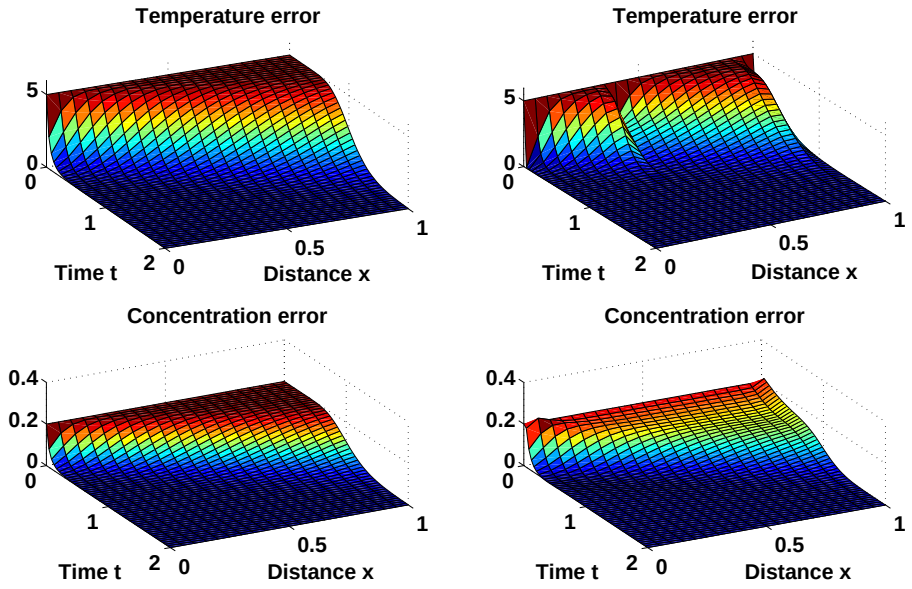

Figure 5.5: Convergence behavior for convection dominated process corresponding to parameters $(P_{e1}, P_{e2}, D_a, \beta, \sigma, \gamma) = (100, 100, 3 \cdot 10^4, 200, 3, 10^4)$, and constant initial profiles $z_0 = [375, 0.2]^T$, $\hat{z}_0 = [380, 0.4]^T$. On the left: natural convergence behavior. On the right: improved convergence behavior corresponding to the observer (5.5) with gains according to (5.39). Top: Temperature estimation error, bottom: concentration estimation error.

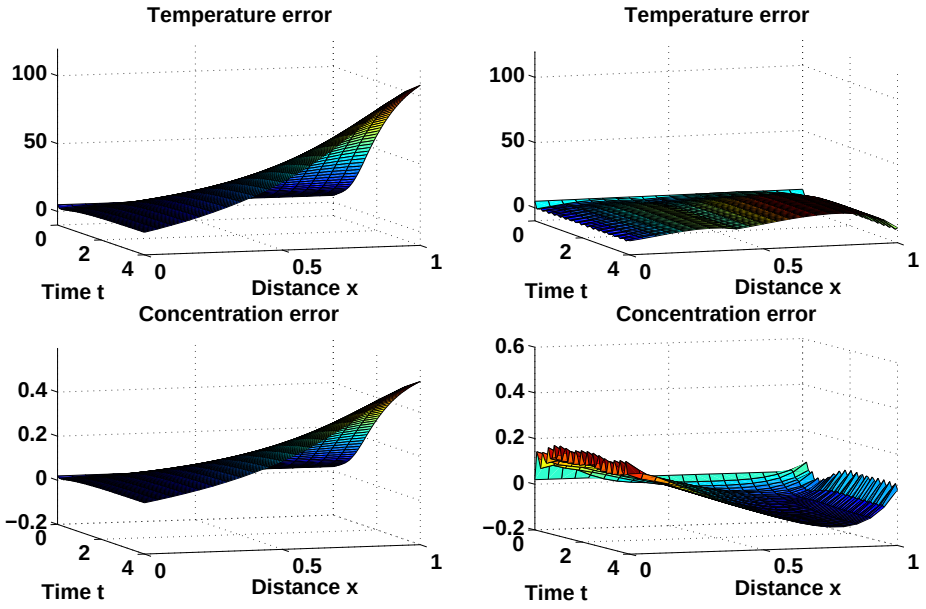

Figure 5.6: Robust convergence behavior for convection dominated process corresponding to parameters $(P_{e1}, P_{e2}, D_a, \beta, \sigma, \gamma) = (100, 100, 3 \cdot 10^4, 200, 3, 10^4)$, and constant initial profiles $z_0 = [375, 0.2]^T$, $\hat{z}_0 = [380, 0.4]^T$. The process is subject to reaction parameter errors of -60 % in σ, γ, and D_a, and measurement noise of 2 K amplitude and 50 Hz frequency. On the left: natural convergence behavior. On the right: improved convergence behavior corresponding to the observer (5.5) with gains according to (5.39). Top: Temperature estimation error, bottom: concentration estimation error.

corresponding to the measurement point $(\delta\varphi_0, \delta\varphi_0, \delta\varphi_0) = (0, 1, 1.5)$. The simulation parameters have been chosen equal to the above simulations, i.e.

$$(P_{e1}, P_{e2}, D_a, \beta, \sigma, \gamma) = (10, 10, 3 \cdot 10^4, 200, 3, 10^4)$$

for the diffusion dominated case study, and

$$(P_{e1}, P_{e2}, D_a, \beta, \sigma, \gamma) = (100, 100, 3 \cdot 10^4, 200, 3, 10^4)$$

for the convection dominated one. The corresponding simulation results are shown in Figures 5.6 and 5.7.

One appreciates that: (i) for the diffusion dominated case (Figure 5.6), the asymptotic convergence offset due to the errors in the reaction parameters σ, γ, k, is attenuated in the corresponding maximum about 70 % (temperature) and 50 %

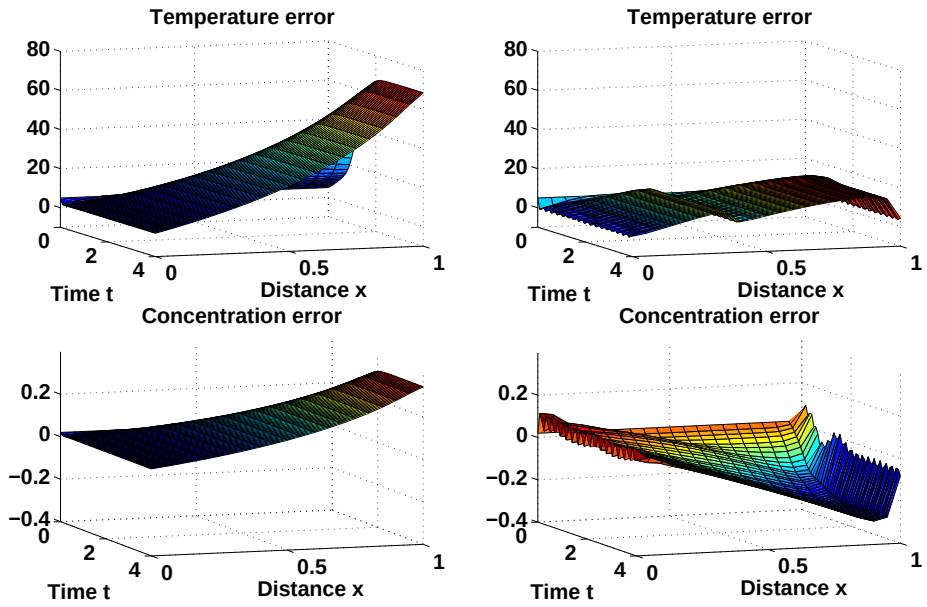

Figure 5.7: Robust convergence behavior for convection dominated process corresponding to parameters $(P_{e1}, P_{e2}, D_a, \beta, \sigma, \gamma) = (100, 100, 3 \cdot 10^4, 200, 3, 10^4)$, and constant initial profiles $z_0 = [375, 0.2]^T$, $\hat{z}_0 = [380, 0.4]^T$. The process is subject to reaction parameter errors of -60 % in σ, γ, and D_a, and measurement noise of 2 K amplitude and 50 Hz frequency. On the left: natural convergence behavior. On the right: improved convergence behavior corresponding to the observer (5.5) with gains according to (5.39). Top: Temperature estimation error, bottom: concentration estimation error.

(concentration), and (ii) for the convection dominated scenario (Figure 5.7), the corresponding offset is strongly propagated up-stream, causing a stronger impact and less attenuation of the maximum in the concentration estimation error offset (about 2 %).

5.4.3 Concluding Remarks

The presented simulation studies show that the employment of the observer (5.5) with (i) collocated point injection of the boundary measurements, (ii) point injection in the temperature dynamics of the temperature measurement in the domain at $x = \xi$, and (iii) (constant) distributed injection in the concentration dynamics of this measurement, improves the convergence behavior in the understanding of faster convergence with more robustness against errors in the reaction parameters under consideration of measurement errors. The presented cases reflect the basic interplay between transport and reaction and show that for strongly convective transport the obtained improvement in the concentration estimation becomes less than in the diffusion-dominated case. The presented results can be improved: (i) by considering more temperature sensors, (ii) if possible employing concentration sensors, and (iii) probably by designing the distributed injection gain in the estimated concentration dynamics in a non-constant (eventually only regionally active) gain function.

5.5 Summary

In this chapter the dissipative observer design methodology, previously employed for the continuous stirred and the isothermal tubular reactor, has been extended to the non-isothermal tubular reactor with boundary and/ or domain point temperature measurements. The main issues addressed were the coupling phenomena caused by (i) the nonlinear non-isothermal chemical reaction kinetic rate, and (ii) the correction terms in the concentration dynamics depending on the temperature. The design approach based on the dissipation properties of the estimation error dynamics have been adapted to the consideration of these issues in the following manner

- an integrally weighted Lipschitz sector condition has been used to bound the dissipation according to the kinetic mechanism
- a modal decomposition has been employed to analyze the influence of a modal

injection structure in the temperature and concentration dynamics

- a coupled point and distributed injection mechanism has been proposed for the correction mechanism, employing direct transformations of the dissipation expression via integration by parts and application of integral inequalities.

Together with the results for the continuous and the isothermal tubular reactor studies, these steps presented the basic issues which had to be discussed for the development of a dissipative observer design methodology for the non-isothermal tubular reactor with temperature and/ or concentration point measurements at the boundary and/ or in the domain.

In comparison with previous studies on non-isothermal tubular reactor observer design based on temperature measurements the presented dissipative observer presents (i) systematic design, (ii) convergence improvement, (iii) mathematical rigor, (iv) physical insight, (v) ensured functioning with only one sensor, and (vi) improved convergence behavior employing various sensors.

Chapter 6

Implications for a class of multi-species transport-reaction systems

In this chapter, some implications of the preceding development of the dissipative observer design methodology for a class of tubular reactors are presented with respect to a class of multi-species transport-reaction systems. For this purpose, a slightly more general framework is used to present a possible approach to the observer design for multi-species systems with multiple simultaneous reactions. The basic idea concerning the interpretation of the system in terms of an interconnection of two subsystems is formulated within a system-theoretic dissipativity framework, and sufficient conditions for the global and exponential convergence of a dissipative observer are given. Due to the particular structure of the considered system class, it is clarified that the observer correction structure can be designed by following either of the approaches developed in the preceding chapters 4 and 5.

In the context of multi-species transport reaction system observer design, already no specific studies are recorded in the literature. From an application point of view, in particular considering chemical, biological or biochemical reaction systems, the principal approaches have been mentioned in the introduction and it has already been clarified, that there is a lack of a methodology which unifies the basic requirements of (i) a systematic design approach, (ii) mathematically rigorous non-local convergence criteria with physical meaning, (iii) convergence improvement, and (iv) simple implementation and tuning. Thus the present implications for multi-

species-transport-multi-reaction systems represent a methodological contribution in the field of transport-reaction system observer design, and, as has been illustrated in the previous chapters, allows for innovating results in agitated and tubular reactor applications.

6.1 Introduction

The emphasis of this chapter is focussed on a direct generalization of the preceding results, in the understanding that: (i) various state variables $z_i(x,t)$ are considered which belong each to the corresponding state space $Z_i = L^2([0,1], X_i \subseteq \mathbb{R})$, (ii) each of the variables z_i is transported through the system by diffusion and convection, in a linear fashion, (iii) the reaction rate expression represents a pointwise source (sink), in the sense that the nonlinear terms do not invoke any differentials of the variables, and (iii) the boundary conditions are such that the previously considered Damköhler boundary conditions are covered. Technically speaking, the considered systems have the following structure

$$\begin{aligned} &\frac{\partial z_i(x,t)}{\partial t} = D_i \frac{\partial^2 z_i(x,t)}{\partial x^2} - v_i \frac{\partial z_i(x,t)}{\partial x} + k_i z_i(x,t) + b_i u_{d,i}(x,t) + g_i^T r[\sigma(x,t)] \\ &z(x,t) = \left[\; z_1(x,t), \;\; \cdots, \;\; z_n(x,t) \; \right]^T \\ &\sigma(x,t) = Hz(x,t), \end{aligned} \tag{6.1}$$

for $x \in (0,1), t > 0, i = 1, \ldots, n$, boundary conditions

$$\begin{aligned} x = 0: \; &\frac{\partial z_i}{\partial x}(0,t) = \alpha_{0,i} z_i(0,t) + \gamma_{0,i} u_{0,i}(t), \\ x = 1: \; &\frac{\partial z_i}{\partial x}(1,t) = \alpha_{1,i} z_i(1,t) + \gamma_{1,i} u_{1,i}(t) \end{aligned} \tag{6.2}$$

for $t \geq 0$, initial conditions $x \in [0,1]: \; z(x,t_0) = z_0(x)$, and measurement

$$y(t) = Cz(x,t). \tag{6.3}$$

Here, $z(x,t) = [z_1(x,t), \ldots, z_n(x,t)]^T \in L^2([0,1], X \subseteq \mathbb{R}^n), \forall t \geq 0$ is the state with image $X = \bigcup_{i \leq n} X_i$ for all pairs (x,t), and for all $i = 1, \ldots, n$, D_i is the diffusion coefficient, v_i the superficial velocity of the flow, k_i the gain of the linear source (sink) term, b_i is a distributed control, $u_{d,i}$ a distributed exogenous input, $g_i \in \mathbb{R}^q$ is the *kinetic gain matrix* according to the reaction $r : (L^2)^p \to (L^2)^q$ with argument $\sigma \in (L^2)^p$ defined by the matrix $H \in \mathbb{R}^{p \times n}$, α_{ij}, $j = 0, 1$ are constants according to the boundary conditions, γ_i is a boundary control gain, $u_{i,j}$, $j = 0, 1$ are exogenous boundary inputs, and $y \in \mathbb{R}^m$ is the output corresponding to the measurement operator C, characterized by the k measurement points $\xi = (\xi_1, \ldots, \xi_k) \in \mathbb{R}^n$, where

one ore more state variables are measured, i.e. the elements of y are given by real-valued signals $y_i(t) = z_j(\xi_l), j \in \{1, \ldots, n\}, 0 \leq l \leq k$.

Obviously, the tubular reactors considered in Chapters 4 and 5 (and thus the CSTR in Chapter 3 [9]) are particular cases of system (6.1) with $z = [c(x,t),\, T(x,t)]^T$. In particular, in the case of the non-isothermal tubular reactor (Chapter 5), one identifies e.g. for $z_2 = T$: $D_2 = \alpha/(\rho c_P)$, $v_2 = v/(\rho c_P)$, $k_2 = -UA_U/(\rho c_P)$, $b_2 = UA_U/(\rho c_P)$, $u_{d,2}(x,t) = T_c(x,t)$, $g_2 = k(-\Delta H)/(\rho c_P)$, $q = 1$, $p = 2$, $\sigma = z$, $\alpha_{0,j} = P_{e,T}/L_e = -\gamma_{0,2}$, $j = 0, 1$, $\gamma_{1,2} = 0$, $u_{0,2} = T_{in}$ and $u_{1,2} = 0$.

6.2 Dissipative Observer

6.2.1 Observer Construction

The dissipative observer with linear constant gain structure and point or distributed injection mechanism in the domain is given by

$$\begin{aligned} \frac{\partial \hat{z}_i}{\partial t} &= D_i \frac{\partial^2 \hat{z}_i}{\partial x^2} - v_i \frac{\partial \hat{z}_i}{\partial x} + k_i \hat{z}_i + b_i u_{d,i} + g_i^T r[\hat{\sigma}] - L_{d,i}(C\hat{z} - y) \\ \hat{z} &= \left[\begin{array}{ccc} \hat{z}_1, & \cdots, & \hat{z}_n \end{array} \right]^T \\ \hat{\sigma} &= H\hat{z} \end{aligned} \tag{6.4}$$

for $x \in (0,1), t > 0$, boundary conditions

$$\begin{aligned} x = 0 : \frac{\partial \hat{z}_i}{\partial x}(0,t) &= \alpha_{0,i}\hat{z}_i(0,t) + \gamma_{0,i}u_{0,i}(t) - L_0(C\hat{z} - y), \\ x = 1 : \frac{\partial \hat{z}_i}{\partial x}(1,t) &= \alpha_{1,i}\hat{z}_i(1,t) + \gamma_{1,i}u_{1,i}(t) - L_1(C\hat{z} - y) \end{aligned} \tag{6.5}$$

and initial conditions $x \in [0,1] : \hat{z}(x,t_0) = \hat{z}_0(x)$. The role of the correction mechanism in the domain corresponding to L_d is of high importance for the design, in terms of convergence speed up and robustness improvement, as has become clear from the preceding tubular reactor studies. This degree of freedom is kept free, in the understanding that the approaches discussed in the previous chapters can be employed, i.e. modal, point or other distributed mechanisms can be used. The following general results are not affected by the particular choice of the domain injection mechanism.

6.2.2 Estimation Error Dynamics

The estimation error dynamics ($e(x,t) = \hat{z}(x,t) - z(x,t)$), is given by the difference of (6.4)-(6.5) and (6.1)-(6.2),

$$\begin{aligned} \frac{\partial e_i}{\partial t} &= D_i \frac{\partial^2 e_i}{\partial x^2} - v_i \frac{\partial e_i}{\partial x} + k_i e_i + g_i^T \left(r[\sigma + \zeta] - r[\sigma] \right) - L_d(C\hat{z} - y) \\ e(x,t) &= \left[\begin{array}{ccc} e_1(x,t), & \cdots, & e_n(x,t) \end{array} \right]^T \\ \zeta(x,t) &= He(x,t) \end{aligned} \tag{6.6}$$

for $x \in (0,1), t > 0$, $i = 1, \ldots, n$, boundary conditions

$$\begin{aligned} x = 0, \qquad t \geq 0 : \ & \frac{\partial e_i}{\partial x}(0,t) = \alpha_{0,i} e_i(0,t) - L_0(C\hat{z} - y), \\ x = 1, \qquad t \geq 0 : \ & \frac{\partial e_i}{\partial x}(1,t) = \alpha_{1,i} e_i(1,t) - L_1(C\hat{z} - y), \end{aligned} \tag{6.7}$$

$i = 1, \ldots, n$, and initial conditions $x \in [0,1] : e(x,t_0) = e_0(x)$.

In the spirit of the preceding tubular reactor application studies, two main mechanisms can be identified: (i) a linear transport mechanism, and (ii) a kinetic mechanism. Accordingly, the estimation error dynamics can be viewed as a (feedback) interconnection of (i) a linear dynamical transport subsystem Σ_T and (ii) a nonlinear static kinetic subsystem Σ_K. Figure 6.1 illustrates this dynamical inter-

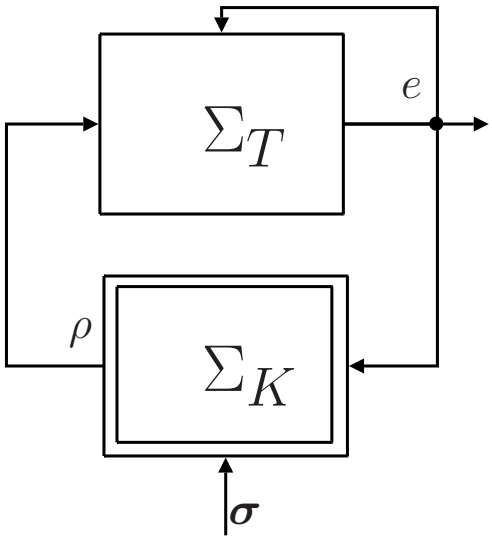

Figure 6.1: Basic Interconnection Structure of transport and kinetic component of the estimation error dynamics (6.6)-(6.7).

connection structure. In correspondence to these main components, the estimation error dynamics is written in Popov-Lur'e form [101, 73]

$$\begin{aligned} \frac{\partial e(x,t)}{\partial t} &= A_L e(x,t) + G\nu(x,t), \\ \zeta(x,t) &= He(x,t) \\ \nu(x,t) &= -\rho(\sigma(x,t);\zeta(x,t)), \end{aligned} \tag{6.8}$$

with $A_L \triangleq A - LC$, $L(0) = L_0, L(1) = L_1, L\big|_{x\in(0,1)} = L_d(x)$ and the operator

$$A = \mathrm{diag}(A_i), \quad A_i = D_i \frac{\partial^2}{\partial x^2} - v_i \frac{\partial}{\partial x} + k_i, \tag{6.9}$$

with domain of definition characterized by the boundary conditions

$$\mathrm{Dom}(A) = \left\{ e \in L^2([0,1], X \subseteq \mathbb{R}^n) : e, \frac{de}{dx} \text{ a.c. and (6.7) holds.} \right\}, \tag{6.10}$$

and the kinetic gain vector

$$G = \begin{bmatrix} g_1^T \\ \vdots \\ g_n^T \end{bmatrix}. \tag{6.11}$$

Based on this identification of two main components of the estimation error dynamics, the dissipation properties are analyzed in the sequel, in order to obtain a Lyapunov-like exponential convergence criteria.

6.2.3 Error Dissipation

In the light of Lyapunov theory for distributed parameter systems [63, 65], the squared error potential energy dissipation is analyzed, for the sake of general convergence conditions, in the understanding that the deviation from the zero estimation error $e(x,t) = 0$ can be measured using this energy. For this aim, the dissipation components corresponding to the linear dynamical transport and the nonlinear kinetic subsystem are identified.

The squared error potential energy is given by

$$E(e(x,t)) = \int_0^1 e^T(x,t)W(x)e(x,t)dx, \tag{6.12}$$

where $W(x) = W^T(x) > 0$ is a positive definite matrix-valued function, which represents an important design degree of freedom, as has turned out in the preceding application studies on the tubular reactor estimation problem. The corresponding dissipation is given by

$$\begin{aligned} \frac{dE(e)}{dt} &= \mathcal{D}_K + \mathcal{D}_T \\ \mathcal{D}_K &= -2\int_0^1 e^T WG\rho dx \\ \mathcal{D}_T &= -\int_0^1 e^T \left(WA_L + A_L^* W\right) e dx, \end{aligned} \tag{6.13}$$

where $A_L^* = A^* - (LC)^*$ is the adjoint of the innovated transport operator [34, 91, 92, 93, 95, 38, 39], with

$$\begin{aligned} x \in (0,1):\ A^*e &= D\frac{\partial^2 e}{\partial x^2} + V\frac{\partial e}{\partial x} + Ke, \quad i = 1,\ldots,n \\ x = 0:\ \frac{\partial e}{\partial x}(0,t) &= \alpha_{1,i}e(0,t), \\ x = 1:\ \frac{\partial e}{\partial x}(1,t) &= \alpha_{0,i}e(1,t), \end{aligned} \tag{6.14}$$

and $(L_dC)^*$ depends on the structure of the chosen correction mechanism. [1] According to the preceding tubular reactor studies, the design is based on the requirement of the strict dissipation property

$$\frac{d}{dt}E \leq -2\lambda E, \tag{6.15}$$

in the understanding that such an inequality implies exponential stability (see Lemma 2.1). As discussed in the preceding chapters, the bounding of the dissipation components $\mathcal{D}_K$ and $\mathcal{D}_T$ in equation (6.13) to achieve an inequality of the kind (6.15) is a non-trivial task. Due to the quadratic structure of the energy function $E(e)$ (6.12), the strict dissipation condition (6.15) requires to find quadratic bounds for the dissipation components $\mathcal{D}_T$ and $\mathcal{D}_K$. In virtue of the particular structure of the linear

[1] Remember that the adjoint B^* of an operator B can be determined via the relation $\langle v, Bw\rangle = \langle B^*v, w\rangle$ and taking into account the particular form of the inner product $\langle\cdot,\cdot\rangle$ used for the design.

transport subsystem, the bounds for the linear dissipation component can, in principle, be drawn employing the approaches presented in the preceding tubular reactor studies, i.e. (i) modal innovation and corresponding bounding of the linear dissipation $\mathcal{D}_T$ in terms of the dominant eigenvalues, or (ii) using point and distributed injection mechanisms and bounding the dissipation $\mathcal{D}_T$ using direct functional analytic integral transformations. The nonlinear kinetic dissipation component $\mathcal{D}_K$ can, in principle, be bounded using sector conditions of the type employed in the preceding analysis. This shows, that the proposed design methodology for the tubular reactor applications, are generic, in the sense that they can be applied directly to the class of considered multi-species transport reaction systems with several simultaneous reactions.

From a system theoretic viewpoint, the proposed dissipative observer design method can be formulated in the more general context of dissipativity properties of the invoked open subsystems, interconnected in the estimation error dynamics, in the understanding that the theory of Lyapunov for the present class of systems (6.6)-(6.7) can be concluded from closing the open dissipative subsystems by interconnection. In order to illustrate this generalization within the system theoretic dissipativity framework, in the next section some important dissipativity concepts and properties for infinite-dimensional systems are shortly discussed.

6.3 Some dissipativity concepts in an infinite dimensional set-up

In the spirit of the preceding discussion, some basic dissipativity properties of linear dynamical and nonlinear static systems, and their interconnection in an infinite-dimensional state space set-up are shortly discussed. This allows to identify the dissipative observer design methodology developed for the previous tubular reactor studies in a more general framework,representing an extension of the dissipativity concepts used in lumped systems theory (compare [56, 57, 6]) in the spirit of infinite-dimensional dissipativity theory (some work on this subject can be found e.g. in [102, 103, 58]).

6.3.1 General Concepts

In a system-theoretic framework, the concept of dissipativity is strictly related to the concept of power supply ω, which represents a measure of energy change in a system in terms of its inputs and outputs, i.e. $\omega(\Psi, \nu)$ is a function of inputs ν and outputs Ψ (compare Figure 6.2).[2] The concept of dissipativity, represents a

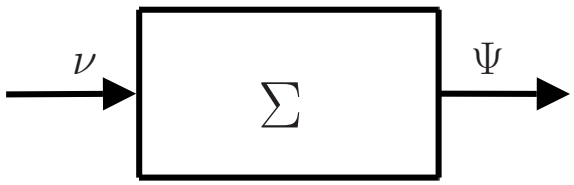

Figure 6.2: General inputν-outputΨ system Σ.

generalization of the concept of passivity, in the sense that it applies to non-quadratic systems [56, 57, 6]. For reasons of applicability, supply rates given by quadratic forms in inputs and outputs are considered, i.e.

$$\omega(\Psi(x,t),\nu(x,t)) = \int_0^1 \begin{bmatrix} \Psi(x,t) \\ u(x,t) \end{bmatrix}^T \begin{bmatrix} Q(x) & S(x) \\ S^T(x) & R(x) \end{bmatrix} \begin{bmatrix} \Psi(x,t) \\ \nu(x,t) \end{bmatrix} dx \qquad (6.16)$$

with appropriate functions $Q(x), = Q^T(x), R(x) = R^T(x), S(x)$. Dissipativity of the system (6.6) with respect to the supply rate ω given by (6.16) can therefore be identified with the fulfillment of an inequality characterizing the change in stored energy $E(e(x,t))$ (6.12) in terms of the supplied power of the kind

$$\frac{dE(e(x,t))}{dt} \leq \int_0^1 \begin{bmatrix} \Psi(x,t) \\ \nu(x,t) \end{bmatrix}^T \begin{bmatrix} Q(x) & S(x) \\ S^T(x) & R(x) \end{bmatrix} \begin{bmatrix} \Psi(x,t) \\ \nu(x,t) \end{bmatrix} dx. \qquad (6.17)$$

[2]The consideration of this issue is actually motivated by the definition of electrical power as a product of voltage and current, i.e. $\omega(V, I) = VI$, taking into account that the input to an electrical circuit is normally given by either of them and the output by the other. Correspondingly, an electrical circuit with m inputs ν (voltages or currents) and m outputs Ψ (currents or voltages, correspondingly) is called passive if $\omega(\Psi, \nu) = \Psi^T\nu \geq 0$, in the sense that, the net-flow of electrical energy (the time-integral over the supplied power) is into the circuit. The concept of passivity found its generalizations directly by the consideration of supply rates given by the product of inputs and outputs of arbitrary systems. Nevertheless, this restricts the class of systems to quadratic ones, in the understanding that the input and output spaces' dimensions are the same, or, more generally speaking, that the input space is dual to the output space, in the sense that an inner product of the form $\omega(\Psi, \nu) = \langle \Psi, \nu \rangle$ is defined.

Correspondingly the system is characterized as (Q, S, R)-dissipative (compare [56, 57, 6, 62] for the finite-dimensional correspondence). It is important to notice that, in this definition, the input ν and output Ψ not necessarily correspond to the physical input and output sets of the system, but represent variables for which the considered dissipativity condition is analyzed. If the system internal states are denoted by $e(x,t)$ and the output Ψ is given by the relation $\Psi = He$, the condition for (Q, S, R)-dissipativity of (6.6) takes the form

$$\frac{dE(t)}{dt} \leq \int_0^1 \begin{bmatrix} e(x,t) \\ \nu(x,t) \end{bmatrix}^T \begin{bmatrix} H^T Q(x) H & H^T S(x) \\ S^T(x) H & R(x) \end{bmatrix} \begin{bmatrix} e(x,t) \\ \nu(x,t) \end{bmatrix} dx. \tag{6.18}$$

Furthermore, the corresponding condition for strict dissipation in the sense of (6.15) takes the form

$$\frac{dE(e(x,t))}{ddt} \leq \int_0^1 \begin{bmatrix} e(x,t) \\ \nu(x,t) \end{bmatrix}^T \begin{bmatrix} H^T R(x) H - 2\lambda W(x) & H^T S(x) \\ S^T(x) H & Q(x) \end{bmatrix} \begin{bmatrix} e(x,t) \\ \nu(x,t) \end{bmatrix} dx. \tag{6.19}$$

In order to exploit this definition for the purpose of designing the data-assimilation structure of the observer (6.4), the dissipativity of (i) linear systems with state-space representation, (ii) static nonlinear systems, and (iii) linear systems with nonlinear state-feedback has to be characterized.

6.3.2 Linear Systems

First consider the case of a linear system with a state-space representation ([104, 105, 80, 106, 107, 39])

$$\begin{aligned} \frac{\partial e(x,t)}{\partial t} &= Ae(x,t) + G\nu(x,t) \\ \Psi(x,t) &= He(x,t), \end{aligned} \tag{6.20}$$

where $A = D\dfrac{\partial^2}{\partial x^2} - V\dfrac{\partial}{\partial x} + K$ is the convective-diffusive transport operator corresponding to system (6.6), with D, V and K are diagonal matrixes containing the respective parameters D_i, v_i and k_i. Actually, (6.20) represents the linear part of the estimation error dynamics (6.6) with (i) A being the linear transport operator with correction mechanisms L_i, $i = 0, d, 1$, (ii) $\nu = \rho(\sigma; \zeta)$ being the induced reaction rate

error, and (iii) $\Psi = \zeta = He$ being the argument of $\rho(\sigma;\cdot)$. In order to formulate the dissipation of the energy

$$E(e) = \int_0^1 e^T W e dx \tag{6.21}$$

in terms of the operator A, note that actually E can be expressed as a weighted inner product of the Hilbert space $Z = L^2([0,1], X)$, i.e. $E(e) = \langle e, We\rangle$. Correspondingly, the dissipation can be written in the following form

$$\begin{aligned}\frac{dE(e)}{dt} &= \left\langle \frac{\partial e}{\partial t}, We \right\rangle + \left\langle e, W\frac{\partial e}{\partial t} \right\rangle = \langle (Ae + G\nu), We\rangle + \langle e, W(Ae+G\nu)\rangle \\ &= \langle e, (A^*W + WA)e\rangle + 2\langle e, WG\nu\rangle ,\end{aligned}$$

with A^* given in (6.14). Accordingly, the strict (Q,S,R) dissipation inequality (6.19) becomes (cp. [102])

$$\begin{aligned}\frac{dE(e)}{dt} &= \int_0^1 \begin{bmatrix} e(x,t) \\ \nu(x,t)\end{bmatrix}^T \begin{bmatrix} W(x)A + A^*W(x) & G \\ G^T & 0\end{bmatrix} \begin{bmatrix} e(x,t) \\ \nu(x,t)\end{bmatrix} dx \\ &\leq \int_0^1 \begin{bmatrix} e(x,t) \\ \nu(x,t)\end{bmatrix}^T \begin{bmatrix} H^TQ(x)H - 2\lambda W(x) & H^TS(x) \\ S^T(x)H & R(x)\end{bmatrix} \begin{bmatrix} e(x,t) \\ \nu(x,t)\end{bmatrix}.\end{aligned} \tag{6.22}$$

Note that condition (6.22) implies two degrees of freedom: (i) the strict dissipation λ (directly related to convergence velocity), and (ii) the (spatial) weighting function $W(x) = W^T(x) > 0$ in the sense of modulating the spatial shape of the considered projection in requirement (6.22).

6.3.3 Static (nonlinear) systems

If one considers the static relation

$$\Psi = \rho(\sigma;\nu), \quad \rho(\sigma;0) = 0, \tag{6.23}$$

the (Q,S,R)-dissipativity inequality (6.16) obtains another form, because the system is memoryless. As dissipativity with respect to a given supply rate ω, depending on the input-output pair (here correspondingly (ν,Ψ)), signifies that the net flux of power supply is into the system [56], the corresponding (Q,S,R)-dissipativity

condition takes the form

$$0 \leq \int_0^1 \begin{bmatrix} \Psi(x,t) \\ \nu(x,t) \end{bmatrix}^T \begin{bmatrix} Q(x) & S(x) \\ S^T(x) & R(x) \end{bmatrix} \begin{bmatrix} \Psi(x,t) \\ \nu(x,t) \end{bmatrix} dx \tag{6.24}$$

(see [56, 57, 62, 6] for the finite-dimensional correspondence). Note that this concept in particular includes the sector conditions employed in Chapters 4 and 5. Consequently, such a static system's dissipativity condition can be employed in order to characterize the corresponding dissipation of the nonlinear part of the estimation error dynamics' dissipation (6.13) (compare Chapters 4 and 5).

6.3.4 Linear systems with (nonlinear) output-feedback

With these definitions the internal stability of a linear system with (nonlinear) output feedback can be treated in a straight forward manner. Consider the system

$$\begin{aligned} \frac{\partial e(x,t)}{\partial t} &= Ae(x,t) + G\nu(x,t) \\ \Psi(x,t) &= He(x,t) \\ \nu(x,t) &= -\rho(\sigma(x,t); \zeta(x,t)), \end{aligned} \tag{6.25}$$

representing the two-subsystem interconnection (6.8), i.e. the interconnection of (i) a dynamic system with exogenous input $\nu(x,t)$ and output $\Psi(x,t) = \zeta(x,t) = He(x,t)$ and (ii) a static (nonlinear) system $\nu(x,t) = -\rho(\sigma(x,t); \Psi(x,t))$. Note that this type of systems forms the basis of the study of absolute stability of linear systems in nonlinear feedback interconnections (see e.g. [101, 73, 108, 6, 109, 5, 110, 111]). Actually the presented concepts are already sufficient to state a powerful tool in the stability analysis of such system interconnections, which is stated next considering the natural convergence behavior of the estimation error dynamics without correction mechanisms (i.e. $L_i = 0$, $i = 0, d, 1$), and which will be subsequently employed to draw sufficient conditions for the observer convergence.

Theorem 6.1. *Consider the system*

$$\begin{aligned} \frac{\partial e(x,t)}{\partial t} &= Ae(x,t) + G\nu(x,t) \\ \zeta(x,t) &= He(x,t) \\ \nu(x,t) &= -\rho(\sigma(x,t); \zeta(x,t)), \end{aligned} \tag{6.26}$$

with A corresponding to the linear diagonal transport operator in (6.6) (with $L_i = 0$, $i = 0, d, 1$) and the corresponding boundary conditions. Let $\rho(\sigma; \cdot)$ satisfy a (Q, S, R)-dissipativity condition (6.24). The zero solution $e(x,t) = 0$ is g.e.s. with convergence rate $\lambda > 0$ and amplitude $a = \sqrt{w^*/w_*}$, $w^* = \max_{x\in[0,1]} eig(W(x))$, $w_* = \min_{x\in[0,1]} eig(W(x))$, i.e.

$$||e(x,t)||_{L^2([0,1], X\subseteq\mathbb{R}^n)} \leq a\, ||e_0(x)||_{L^2([0,1], X\subseteq\mathbb{R}^n)}\, e^{-\lambda t}, \tag{6.27}$$

if the linear system $\Sigma(A, G, H)$ is $(-R, S^T, -Q)$ strictly dissipative (6.22), with strict dissipation $\lambda > 0$, then .

(*Proof in Appendix O.*)

Note that the corresponding condition can be expressed in terms of the compact linear operator inequality (LOI)

$$\int_0^1 \begin{bmatrix} e \\ \nu \end{bmatrix}^T \begin{bmatrix} WA + A^*W + 2\lambda W + H^TRH & WG - H^TS^T \\ G^TW - SH & Q \end{bmatrix} \begin{bmatrix} e \\ \nu \end{bmatrix} dx \leq 0. \tag{6.28}$$

6.4 Convergence Criteria for the Dissipative Observer

Based on the preceding analysis and results, sufficient conditions for the observer convergence are drawn, invoking (i) the dissipativity properties of the nonlinear rate error $\rho(\sigma; \zeta)$, and inherently (ii) the correction gain structure corresponding to the injection mechanisms L_i, $i = 0, d, 1$, and (iii) the system specific transport and reaction parameters.

Theorem 6.2. *Consider the system (6.1), together with the observer (6.4). Let (i) A be given by (6.9), where D, V and K are diagonal matrixes containing the respective parameters D_i, v_i and k_i, and L is a vector consisting of all the $L_{d,i}, i = 1, \ldots, n$, (ii) $D(A_L)$ given by (6.10), and (iii) $\rho(\sigma; \zeta) = r(\sigma + \zeta) - r(\sigma)$ be (Q, S, R)-dissipative (6.24) for all σ. The zero estimation error $e(x,t) = 0$ is g.e.s. with rate $\lambda > 0$, and amplitude $a = \sqrt{w^*/w_*}$, $w^* = \max_{x\in[0,1]} eig(W(x))$, $w_* = \min_{x\in[0,1]} eig(W(x))$, i.e.*

$$||e(x,t)||_{L^2([0,1], X\subseteq\mathbb{R}^n)} \leq a\, ||e_0(x)||_{L^2([0,1], X\subseteq\mathbb{R}^n)}\, e^{-\lambda t}, \tag{6.29}$$

if the following LOI is satisfied

$$\int_0^1 \begin{bmatrix} e \\ \nu \end{bmatrix}^T \begin{bmatrix} WA_L + A_L^* W + 2\lambda W + H^T R H & WG - H^T S^T \\ G^T W - SH & Q \end{bmatrix} \begin{bmatrix} e \\ \nu \end{bmatrix} dx \leq 0, \tag{6.30}$$

i.e. if the linear system $\Sigma(A_L, G, H)$ *is* $(-R, S^T, -Q)$*-strictly dissipative in the state.*

(*Proof in Appendix P.*)

6.5 Discussion of the results

Linear operator inequalities (LOIs) of the type (6.30) and (6.22) are known to be difficult to solve in the general case [102, 66]. Nevertheless, it is known, that for parabolic systems analytic solutions can be found (see e.g. [112, 66]) as has been shown in the previous tubular reactor studies. In particular, the satisfaction of such LOI can be carried out using either of the approaches presented for the particular tubular reactor cases, i.e.

- *Spectral approach*: Fourier series expansion of the estimation error in the basis of eigenfunctions of the linear transport operator $A = D\frac{\partial^2}{\partial x^2} - V\frac{\partial}{\partial x} + K$ over the domain $[0, 1]$ corresponding to the boundary conditions in (6.6), and modal innovation over a finite number of modes corresponding to the slow eigenvalues, such that the resulting maximal improved eigenvalue λ^*, which bounds the linear dissipation according to

$$\int_0^1 e^T(WA[e] + A^*[We] - LC[e])dx \leq \lambda^* \int_0^1 e^T We dx \tag{6.31}$$

  is sufficiently negative to ensure the fulfillment of the LOI (6.30). This approach implies a requirement on the sensor location related to the possibility of improving the eigenvalue distribution of the operator A.

- *Variational approach*: Integrating the linear differential expressions by parts and employing integral inequalities, to express them in a quadratic form invoking $e(x, t)$ and the values it attains on the boundaries $x = 0, 1$. The correction expression in the domain L_d can be chosen as a mixed collocated point and/ or distributed injection mechanism.

These approaches are not presented in a general manner because (i) their development in the preceding chapters 4 and 5 showed in a clear fashion how they can be applied to particular cases of practical interest, and (ii) their formulation for the system (6.1) does not reveal fundamentally new insight in comparison to the presented tubular reactor studies.

6.6 Summary

Some implications of the previously developed dissipative observer design methodology have been presented for a class of multi-species transport reaction systems with multiple simultaneous reactions. A generalized dissipativity framework has been presented for the convergence analysis. Furthermore, it has been clarified that the basic approaches used in the tubular reactor studies presented in the previous chapters can be employed in order to obtain explicit criteria for the assignment of the correction mechanism structure and corresponding explicit convergence conditions.

As pointed out in the introduction and at the beginning of this chapter, the presented generalized design framework represents a methodological contribution in the field of transport-reaction system observer design, because

- there are already no specific design methods for multi-species transport-reaction systems with multiple simultaneous reactions
- the existing methods which apply to this system class are either very sophisticated and hard to imply, or bear mathematical rigor
- for continuous and tubular reactor application problems it turned out in the previous chapters, that the dissipative observer allows for innovating results with respect to (i) systematic design, (ii) convergence improvement, (iii) physical interpretation and (iv) mathematical rigor.

Chapter 7

Conclusions

The present study contributed some important issues concerning the design of nonlinear observers for a class of agitated and tubular reactors. The particular object of study has been a class of non-isothermal tubular reactors with boundary and/ or domain point temperature (and concentration) measurements. The corresponding estimation problem has been tackled using a dissipativity approach. The particular cases which have been considered are

- the concentration and temperature estimation and OF control problems for a jacketed, exothermic continuous stirred tank reactor with non-monotonic reaction rate,
- the concentration profile estimation problem for an isothermal tubular reactor with concentration measurements at the boundary and in some point(s) of the domain,
- the estimation of concentration and temperature profiles of a non-isothermal tubular reactor with boundary and/ or domain temperature point measurements.

The corresponding solutions are drawn in the light of a phenomenologically motivated exploitation of the process inherent dissipation mechanisms corresponding to linear (convective-diffusive) transport and nonlinear reaction.

The problems have been addressed in a unifying framework by combining concepts and methods of (i) chemical engineering sciences, (ii) modern estimation (and control) theory for lumped and distributed parameter systems, (iii) physical and system-theoretic concepts of dissipativity, and (iv) mathematical analysis.

In the light of previous studies recorded in the chemical process engineering literature, the dissipative observers designed for these case studies represent important innovations, in the understanding of

- systematic design
- convergence behavior improvement
- mathematical rigor
- simple implementation
- convergence criteria with physical meaning.

These results have been possible due to a fruitful combination of the above mentioned mathematical, physical and system theoretic concepts, as well as analysis and design methods.

Finally, some implications of the obtained design method in the perspective of more general multi-species transport-reaction systems with various simultaneous chemical reactions have been drawn yielding a general exponential convergence result for a dissipative observer with injections of general kind for the regarded system class.

Appendix A

Proof of Proposition 3.1

Proof. Let $\xi \triangleq [\epsilon_T, \quad \zeta]^T$. In the case that the LMI (3.24) is satisfied, the function $E = 1/2\,||\xi||^2$ (3.15) is a Lyapunov function. It follows by the comparison lemma [73]

$$||\xi(t)||^2 \leq ||\xi(0)||^2 e^{-\min\hat{\lambda}\,t},$$

with $\min\hat{\lambda}$ being the minimal eigenvalue of the matrix in (3.24). It follows

$$||\xi(t)|| \leq ||\xi(0)||\, e^{-\min\hat{\lambda}/2\,t},$$

i.e. if there are no parameter ($\tilde{p}$), exogenous inputs ($\tilde{d}$), and measurement ($\tilde{y}$) errors, the estimation error converges exponentially to zero with rate $\lambda = \min\hat{\lambda}/2$. Furthermore, in the presence of such errors, the estimation error dynamics read

$$\begin{aligned}\dot{\xi} &= \begin{bmatrix} -(\theta+\eta+\kappa_T) & 0 \\ -\kappa_c + \kappa_r(\eta+\kappa_T) & -\theta \end{bmatrix} \xi + \begin{bmatrix} -\beta \\ 1+\kappa_r\beta \end{bmatrix} \nu - \begin{bmatrix} \kappa_c \\ \kappa_T \end{bmatrix} \tilde{y} + \varphi(x,\xi;\tilde{p},\tilde{d},\tilde{y}) \\ \nu &= -\rho(\zeta + \kappa_r\epsilon_T, y; \zeta),\end{aligned} \tag{A.1}$$

where φ is a Lipschitz-continuous function in its arguments and $\varphi(x,\xi;0,0,0) = 0$. It follows that

$$\dot{E} \leq -\min\hat{\lambda}E + \xi^T \left(\begin{bmatrix} -\kappa_c \\ -\kappa_T \end{bmatrix} \tilde{y} + \varphi(x,\xi;\tilde{p},\tilde{d},\tilde{y}) \right).$$

Consequently, the P-stability of $\xi = 0$ follows by Definition 2.1.

Furthermore, it is necessary that all diagonal elements are positive. This condition can always be met, if and only if $\theta + s_u s_l$ for all $\theta \geq \theta^-$. On the other hand, if this condition holds, the particular choice of the gains

$$\begin{aligned} \kappa_r &= \frac{s_u + s_l - 1}{\beta} \\ \kappa_T &> \frac{\beta^2}{4} - \theta - \eta \\ \kappa_c &= \kappa_r(\eta + \kappa_T), \end{aligned}$$

ensures the fulfillment of the LMI (3.24) according to Schur's Lemma. □

Appendix B

Derivation of the closed-loop dynamics (3.35)

Remember the reactor dynamics in deviation form

$$\begin{aligned} \dot{e_c} &= -r(c, T, p_r) + \theta_r(c_e - c), \quad c(0) = c_0 \\ \dot{e_T} &= \beta r(c, T, p_r) + \theta_r(T_e - T) - \eta(T - T_{c,r}), \quad T(0) = T_0 \end{aligned} \tag{B.1}$$

where $\theta_r, T_{c,r}$ correspond to the real control signals, derived from the designed control laws

$$\begin{aligned} \theta^* &= \frac{-k_c e_c + r}{c_e - c}, \\ T_c^* &= \frac{-k_T e_T - \beta r - \theta^*(T_e - T) + \eta T}{\eta}, \end{aligned} \tag{B.2}$$

through the substitution of the real states T, c by the estimated ones $\hat{T}, \hat{c}$ (and corresponding estimation errors $\epsilon_T = \hat{T} - T, \epsilon_c = \hat{c} - c$). The real inputs are thus

$$\begin{aligned} \theta_r &= \frac{-k_c e_c + r - k_c \epsilon_c + \rho}{c_e - \hat{c}}, \\ T_{c,r} &= \frac{-k_T(e_T + \epsilon_T) - \beta(r + \rho) - [\theta^* + \theta_r - \theta^*](T_e - \hat{T}) + \eta \hat{T}}{\eta}. \end{aligned} \tag{B.3}$$

Further, from (3.18) it follows that ρ can be expressed using the reaction rate slope function σ

$$\rho = r(c + \epsilon_c - \kappa_r \epsilon_T, y) - r(c, y) = \sigma(c, \epsilon_c, y) \left[\epsilon_c - \kappa_r \epsilon_T\right]. \tag{B.4}$$

Consequently the resulting control-signal offset can be expressed as

$$\begin{aligned}
\theta_r - \theta^* &= \frac{[-k_c e_c + r - k_c\epsilon_c + \rho](c_e - c) - [-k_c e_c + r](c_e - c - \epsilon_c)}{(c_e - \hat{c})(c_e - c)} \\
&= (\theta^* - k_c)\,\frac{\epsilon_c}{c_e - \hat{c}} + \frac{\rho}{c_e - \hat{c}} \\
&= (\theta^* - k_c + \sigma)\,\frac{\epsilon_c}{c_e - \hat{c}} - \frac{\kappa_r\sigma\epsilon_T}{c_e - \hat{c}}, \\
T_{c,r} - T_c^* &= \frac{-k_T(e_T + \epsilon_T) - \beta(r + \rho) - [\theta^* + \theta_r - \theta^*](T_e - T - \epsilon_T) + \eta(T + \epsilon_T)}{\eta} \\
&\quad - \frac{-k_T e_T - \beta r - \theta^*(T_e - T) + \eta T}{\eta} \\
&= -\frac{(k_T - \eta - \theta_r)\epsilon_T + \beta\rho + [\theta_r - \theta^*](T_e - T)}{\eta} \\
&= -\frac{(k_T - \eta - \theta_r)\epsilon_T + \beta\sigma\,[\epsilon_c - \kappa_r\epsilon_T] + [\theta_r - \theta^*](T_e - T)}{\eta} \\
&= -\frac{(k_T - \eta - \theta_r - \kappa_r\beta\sigma)\,\epsilon_T + \beta\sigma\epsilon_c + [\theta_r - \theta^*](T_e - T)}{\eta}.
\end{aligned} \tag{B.5}$$

$$\tag{B.6}$$

With these signals the control error dynamics are determined (compare (B.1),(B.5),(B.6)):

$$\begin{aligned}
\dot{e}_c &= -r + [\theta_r + \theta^* - \theta^*](c_e - c) \\
&= -k_c e_c + [\theta_r - \theta^*](c_e - c) \\
&= -k_c e_c + (\theta^* - k_c + \sigma)\,\frac{c_e - c}{c_e - \hat{c}}\epsilon_c - \kappa_r\sigma\frac{c_e - c}{c_e - \hat{c}}\epsilon_T \\
&= -k_c e_c + \frac{(\theta^* - k_c + \sigma)(c_e - c)}{c_e - \hat{c}}\epsilon_c - \kappa_r\sigma\frac{c_e - c}{c_e - \hat{c}}\epsilon_T, \\
\dot{e}_T &= \beta r + [\theta_r + \theta^* - \theta^*](T_e - T) - \eta(T - [T_{c,r} + T_c^* - T_c^*]) \\
&= -k_T e_T + [\theta_r - \theta^*](T_e - T) + \eta(T_{c,r} - T_c^*) \\
&= -k_T e_T + [\theta_r - \theta^*](T_e - T) + \eta\left(-\frac{(k_T - \eta - \theta_r - \kappa_r\beta\sigma)\,\epsilon_T + \beta\sigma\epsilon_c + [\theta_r - \theta^*](T_e - T)}{\eta}\right) \\
&= -k_T e_T - \beta\sigma\epsilon_c - (k_T - \eta - \theta_r - \kappa_r\beta\sigma)\,\epsilon_T.
\end{aligned}$$

On the other hand the estimation error dynamics for the chosen data-assimilation scheme is given by

$$\begin{aligned}
\dot{\epsilon}_c &= -\rho - \theta_r\epsilon_c - \kappa_c\epsilon_T = -\left[\sigma + \theta_r\right]\epsilon_c - \left[\kappa_c - \kappa_r\sigma\right]\epsilon_T \\
\dot{\epsilon}_T &= \beta\rho - \left[\kappa_T + \theta_r + \eta\right]\epsilon_T = -\left[\kappa_T + \theta_r + \eta + \kappa_r\beta\sigma\right]\epsilon_T + \beta\sigma\epsilon_c
\end{aligned} \tag{B.7}$$

Consequently one obtains the following closed-loop interconnection dynamics

$$\begin{aligned}
\dot{e}_c &= -k_c e_c + \frac{(\theta^* - k_c + \sigma)(c_e - c)}{c_e - \hat{c}}\epsilon_c - \kappa_r \sigma \frac{c_e - c}{c_e - \hat{c}}\epsilon_T \\
\dot{e}_T &= -k_T e_T - \beta\sigma\epsilon_c - (k_T - \eta - \theta_r - \kappa_r\beta\sigma)\,\epsilon_T \\
\dot{\epsilon}_c &= -[\theta_r + \sigma]\epsilon_c - [\kappa_c - \kappa_r\sigma]\,\epsilon_T \\
\dot{\epsilon}_T &= -[\theta_r + \eta + \kappa_T + \kappa_r\beta\sigma]\epsilon_T + \beta\sigma\epsilon_c.
\end{aligned} \tag{B.8}$$

Appendix C

Proof of Proposition 3.2

Proof. Consider the closed-loop dynamics in the following re-ordered form

$$\begin{aligned}
\dot{e}_c &= -k_c e_c + \frac{(\theta^* - k_c + \sigma)(c_e - c)}{c_e - \hat{c}}\epsilon_c - \kappa_r \sigma \frac{c_e - c}{c_e - \hat{c}}\epsilon_T \\
\dot{\epsilon}_c &= -[\theta_r + \sigma]\epsilon_c - [\kappa_c - \kappa_r \sigma]\,\epsilon_T, \\
\dot{e}_T &= -k_T e_T - \beta\sigma\epsilon_c - (k_T - \eta - \theta_r - \kappa_r\beta\sigma)\,\epsilon_T \\
\dot{\epsilon}_T &= -[\theta_r + \eta + \kappa_T + \kappa_r\beta\sigma]\epsilon_T + \beta\sigma\epsilon_c.
\end{aligned} \tag{C.1}$$

Correspondingly, as a first step, a closed-loop stability condition is given in the following Lemma.

Lemma C.1. *The actual reactor (2.14) with the proposed dynamic OF controller (3.34) yields a P-stable (2.16) closed loop system (3.35) if: the (reactor and estimator states, exogenous input, measurement and actuator) disturbance sizes (δ, ϵ), and the control (k_c, k_T) and estimator $(\kappa_c, \kappa_T, \kappa_r)$ gains satisfy the LMI*

$$Q \triangleq \begin{bmatrix}
k_c & -\frac{[\theta^* - k_c + \sigma](c_e - c)}{2(c_e - \hat{c})} & 0 & \kappa_r\sigma\frac{c_e - c}{2(c_e - \hat{c})} \\
-\frac{[\theta^* - k_c + \sigma](c_e - c)}{2(c_e - \hat{c})} & \theta_r + \sigma & \frac{\beta\sigma}{2} & \frac{\kappa_c - (\kappa_r + \beta)\sigma}{2} \\
0 & \frac{\beta\sigma}{2} & k_T & \frac{k_T - \eta - \theta_r - \kappa_r\beta\sigma}{2} \\
\kappa_r\sigma\frac{c_e - c}{2(c_e - \hat{c})} & \frac{\kappa_c - (\kappa_r + \beta)\sigma}{2} & \frac{k_T - \eta - \theta_r - \kappa_r\beta\sigma}{2} & \theta_r + \eta + \kappa_T + \kappa_r\beta\sigma
\end{bmatrix} > 0, . \tag{C.2}$$

for all $y \in [T^-, T^+]$. Furthermore, if $(\tilde{d}, \tilde{p}) = (0, 0)$, the exponential convergence follows.

Proof. Consider the Lyapunov function $V = 1/2(e_c^2 + \epsilon_c^2 + e_T^2 + \epsilon_T^2)$. The corre-

sponding dissipation is strictly negative if the LMI (C.2) is satisfied. The exponential convergence in the errorless case follows with rate fixed by the smallest eigenvalue $\min \lambda(Q) > 0$. Furthermore, as $||B_e||$ (in (3.38)) is bounded, and the error-dependence of the estimation error dynamics is Lipschitz bounded, the P-stability follows for bounded parameter ($\tilde{p}$), exogenous input ($\tilde{d}$), and measurement ($\tilde{y}$) errors. □

According to Lemma C.1 the accomplishment of LMI (C.2) is sufficient for exponential stability of the nominal closed-loop dynamics. The positive definiteness can be concluded if the leading principal minors M_1 to M_4 are all positive. Accordingly the following conditions have to be satisfied:

$$\theta_r + \sigma > 0,\ M_2 = k_c(\theta_r + \sigma) - \frac{[\theta^* - k_c + \sigma]^2(c_e - c))^2}{4(c_e - \hat{c})^2} > 0,$$
$$M_3 = k_T M_2 - k_c \frac{\beta^2 \sigma^2}{4} > 0.$$

Note that, due to physical reasons (mass conversion), the terms $c_e - c$ and $c_e - \hat{c}$ are always positive (in the last case this holds at least in a practical, sufficiently small, region around the SS). Finally it has to be shown that $M_4 = \det Q > 0$. Sufficient for this requirement is that the Schur complement of the lower-right 2×2 temperature submatrix in Q is positive. The positivity of this submatrix is a necessary condition for the positivity of Q which reads

$$k_T(\theta_r + \eta + \kappa_T + \kappa_r \beta \sigma) > \frac{(k_T - \eta - \theta_r - \kappa_r \beta \sigma)^2}{4}.$$

If this holds, and the above condition for $M_2 > 0$ is satisfied, then the positivity of the Schur complement of the lower-right 2×2-temperature-submatrix in Q is

sufficient for the positivity of Q. The corresponding condition reads

$$\mathcal{C}_T = \begin{bmatrix} k_T & \frac{k_T-\eta-\theta_r-\kappa_r\beta\sigma}{2} \\ \frac{k_T-\eta-\theta_r-\kappa_r\beta\sigma}{2} & \theta_r+\eta+\kappa_T+\kappa_r\beta\sigma \end{bmatrix} -$$
$$\begin{bmatrix} 0 & \frac{\beta\sigma}{2} \\ \kappa_r\sigma\frac{c_e-c}{2(c_e-\hat{c})} & \frac{\kappa_c-(\kappa_r+\beta)\sigma}{2} \end{bmatrix} \begin{bmatrix} k_c & -\frac{[\theta^*-k_c+\sigma](c_e-c)}{2(c_e-\hat{c})} \\ -\frac{[\theta^*-k_c+\sigma](c_e-c)}{2(c_e-\hat{c})} & \theta_r+\sigma \end{bmatrix}^{-1} \begin{bmatrix} 0 & \kappa_r\sigma\frac{c_e-c}{2(c_e-\hat{c})} \\ \frac{\beta\sigma}{2} & \frac{\kappa_c-(\kappa_r+\beta)\sigma}{2} \end{bmatrix}$$
$$= \begin{bmatrix} k_T & \frac{k_T-\eta-\theta_r-\kappa_r\beta\sigma}{2} \\ \frac{k_T-\eta-\theta_r-\kappa_r\beta\sigma}{2} & \theta_r+\eta+\kappa_T+\kappa_r\beta\sigma \end{bmatrix}$$
$$-\frac{1}{M_2}\begin{bmatrix} k_c\frac{\beta^2\sigma^2}{4} & \frac{\beta\sigma}{2}\left(\frac{\kappa_r\sigma(c_e-c)}{2(c_e-\hat{c})}\left[\frac{[\theta^*-k_c+\sigma](c_e-c)}{2(c_e-\hat{c})}\right]+k_c\frac{\kappa_c-[\kappa_r+\beta]\sigma}{2}\right) \\ \star & \kappa_r\sigma\frac{[\theta^*-k_c+\sigma](c_e-c)(\kappa_c-[\kappa_r+\beta]\sigma)(c_e-c)}{4(c_e-\hat{c})^2}+(\theta_r+\sigma)\frac{(\kappa_r\sigma(c_e-c))^2}{4(c_e-\hat{c})^2}+k_c\frac{(\kappa_c-[\kappa_r+\beta]\sigma)^2}{4} \end{bmatrix} > 0$$

Consequently, choosing k_T so that $M_3 > 0$, the gain κ_T has to be chosen so that the above difference is positive, what is equivalent to

$$\kappa_T > \varpi(k_c, k_T, \kappa_c, \kappa_r),$$

where $\varpi(\cdot)$ is a bounded function of its arguments (if the condition $M_2 > 0$ holds). Finally, rewriting the given conditions in terms of the functions (3.37), one obtains the conditions (3.36). □

Appendix D

Fourier expansion of the linear mass transport dynamics

Let $\{\Phi_n(x)\}_{n\in\mathbb{N}}$ be any orthonormal basis of the Hilbert-space $Z = L^2$, i.e. $\langle \Phi_l, \Phi_m \rangle = \delta_{lm}$ where δ_{lm} is the Kronecker-δ function. Then any function e in Z can be expressed as a Fourier-expansion

$$e(x,t) = \sum_{k=1}^{\infty} \underbrace{\left(\int_0^1 e(x,t)\Phi_k(x)dx \right)}_{e_k(t)} \Phi_k(x). \tag{D.1}$$

Correspondingly one obtains

$$-\frac{\partial^2 e(x,t)}{\partial x^2} + P_e \frac{\partial e(x,t)}{\partial x} = -\sum_{k=1}^{\infty} e_k(t) \left(\Phi_k'' - P_e \Phi_k' \right). \tag{D.2}$$

Of particular interest are such function basis' $\{\Phi_k\}_{k\in\mathbb{N}}$ in which the derivatives are related for each $k \in \mathbb{N}$ such that for some λ_k

$$\Phi_k'' - P_e \Phi_k' = \lambda_k \Phi_k, \tag{D.3}$$

and the boundary conditions are satisfied

$$\Phi'(0) - P_e \Phi(0) = 0, \quad \Phi'(1) = 0, \tag{D.4}$$

for in this case it holds that

$$-\frac{\partial^2 e(x,t)}{\partial x^2} + P_e \frac{\partial e(x,t)}{\partial x} = -\sum_{k=1}^{\infty} \lambda_k e_k(t) \Phi_k(x). \tag{D.5}$$

One recognizes that (D.3) with (D.4) is the eigenvalue problem corresponding to the linear transport operator

$$Ae = \frac{\partial^2 e}{\partial x^2} - P_e \frac{\partial e}{\partial x}, \quad x = 0: \ \frac{\partial e}{\partial x} = P_e e, \quad x = 1: \ \frac{\partial e}{\partial x} = 0, \tag{D.6}$$

and Φ_k is its k-th eigenfunction associated with the k-th eigenvalue λ_k. Furthermore, the negative of the operator A is a Sturm-Liouville operator [96] and consequently the eigenvalues of A form a decreasing, discrete set and consequently it makes sense to think about a discrete expansion in terms of a sum over the eigenfunctions Φ_k.

Note that the eigenfunctions Φ_k of the operator A do not form an orthogonal set and thus the representation (D.1) can not be employed. Nevertheless, invoking the adjoint operator A^* of A, defined by $\langle Av, w\rangle = \langle v, A^* w\rangle, \quad \forall v, w \in Z$, and the corresponding adjoint eigenfunctions Ψ_k, i.e. the solutions of $A^*\Psi_k = \bar{\lambda}_k \Psi_k$ ($\bar{\lambda}_k$ being the complex conjugate of λ_k), it follows

$$\lambda_l \langle \Phi_l, \Psi_m\rangle = \langle A\Phi_l, \Psi_m\rangle = \langle \Phi_l, A^*\Psi_m\rangle = \left\langle \Phi_l, \bar{\lambda}_m \Psi_m\right\rangle = \lambda_m \langle \Phi_l, \Psi_m\rangle,$$

and consequently

$$(\lambda_l - \lambda_m) \langle \Phi_k, \Psi_l\rangle = 0. \tag{D.7}$$

If $\lambda_l \neq \bar{\lambda}_m$ it follows that the Ψ_k can be normalized such that Φ_k and Ψ_k form a bi-orthogonal set of functions, i.e. $\langle \Phi_l, \Psi_m\rangle = \delta_{lm}$, with δ_{lm} the Kronecker-δ function. Furthermore it can be shown that the set $\{\Phi_k\}_{k\in\mathbb{N}}$ forms a Riesz-basis of $Z = L^2$ [39, 96]. Correspondingly one can express any function $e(x,t) \in Z$ in terms of the bi-orthogonal basis set $(\{\Phi_k\}_{k\in\mathbb{N}}, \{\Psi_k\}_{k\in\mathbb{N}})$ as follows

$$e(x,t) = \sum_{k=1}^{\infty} \langle e(x,t), \Psi_k(x)\rangle \, \Phi_k(x). \tag{D.8}$$

Using this representation of the estimation error $e(x,t)$ one obtains the expression

(D.5) with

$$e_k(t) = \langle e(x,t), \Psi_k(x) \rangle = \int_0^1 e(x,t)\Psi_k(x)dx. \tag{D.9}$$

Appendix E

Proof of Lemma 4.1

The proof is separated into two parts: (i) expression of the dissipation in the light of the Fourier expansion, and (ii) dependence of the dissipation on the modal injection gains.

Dissipation in terms of the Fourier expansion

According to (D.8), the linear integral square error dissipation term in (4.14), without innovation, can be bounded

$$\begin{aligned}
&-\int_0^1 w(x)e(x,t)\left\{-P_e^{-1}\frac{\partial^2 e(x,t)}{\partial x^2}+\frac{\partial e(x,t)}{\partial x}\right\}dx\\
&=-\int_0^1 w(x)\sum_{k=1}^{\infty}e_k(t)\Phi_k(x)\sum_{l=1}^{\infty}(-\lambda_l)e_l(t)\Phi_l(x)dx\\
&=\sum_{k=1}^{\infty}\left(\sum_{l=1}^{k}\lambda_l e_{k-l}(t)e_l(t)\int_0^1\Phi_{k-l}(x)w(x)\Phi_l(x)dx\right).
\end{aligned}$$

Unless the Φ_k are not pairwise orthogonal, one can chose the weighting function

$$w=\exp(-P_e x) \tag{E.1}$$

so that they are with respect to the corresponding weighted inner product $\langle \cdot, w\cdot \rangle$, because in this case

$$\begin{aligned}
&\lambda_k \langle \Phi_k, w\Phi_l \rangle = \langle A\Phi_k, w\Phi_l \rangle = \int_0^1 \left(\frac{\partial^2 \Phi_k}{\partial x^2} - P_e \frac{\partial \Phi_k}{\partial x} \right) w\Phi_l dx \\
&= \left[w\frac{\partial \Phi_k}{\partial x}\Phi_l - w\Phi_k \frac{\partial \Phi_l}{\partial x} - \left(\frac{\partial w}{\partial x} + P_e w \right) \Phi_k \Phi_l \right]_0^1 + \\
&\quad + \int_0^1 \left\{ \Phi_k w \left(\frac{\partial^2 \Phi_l}{\partial x^2} - P_e \frac{\partial \Phi_l}{\partial x} \right) + 2\Phi_k \Phi_l \left[\frac{\partial w}{\partial x} + P_e w \right] + \left[\frac{\partial^2 w}{\partial x^2} + P_e \frac{\partial w}{\partial x} \right] \Phi_k \Phi_l \right\} dx \\
&= \underbrace{\left[w\frac{\partial \Phi_k}{\partial x}\Phi_l - w\Phi_k \frac{\partial \Phi_l}{\partial x} \right]_0^1}_{\stackrel{!}{=} 0} + \int_0^1 \Phi_k w \left(\frac{\partial^2 \Phi_l}{\partial x^2} - P_e \frac{\partial \Phi_l}{\partial x} \right) dx \\
&= \langle \Phi_k, wA\Phi_l \rangle = \langle \Phi_k, w\lambda_l \Phi_l \rangle = \bar{\lambda}_l \langle \Phi_k, w\Phi_l \rangle ,
\end{aligned}$$

and as the eigenvalues are real $\bar{\lambda}_l = \lambda_l$ and one has

$$\langle \Phi_k, w\Phi_l \rangle = 0, \quad \forall k \neq l.$$

Furthermore one can normalize the eigenfunction in such a way that

$$\langle \Phi_k, w\Phi_l \rangle = \delta_{k,l}, \tag{E.2}$$

with $\delta_{k,l}$ being the Kronecker-δ. Correspondingly one can bound the above linear dissipation by the square of the un-weighted L^2 norm of the estimation error

$$\begin{aligned}
&- \int_0^1 w(x)e(x,t) \left\{ -P_e^{-1} \frac{\partial^2 e(x,t)}{\partial x^2} + \frac{\partial e(x,t)}{\partial x} \right\} dx \\
&\leq \sup_{k \in \mathbb{N}} \lambda_k \sum_{k=1}^{\infty} \left(\sum_{l=1}^{k} e_{k-l}(t) e_l(t) \int_0^1 \Phi_{k-l}(x) w(x) \Phi_l(x) dx \right) \\
&= \sup_{k \in \mathbb{N}} \lambda_k \sum_{k=1}^{\infty} e_k^2 \\
&= \sup_{k \in \mathbb{N}} \lambda_k \left|\left| e(x,t) \right|\right|_{L^2}^2 .
\end{aligned} \tag{E.3}$$

This shows that the linear (un-innovated) dissipation is bounded by the dominant eigenvalues of the linear transport operator A (D.6). Furthermore, as $-A$ is a Sturm-Liouville operator [96] and the eigenvalues λ_k, $k \in \mathbb{N}$ of A form a decreasing, discrete set, the above supremum is actually given by the first eigenvalue λ_1 [113, 96, 26].

Influence of the modal injection gains

Having as a point of departure the bi-orthogonal Fourier expansion (D.8) of all elements of L^2 one can express the measurement of the concentration in $x = \xi$ as

$$y(t) = c(\xi, t) = \sum_{k=1}^{\infty} c_k(t)\Phi_k(\xi), \tag{E.4}$$

with c_k being the k-th Fourier coefficient. Accordingly, the action of the measurement injection in (4.6) can be expressed as

$$\frac{\partial^2 e(x,t)}{\partial x^2} - P_e \frac{\partial e(x,t)}{\partial x} - l_\xi e(\xi, t) = \sum_{k=1}^{\infty} e_k(t)\lambda_k \Phi_k(x) - l_\xi \sum_{l=1}^{\infty} e_l(t)\Phi_l(\xi). \tag{E.5}$$

Correspondingly, one has to choose the injection mechanism l_ξ in such a way that the first N eigenmodes are directly modified. This can be achieved [35, 37, 39] employing a modal innovation mechanism proportional to the measurement offset $e(\xi, t)$ in $x = \xi$

$$l_\xi e(\xi, t) = \sum_{k=1}^{\infty} l_{\xi,k}\Phi_k(x)e(\xi, t) = \sum_{k=1}^{\infty} l_{\xi,k}\Phi_k(x) \left(\sum_{l=1}^{\infty} e_l(t)\Phi_l(\xi) \right), \tag{E.6}$$

i.e. l_ξ is given by a modal injection operator with modal gains [35, 37, 39]. Accordingly, the action of the innovated transport operator $A_L = A_c - LC$ (4.10) is given by

$$A_L e(x,t) = \frac{\partial^2 e}{\partial x^2} - P_e \frac{\partial e}{\partial x} - l_\xi e(\xi, t) = \sum_{k=1}^{\infty} e_k(t)\Phi_k(x) \left[\lambda_k - l_{\xi,k} \left(\sum_{l=1}^{\infty} e_l(t)\Phi_l(\xi) \right) \right]. \tag{E.7}$$

Based on this representation of the innovated linear operator, one can express the corresponding linear dissipation (E.3), in its innovated form using (E.1) and (E.2)

$$\begin{aligned}
&-\int_0^1 w(x)e(x,t)\left\{-P_e^{-1}\frac{\partial^2 e(x,t)}{\partial x^2}+\frac{\partial e(x,t)}{\partial x}-l_\xi e(\xi,t)\right\}dx\\
&=\sum_{k=1}^{\infty}\left(\sum_{l=1}^{k}\left[\lambda_l e_l-l_{\xi,l}e(\xi,t)\right]e_{k-l}\int_0^1\Phi_{k-l}(x)w(x)\Phi_l(x)dx\right)\\
&=\sum_{k=1}^{\infty}\left(\lambda_k e_k^2-l_{\xi,k}e(\xi,t)e_k\right)\\
&=\sum_{k=1}^{\infty}\left(\lambda_k e_k^2-l_{\xi,k}e_k\left[\sum_{l=1}^{\infty}e_l(t)\Phi_l(\xi)\right]\right)\\
&=\sum_{k=1}^{\infty}\lambda_k e_k^2-\sum_{k=1}^{\infty}\sum_{l=1}^{k}l_{\xi,l}\Phi_{k-l}(\xi)e_l e_{k-l}.
\end{aligned}$$

As actually only a finite number N of eigenvalues has to be relocated,

$$l_{\xi,k}=0,\quad k>N, \tag{E.8}$$

and consequently the above dissipation becomes

$$\begin{aligned}
&-\int_0^1 w(x)e(x,t)\left\{-P_e^{-1}\frac{\partial^2 e(x,t)}{\partial x^2}+\frac{\partial e(x,t)}{\partial x}-l_\xi e(\xi,t)\right\}dx\\
&=\sum_{k=1}^{\infty}\lambda_k e_k^2-\sum_{k=1}^{\infty}\sum_{l=1,\,l\le N}^{k}l_{\xi,l}\Phi_l(\xi)e_l e_{k-l}.
\end{aligned} \tag{E.9}$$

In seek of comprehensiveness, the innovated dissipation (E.9) is expressed in a modal state space form. In the chosen basis, one can view the state as an infinite-dimensional vector with elements e_k (the modes) [34, 91], and correspondingly one

can write (E.9) in the following quadratic way

$$
\begin{aligned}
&-\int_0^1 w(x)e(x,t)\left\{-P_e^{-1}\frac{\partial^2 e(x,t)}{\partial x^2}+\frac{\partial e(x,t)}{\partial x}-l_\xi e(\xi,t)\right\}dx \\
&=\begin{bmatrix} e_1 \\ e_2 \\ \vdots \\ e_N \\ e_{N+1} \\ \vdots \end{bmatrix}^T \left(\left[\begin{array}{cccc|cc} \lambda_1 & 0 & 0 & 0 & 0 & \dots \\ 0 & \lambda_2 & 0 & 0 & 0 & \dots \\ \vdots & & \ddots & & \vdots & \vdots \\ 0 & 0 & 0 & \lambda_N & 0 & \dots \\ \hline & & & & & \\ 0 & 0 & 0 & 0 & \lambda_{N+1} & \dots \\ \vdots & & & \vdots & \vdots & \ddots \end{array}\right] - \right. \\
&\qquad \left. - \left[\begin{array}{cccc|cc} l_{\xi,1}\Phi_1(\xi) & l_{\xi,1}\Phi_2(\xi) & \cdots & l_{\xi,1}\Phi_N(\xi) & l_{\xi,1}\Phi_{N+1}(\xi) & \dots \\ l_{\xi,2}\Phi_1(\xi) & l_{\xi,2}\Phi_2(\xi) & \cdots & l_{\xi,2}\Phi_N(\xi) & l_{\xi,1}\Phi_{N+1}(\xi) & \dots \\ \vdots & & \ddots & \vdots & \vdots & \\ l_{\xi,N}\Phi_1(\xi) & l_{\xi,N}\Phi_2(\xi) & \cdots & l_{\xi,N}\Phi_N(\xi) & l_{\xi,N}\Phi_{N+1}(\xi) & \dots \\ \hline & & & & & \\ 0 & 0 & 0 & 0 & 0 & \dots \\ 0 & 0 & 0 & 0 & \vdots & \ddots \end{array}\right] \right) \begin{bmatrix} e_1 \\ e_2 \\ \vdots \\ e_N \\ e_{N+1} \\ \vdots \end{bmatrix}
\end{aligned}
\tag{E.10}
$$

Accordingly, the new bound λ^* of the innovated linear dynamics corresponds to the maximal eigenvalue of the innovated dominant (slow) dynamics, i.e. the maximal eigenvalue of the matrix

$$
A_L^s \triangleq \begin{bmatrix} \lambda_1 - l_{\xi,1}\Phi_1(\xi) & -l_{\xi,1}\Phi_2(\xi) & \cdots & -l_{\xi,1}\Phi_N(\xi) \\ -l_{\xi,2}\Phi_1(\xi) & \lambda_2 - l_{\xi,2}\Phi_2(\xi) & \cdots & -l_{\xi,2}\Phi_N(\xi) \\ \vdots & & \ddots & \vdots \\ -l_{\xi,N}\Phi_1(\xi) & -l_{\xi,N}\Phi_2(\xi) & \cdots & \lambda_N - l_{\xi,N}\Phi_N(\xi) \end{bmatrix}. \tag{E.11}
$$

It has to be pointed out, that the possibility of changing the eigenvalues resides in the choice of the measurement point $x = \xi$. In more detail, the eigenfunctions corresponding to the dominant modes must not vanish in this point, or in other words, $x = \xi$ *must not correspond to any of the k roots of the k-th eigenfunction* Φ_k.

Taking into account to above relations (E.9) and (E.10), the innovated dissipa-

tion of the linear transport system is bounded according to

$$-\int_0^1 ew\left\{-\frac{\partial^2 e}{\partial x^2}+P_e\frac{\partial e}{\partial x}+l_\xi e(\xi,t)\right\}dx \leq \max\{\lambda^*,\lambda_{N+1}\}\,||e||^2_{L^2_w}\,, \tag{E.12}$$

where λ^* is the maximal eigenvalues of the $N\times N$ matrix A^s_L (E.11), and $||e||_{L^2_w}$ the weighted L^2-norm

$$||e||_{L^2_w}=\langle e,we\rangle=\int_0^1 we^2dx=\sum_{k=1}^{\infty}e_k^2. \tag{E.13}$$

Appendix F

Proof of Lemma 4.2

Proof. Considering a collocated point injection of the measurement in $x = \xi$, i.e.

$$l_\xi = l_\xi^0 \delta(x - \xi), \tag{F.1}$$

the linear part of the dissipation expression (4.14) can be rewritten as

$$\begin{aligned}
&-2\int_0^1 we\left\{-\frac{1}{P_{ec}}\frac{\partial^2 e}{\partial x^2} + \frac{\partial e}{\partial x} + l_\xi e(\xi,t)\right\}dx \\
&= 2\left[\frac{1}{P_{ec}} we\frac{\partial e}{\partial x}\right]_0^1 - 2\int_0^1 \left[\frac{1}{P_{ec}}\left(\frac{\partial w}{\partial x}e + w\frac{\partial e}{\partial x}\right)\frac{\partial e}{\partial x} + we\frac{\partial e}{\partial x} + l_\xi^0\delta(x-\xi)wee(\xi,t)\right]dx \\
&= 2\left[\frac{1}{P_{ec}} we\frac{\partial e}{\partial x}\right]_0^1 - 2\int_0^1 \left[\left(\frac{1}{P_{ec}}\frac{\partial w}{\partial x} + w\right)e\frac{\partial e}{\partial x} + \frac{1}{P_{ec}}w\left(\frac{\partial e}{\partial x}\right)^2\right]dx + l_\xi^0 w(\xi)e^2(\xi,t).
\end{aligned}$$

Next, the mixed term in the estimation error and its gradient is expressed as follows

$$\begin{aligned}
&-2\int_0^1 \left(\frac{1}{P_{ec}}\frac{\partial w}{\partial x} + w\right)e\frac{\partial e}{\partial x}dx = -\int_0^1 \left(\frac{1}{P_{ec}}\frac{\partial w}{\partial x} + w\right)\frac{\partial}{\partial x}e^2 dx \\
&= \left[-\left(\frac{1}{P_{ec}}\frac{\partial w}{\partial x} + w\right)e^2\right]_0^1 + \int_0^1 \left(\frac{1}{P_{ec}}\frac{\partial^2 w}{\partial x^2} + \frac{\partial w}{\partial x}\right)e^2 dx.
\end{aligned}$$

Further, following Wirtinger's Lemma [97, 98, 66], by which it holds that all functions $h(x)$ in $L^2([a,b],\mathbb{R})$ with $h(a) = 0$ satisfy

$$\int_a^b h^2 dx \leq \frac{4(b-a)^2}{\pi}\int_a^b \left(\frac{\partial h}{\partial x}\right)^2 dx, \tag{F.2}$$

the quadratic term in the gradient can be bounded by a quadratic term in the estimation error

$$-2\int_0^1 \frac{1}{P_{ec}} w \left(\frac{\partial e}{\partial x}\right)^2 dx \leq -2\frac{1}{P_{ec}} w_{\min} \int_0^1 \left(\frac{\partial e}{\partial x}\right)^2 dx \leq -\frac{w_{\min}\pi}{2P_{ec}} \int_0^1 (e(x,t) - e(0,t))^2 dx,$$

where $w_{\min}$ is the minimum of the weighting function over the spatial extension $[0, 1]$. Finally, the boundary term can be expressed in function of the injection gains l_0 and l_1 according to (4.6)

$$\begin{aligned}\left[\frac{2}{P_{ec}} we\frac{\partial e}{\partial x} - \left(\frac{1}{P_{ec}}\frac{\partial w}{\partial x} + w\right)e^2\right]_0^1 &= \left(-\frac{2}{P_{ec}} w(1) l_1 e^2(1,t) - \left(\frac{1}{P_{ec}}\frac{\partial w}{\partial x}(1) + w(1)\right)e^2(1,t)\right) - \\ &- \left(\frac{2}{P_{ec}} w(0)[1-l_0]e^2(0,t) - \left(\frac{1}{P_{ec}}\frac{\partial w}{\partial x}(0) + w(0)\right)e^2(0,t)\right) \\ &= -e^2(1,t)\left(\frac{1}{P_{ec}}\frac{\partial w}{\partial x}(1) + \frac{2l_1 + P_{ec}}{P_{ec}} w(1)\right) - e^2(0,t)\left(-\frac{1}{P_{ec}}\frac{\partial w}{\partial x}(0) - \frac{P_{ec}+\end{aligned}$$

Consequently, one can express the linear dissipation term in (4.14) as follows

$$-\int_0^1 we\left\{-\frac{\partial^2 e}{\partial x^2} + P_e\frac{\partial e}{\partial x} + l_\xi e(\xi,t)\right\}dx = -\int_0^1 \zeta^T \bar{Q}\zeta dx \qquad \text{(F.3)}$$

$$\zeta \triangleq [e(x,t),\, e(0,t),\, e(1,t),\, e(\xi,t)]^T$$

$$\bar{Q} \triangleq \begin{bmatrix} D[w] & \frac{w_{\min}\pi}{2P_{ec}} & 0 & 0 \\ \frac{w_{\min}\pi}{2P_{ec}} & \mathcal{R}_0 & 0 & 0 \\ 0 & 0 & \mathcal{R}_1 & 0 \\ 0 & 0 & 0 & l_\xi^0 w(\xi) \end{bmatrix}$$

$$D[w] = -\frac{d^2 w}{dx^2} - P_e\frac{dw}{dx} + \frac{w_{\min}\pi}{2P_{ec}}$$

$$\mathcal{R}_0 = \frac{1}{P_{ec}}\frac{dw}{dx}(0) + \frac{2 - 2l_0 - P_{ec}}{P_{ec}} w(0) + \frac{w_{\min}\pi}{2P_{ec}}$$

$$\mathcal{R}_1 = \frac{1}{P_{ec}}\frac{dw}{dx}(1) + \frac{2l_1 + P_{ec}}{P_{ec}} w(1).$$

□

Appendix G

Proof of Theorem 4.1

Proof. Let w, h be two continuous positive definite functions, such that for all k for which (4.42) does not hold, ξ does not correspond to any root of the $\Phi_k(x)$, i.e. $\Phi_k(\xi) \neq 0$. As $-A$ is a Sturm-Liouville operator, the eigenvalues λ_k form a monotonically decreasing discrete set. Accordingly, there exists a number N, so that (4.42) holds and by assumption for all $k \leq N$ it holds that $\Phi_k(\xi) \neq 0$. According to (E.11) the modified eigenvalues $\lambda_k^*, k \leq N$ of the matrix A_L^s can be reassigned. Now, consider the functional $E = \langle e, we \rangle$ and the corresponding upper bound for its time derivative (4.39). Now let (4.43) hold for $\lambda > 0$. Then it follows that the following LMI is satisfied

$$\begin{bmatrix} -2\max\{\lambda^*, \lambda_{N+1}\}w(x) + h(x)s_l s_u + 2\lambda w(x) & \frac{D_a w(x) - [s_l + s_u]h(x)}{2} \\ \frac{D_a w(x) - [s_l + s_u]h(x)}{2} & h(x) \end{bmatrix} > 0,$$

where λ^* is the maximal eigenvalue of the matrix A_L^s (E.11). Thus it follows $\dot{E}(e(x,t)) \leq -2\lambda E(e(x,t))$ for some positive $\lambda > 0$. The exponential stability follows by Lemma 2.1. □

Appendix H

Proof of Theorem 4.2

Proof. Combining on Lemma 4.2 and the integrally weighted sector condition (4.18), one can express the strict dissipation condition

$$\frac{dE(e)}{dt} + 2\lambda E \leq 0 \tag{H.1}$$

as in (4.45)-(4.46). Consequently, if condition (4.47) holds, it follows $\dot{E} \leq -2\lambda E$ and by Lemma 2.1 the exponential stability results. □

Appendix I

Proof of Proposition 4.1

Proof. The proof is separated into the demonstration of two Lemmas which in combination permit the conclusions of Proposition 4.1.

Lemma I.1. *Consider the isothermal tubular reactor (2.11), together with the Luenberger-type observer (4.4), with collocated point measurement injection l_ξ corresponding to (F.1). The estimation error zero solution $e(x,t) = 0$ is g.e.s. with convergence rate $\lambda > 0$, if the following inequalities are met*

$$\begin{aligned} &(I) \quad \mathcal{R}_0 > 0, \\ &(II) \quad h\left[(D[w] - 2\lambda w)\mathcal{R}_0 - \frac{w_*^2\pi^2}{4P_{ec}^2}\right] - \mathcal{R}_0\frac{(D_a w - [s_u + s_l]h)^2}{4} > 0, \quad \forall x \in [0,1] \\ &(III)\ l_\xi^0 > 0, \quad (IV)\ \mathcal{R}_1 > 0. \end{aligned} \tag{I.1}$$

Proof. First of all it is shown that the above conditions imply the strict dissipation of the (quadratic weighted integral) energy (4.13), stored in the estimation error. According to Theorem 4.2, the strict dissipation of the quadratic weighted energy storage (with weighting function $w > 0$) if the LMI (4.47) is satisfied for each point $x \in [0,1]$. This condition is equivalent to the positive definiteness of the corresponding 5 leading principal minors of Q, $M_1, \ldots, M_5$. Note that this positivity is independent of the sequence of the matrix, in the sense that a coordinate change of the type $[a,b,c] \mapsto [c,b,a]$ does not alter this property. Therefore the positivity of the first three leading principal minors is equivalent to the positivity of the rearranged

matrix

$$\begin{bmatrix} h & 0 & \frac{D_a w-[s_u+s_l]h}{2} \\ 0 & -\mathcal{R}_0 & \frac{w_{\min}\pi}{2P_{ec}} \\ \frac{D_a w-[s_u+s_l]h}{2} & \frac{w_{\min}\pi}{2P_{ec}} & D[w]-2\lambda w \end{bmatrix}.$$

This matrix is positive if condition (I) holds, with w being a positive definite solution of the differential inequality (II). The positivity of the fourth (M_4) and fifth (M_5) leading principal minors follows if the conditions (iii) and (iv) are satisfied. Thus the above conditions (I) to (IV) are sufficient for the positivity of the matrix Q and consequently for the strict dissipation of the energy (4.13). Next, due to the continuity of the weighting function w, being the solution of (II), and the compactness of the interval $[0,1]$, it holds for all $t \geq 0$ that $w_* \left|\left|e(x,t)\right|\right|^2 \leq E(e(x,t)) \leq w^* \left|\left|e(x,t)\right|\right|^2$, with w^* being the maximum of the weighting function w over $[0,1]$. By the strict dissipation with rate $\lambda > 0$, i.e. $E(e(x,t)) \leq -\lambda E(e(x,t))$ it follows by the comparison principle that $E(e(x,t)) \leq E(e_0(x))\exp(-2\lambda t)$, and consequently $||e(x,t)|| \leq \alpha\,||e_0(x)||\exp(-\lambda t)$, with amplitude $\alpha = \sqrt{w^*/w_*}$. □

The question for which parameter combinations (P_e, D_a) the exponential convergence conditions of Proposition I.1 are solvable is addressed next. Therefore the integral weight h in the sector condition (4.18) is set equal to the energy weight w. Therefore, note first of all the following result.

Lemma I.2. *Let $\mathcal{K}_0 > 2w_*$. The conditions (I) and (II) of Proposition I.1 are satisfied if the following conditions hold*

$$\begin{aligned} &(i)\ \ \mathcal{R}_0 = \mathcal{K}_0 > 0, \\ &(ii)\ \ -\frac{1}{P_{ec}}\frac{\partial^2 w}{\partial x^2} + \frac{\partial w}{\partial x} = \left(2\lambda - s_u s_l + \mathcal{K}_0 \tfrac{(D_a-[s_u+s_l])^2}{4}\right) w \end{aligned} \tag{I.2}$$

Proof. Note that for $h = w$, and $\mathcal{R}_0 = \mathcal{K}_0 > 0$ (i) condition (II) of Proposition I.1 requires that

$$\begin{aligned} &4\left(-\frac{1}{P_{ec}}\frac{\partial^2 w}{\partial x^2} + \frac{\partial w}{\partial x} - [2\lambda - s_u s_l]w + \tfrac{w_*}{2P_{ec}}\right)\mathcal{K}_0 - 2\frac{w_*^2}{P_{ec}^2} - \mathcal{K}_0(D_a - [s_u+s_l])^2 w \\ &= 4\mathcal{K}_0\left(-\frac{1}{P_{ec}}\frac{\partial^2 w}{\partial x^2} + \frac{\partial w}{\partial x} - \left[2\lambda - s_u s_l + \tfrac{(D_a-[s_u+s_l])^2}{4}\right] w\right) + 2\mathcal{K}_0\frac{w_*\pi}{P_{ec}} - 2\frac{w_*^2\pi^2}{P_{ec}^2} > 0. \end{aligned}$$

Consequently, if (ii) holds, it follows with $\mathcal{K}_0 > 2\dfrac{w_*\pi}{P_{ec}}$, that this condition is satisfied.

□

According to this result, the gain l_0 can always be assigned in such a way that the inhomogeneous differential inequality (II) in Proposition I.1 is satisfied if the homogeneous differential equation (ii) in Lemma I.2 is fulfilled. A particular solution of this differential equation is given by

$$w(x) = w_0 e^{-P_e x/2} \cosh\left(\sqrt{\frac{P_e^2}{4} - P_e\left(2\lambda - s_u s_l + \frac{(D_a - [s_u + s_l])^2}{4}\right)}\, x\right). \tag{I.3}$$

This function is positive if it holds that

$$P_e \geq 8\lambda - 4 s_u s_l + (D_a - [s_u + s_l])^2. \tag{I.4}$$

This condition on the system parameters, together with condition (i) of Lemma I.2 with $\mathcal{K}_0 > 2\dfrac{w_* \pi}{P_{ec}}$, and the remaining conditions (III) and (IV) of Proposition I.1, establish sufficient conditions for the global and exponential stability of the estimation error zero solution $e(x,t) = 0$.

Now, condition (i) of Proposition 4.1 is sufficient for the positivity of the weighting function $w(x)$. With condition (ii) it follows by Proposition 4.1 that conditions (I) and (II) of Lemma I.1 are satisfied. Conditions (iii) and (iv) are the same as conditions (III) and (IV) in Lemma I.1. Accordingly, $e(x,t) = 0$ is g.e.s.. □

Appendix J

Determination of the eigenvalues for the linear transport operator

Consider the following eigenvalue problem for the (Sturm-Liouville) operator A

$$\frac{1}{P_e}\frac{d^2\Phi_n}{dx^2} - \frac{d\Phi_n}{dx} - \lambda_n \Phi_n = 0, \tag{J.1}$$

which leads to the characteristic polynomial

$$\frac{s_n^2}{P_e} - s_n - \lambda_n = 0 \tag{J.2}$$

with solutions

$$s_n^{1,2} = \frac{P_e}{2} \pm \underbrace{\sqrt{\frac{P_e^2 + 4P_e\lambda_n}{4}}}_{\triangleq i\omega_n} \tag{J.3}$$

where the ω_n are the eigenfrequencies. The corresponding eigenfunctions and their derivatives have the form

$$\Phi_n(x) = e^{P_e x/2}\left(A_n \sin(\omega_n x) + B_n \cos(\omega_n x)\right) \tag{J.4}$$

$$\frac{d\Phi_n}{dx}(x) = e^{P_e x/2}\left(\left[A_n\frac{P_e}{2} - B_n\omega_n\right]\sin(\omega_n x) + \left[A_n\omega_n + B_n\frac{P_e}{2}\right]\cos(\omega_n x)\right) \tag{J.5}$$

and have to satisfy the boundary conditions

$$\frac{1}{P_e}\frac{d\Phi_n(0)}{dx} - \Phi_n(0) = 0 \Leftrightarrow B_n = \frac{2A_n\omega_n}{P_e} \tag{J.6}$$

$$\frac{1}{P_e}\frac{d\Phi_n}{dx}(1) = 0 \Leftrightarrow e^{P_e/2}A_n\left(\left[\frac{P_e}{2} - \frac{2\omega_n^2}{P_e}\right]\sin(\omega_n) + 2\omega_n\cos(\omega_n)\right) = 0. \tag{J.7}$$

This last equation characterizes the eigenfrequencies for the eigenfunctions, ω_n, via the implicit relation

$$\tan^{-1}(\omega_n) = \frac{4\omega_n^2 - P_e^2}{4P_e\omega_n}. \tag{J.8}$$

This relation is depicted in Figure J.1 for distinct values of P_e. The solutions can

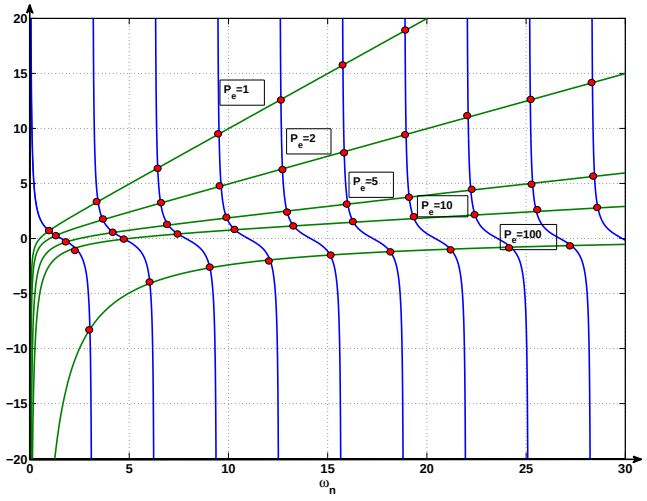

Figure J.1: Relation (J.8) in dependence on the eigenfrequencies ω_n. The solutions are indicated by the red points.

be approximated in a relatively exact manner via graphical or numerical methods. Furthermore, the following bounds can be established (compare [113, 96, 26])

$$\begin{aligned} 0 \leq &\omega_1 \leq \pi \\ (n-1)\pi \leq &\omega_n \leq n\pi. \end{aligned} \tag{J.9}$$

The eigenvalues can be determined from the relation given by (J.3)

$$\lambda_n = -\frac{P_e^2 + 4\omega_n^2}{4P_e}, \tag{J.10}$$

and the corresponding eigenfunctions are

$$\psi_n(x) = A_n e^{P_e x/2} \left(\sin(\omega_n x) + \frac{2\omega_n}{P_e} \cos(\omega_n x) \right). \tag{J.11}$$

The basic behavior of the first four eigenfunctions $\Phi_n, n = 1, 2, 3, 4$ are depicted in Figure J.2 for $P_e = 10$.

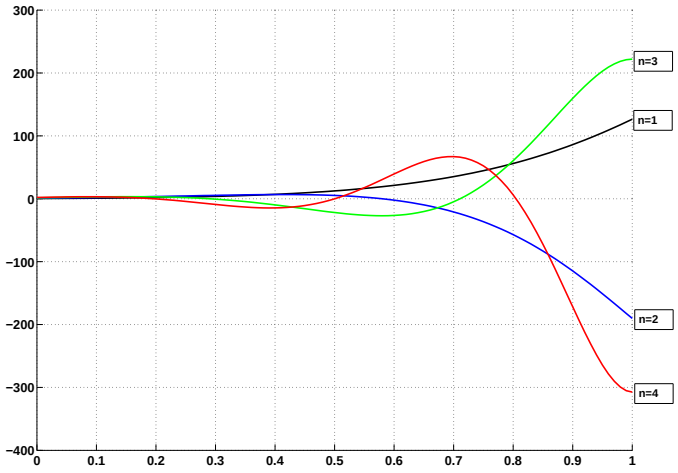

Figure J.2: First four eigenfunctions for $P_e = 10$ and $A_n = 1$.

Appendix K

Proof of Lemma 5.1

Fourier series expansion

Consider the Fourier-expansion

$$e(x,t) = \sum_{k=1}^{\infty} \begin{bmatrix} \langle e_c(x,t), \psi_{k,1} \rangle \, \varphi_{k,1} \\ \langle e_T(x,t), \psi_{k,2} \rangle \, \varphi_{k,2} \end{bmatrix} = \sum_{k=1}^{\infty} \begin{bmatrix} e_{c,k} \varphi_{k,1} \\ e_{T,k} \varphi_{k,2} \end{bmatrix}, \tag{K.1}$$

where the $\varphi_{k,i}$ are the eigenfunctions of the operators $A_j, j = c, T$. Let

$$A = \begin{bmatrix} A_1 & 0 \\ 0 & A_2 \end{bmatrix} = \begin{bmatrix} \dfrac{1}{P_{e,c}} \dfrac{\partial^2}{\partial x^2} - \dfrac{\partial}{\partial x} & 0 \\ 0 & \dfrac{L_e}{P_{e,c}} \dfrac{\partial^2}{\partial x^2} - L_e \dfrac{\partial}{\partial x} - \eta \end{bmatrix} \tag{K.2}$$

and introduce the boundary operators B_0, B_1 such that

$$\begin{aligned} x = 0 : \; B_0 e(0,t) &\triangleq \begin{bmatrix} \dfrac{1}{P_{e,c}} \dfrac{\partial}{\partial x} - I \\ \dfrac{L_e}{P_{e,c}} \dfrac{\partial}{\partial x} - L_e \end{bmatrix} e(0,t) = 0, \\ x = 1 : \; B_1 e(1,t) &\triangleq \begin{bmatrix} \dfrac{\partial}{\partial x} \\ \dfrac{\partial}{\partial x} \end{bmatrix} e(1,t) = 0, \end{aligned} \tag{K.3}$$

with I being the identity. The corresponding eigenvalue problem reads

$$A\Phi_n = \lambda_n \Phi_n, \quad B_0 \Phi_n(0) = B_1 \Phi_n(1) = 0. \tag{K.4}$$

Due to the diagonal structure of the operator A (K.2), and the fact that the boundary conditions are uncoupled, the corresponding eigenvalue-eigenfunction sets are given by the union of the solutions of the diagonal eigenvalue-eigenfunction problems, i.e.

$$\begin{aligned}\sigma(A) &= \bigcup_{i=1,2} \sigma(A_i), \text{ where } \sigma(A_i) = \{\lambda_i : A_i\varphi_{n,i} = \lambda_{n,i}\varphi_{n,i}, \quad n \in \mathbb{N}\}, \quad i = 1,2 \\ \{\Phi_n\}_{n\in\mathbb{N}} &= \left\{ \begin{bmatrix} \varphi_{n,1} \\ 0 \end{bmatrix}, \begin{bmatrix} 0 \\ \varphi_{n,2} \end{bmatrix} \right\}_{n\in\mathbb{N}}.\end{aligned} \tag{K.5}$$

Correspondingly,

$$\begin{aligned} Ae &= \begin{bmatrix} A_1 & 0 \\ 0 & A_2 \end{bmatrix} \begin{bmatrix} e_c \\ e_T \end{bmatrix} = \begin{bmatrix} \sum_{n=0}^{\infty} \lambda_{n,1} \langle e_c, \psi_{n,1} \rangle \varphi_{n,1} \\ \sum_{n=1}^{\infty} \lambda_{n,2} \langle e_T, \psi_{n,2} \rangle \varphi_{n,2} \end{bmatrix} \\ &= \sum_{n=1}^{\infty} \begin{bmatrix} \lambda_{n,1} & 0 \\ 0 & \lambda_{n,2} \end{bmatrix} \begin{bmatrix} e_{c,k}\varphi_{k,1} \\ e_{T,k}\varphi_{k,2} \end{bmatrix}, \end{aligned} \tag{K.6}$$

where the $e_{i,k}$, $i = c, T$, $k \in \mathbb{N}$ are the corresponding concentration and temperature modes.

Modal dissipation bounds

According to the Fourier series representation (K.1) of the elements of $L^2([0,1], X \subset \mathbb{R}^2)$, the temperature measurement signal obtained at the point $x = \xi \in [0,1]$, can be represented correspondingly as

$$y(t) = \sum_{k=1}^{\infty} \int_0^1 \begin{bmatrix} 0 & \delta(x-\xi) \end{bmatrix} \begin{bmatrix} e_{c,k}\varphi_{k,1} \\ e_{T,k}\varphi_{k,2} \end{bmatrix} = \sum_{k=1}^{\infty} e_{T,k}\varphi_{k,2}(\xi). \tag{K.7}$$

Accordingly, if the modal correction mechanisms of the temperature measurement at $x = \xi$ in (5.5) are given by

$$\begin{aligned} l_\xi^c \left(\hat{T}(\xi,t) - y(t) \right) &= \sum_{k=1}^{\infty} l_{\xi,k}^c \varphi_{k,1} \left(\hat{T}(\xi,t) - y(t) \right) \\ l_\xi^T \left(\hat{T}(\xi,t) - y(t) \right) &= \sum_{k=1}^{\infty} l_{\xi,k}^T \varphi_{k,2} \left(\hat{T}(\xi,t) - y(t) \right), \end{aligned} \tag{K.8}$$

then the corresponding linear modal dynamics is given by

$$
\begin{aligned}
Ae - l_\xi e(\xi,t) &= \sum_{k=1}^{\infty}\left(\begin{bmatrix}\lambda_{n,1} & 0\\ 0 & \lambda_{n,2}\end{bmatrix}\begin{bmatrix} e_{c,k}\varphi_{k,1}\\ e_{T,k}\varphi_{k,2}\end{bmatrix} - \begin{bmatrix} l^c_{\xi,k}e_T(\xi,t)\varphi_{k,1}\\ l^T_{\xi,k}e_T(\xi,t)\varphi_{k,2}\end{bmatrix}\right)\\
&= \sum_{k=1}^{\infty}\left(\begin{bmatrix}\lambda_{n,1} & 0\\ 0 & \lambda_{n,2}\end{bmatrix}\begin{bmatrix} e_{c,k}\varphi_{k,1}\\ e_{T,k}\varphi_{k,2}\end{bmatrix} - \sum_{l=1}^{k}\begin{bmatrix} l^c_{\xi,k-l}\varphi_{k-l,1}(x)\\ l^T_{\xi,k-l}\varphi_{k-l,2}(x)\end{bmatrix}\left(\sum_{m=1}^{\infty} e_{T,m}(t)\varphi_{m,2}(\xi)\right)\right),
\end{aligned}
\tag{K.9}
$$

where $l^i_{\xi,k}$, $i = c, T$ is the corresponding k-th modal injection gain of the temperature measurement in $x = \xi$, for the concentration and temperature dynamics, respectively. Introducing the infinite-dimensional (modal) representation of the estimation error vector

$$
\bar{e}(t) \triangleq [e_{c,1}(t),\, e_{T,1}(t),\, \ldots,\, e_{c,N}(t),\, e_{T,N}(t),\, \ldots]^T, \tag{K.10}
$$

and choosing the weighting functions w_1, w_2 as

$$
w_1 = e^{-P_{e,c}x}, \quad w_2 = e^{-P_{e,T}x} \quad \Longleftrightarrow \quad \int_0^1 w_i\varphi_{k,i}\varphi_{l,i}dx = \delta_{k,l},\ i = 1,2, \tag{K.11}
$$

one can express the weighted potential energy E (5.15) as follows

$$
\begin{aligned}
&E(e(x,t)) = \int_0^1 e^T W e dx\\
&= \int_0^1 \left(\sum_{k=1}^{\infty}\begin{bmatrix} e_{c,k}(t)\varphi_{k,1}(x)\\ e_{T,k}(t)\varphi_{k,2}(x)\end{bmatrix}^T\right) W \left(\sum_{m=1}^{\infty}\begin{bmatrix} e_{c,m}(t)\varphi_{m,1}(x)\\ e_{T,m}(t)\varphi_{m,2}(x)\end{bmatrix}\right) dx\\
&= \sum_{k=1}^{\infty}\sum_{m=1}^{k}\left(e_{c,k-m}e_{c,m}\int_0^1 w_1\varphi_{k-m,1}\varphi_{m,1}dx + e_{T,k-m}e_{T,m}\int_0^1 w_2\varphi_{k-m,2}\varphi_{m,2}dx\right)\\
&= \sum_{k=1}^{\infty} e^2_{c,k} + e^2_{T,k} = \bar{e}^T\bar{e}.
\end{aligned}
\tag{K.12}
$$

Now, note that the linear differential part $\mathcal{D}_T$ of the dissipation, with the elements corresponding to the linear measurement injection mechanisms (l^c_ξ, l^T_ξ), is equivalent to the dissipation of the linear dynamics

$$
\frac{\partial e(x,t)}{\partial t} = Ae(x,t) - l_\xi e(\xi,t), \tag{K.13}
$$

where A is given in (K.2) and $l_\xi = [l_\xi^c,\, l_\xi^T]^T$ is the vector corresponding to the measurement injection mechanisms. This dynamics can be represented in terms of the infinite-dimensional modal vector $\bar{e}(t)$ (K.10) according to (K.9) as

$$
\begin{aligned}
&Ae - l_\xi e_T(\xi,t) \\
&= (\Lambda - L_\xi)\bar{e} \triangleq \left(\begin{array}{ccccccc}
\lambda_{1,1} & -l_{\xi,1}^c\varphi_{1,2}(\xi) & \dots & \dots & \dots & 0 & -l_{\xi,1}^c\varphi_{N,2}(\xi) \\
0 & \lambda_{1,2} - l_{\xi,1}^T\varphi_{1,2}(\xi) & \dots & \dots & \dots & 0 & -l_{\xi,1}^T\varphi_{N,2}(\xi) \\
0 & -l_{\xi,2}^c\varphi_{1,2}(\xi) & \ddots & & & \vdots & \\
0 & -l_{\xi,2}^T\varphi_{1,2}(\xi) & & \ddots & & & \\
\vdots & \vdots & & & \ddots & \vdots & \vdots \\
0 & -l_{\xi,N}^c\varphi_{1,2}(\xi) & \dots & \dots & \dots & \lambda_{N,1} & -l_{\xi,N}^c\varphi_{N,2}(\xi) \\
0 & -l_{\xi,N}^T\varphi_{1,2}(\xi) & \dots & \dots & \dots & 0 & \lambda_{N,2} - l_{\xi,N}^c\varphi_{N,2}(\xi) \\
0 & 0 & & & & \vdots & \vdots \\
\vdots & \vdots & & & & \vdots & \vdots \\
\vdots & \vdots & & & & \vdots & \vdots
\end{array}\right| \\
&\qquad\qquad \left|\begin{array}{ccc}
\dots & -l_{\xi,1}^c\varphi_{N+1,2}(\xi) & \dots \\
\dots & -l_{\xi,1}^c\varphi_{N+1,2}(\xi) & \dots \\
& \vdots & \\
& \vdots & \\
& \vdots & \\
& \vdots & \\
& \vdots & \\
\lambda_{N+1,1} & 0 & \dots \\
0 & \lambda_{N+1,2} & \\
\vdots & \vdots & \ddots
\end{array}\right) \left[\begin{array}{c}
e_{c,1} \\ e_{T,1} \\ \vdots \\ \vdots \\ \vdots \\ e_{c,N} \\ e_{T,N} \\ e_{c,N+1} \\ e_{T,N+1} \\ \vdots
\end{array}\right].
\end{aligned}
\tag{K.14}
$$

Correspondingly one has the following representation of the linear differential part of the dissipation $\mathcal{D}_T$ (including boundary conditions) according to (K.13) in terms of $\bar{e}$

$$
\begin{aligned}
\frac{dE(e)}{dt} &= -\int_0^1 \left\{ (-Ae + l_\xi e(\xi,t))^T We + e^T W\left(-Ae + l_\xi e(\xi,t)\right) \right\} dx \\
&= -\bar{e}^T \left[-2\Lambda + \left(L_\xi + L_\xi^T\right) \right] \bar{e}.
\end{aligned}
\tag{K.15}
$$

As the eigenvalue sets $\{\lambda_{i,j}\}_{i\in\mathbb{N}}$, $j = 1, 2$ form continuously decreasing series, the linear dissipation (K.15), of the linear innovated dynamics (K.13), can be bounded by the maximum of the eigenvalues $\lambda_{N+1,1}$, $\lambda_{N+1,2}$, and the dominant eigenvalue λ^*_{LN} of the innovated $N \times N$ matrix $\mathcal{M}^u_N$ given by

$$\mathcal{M}^u_L \triangleq \left[\begin{array}{cccc|cc}
\lambda_{1,1} & -l^c_{\xi,1}\varphi_{1,2}(\xi) & 0 & -l^c_{\xi,1}\varphi_{2,2}(\xi) & \dots & \dots \\
-l^c_{\xi,1}\varphi_{1,2}(\xi) & \lambda_{1,2} - l^T_{\xi,1}\varphi_{1,2}(\xi) & -l^c_{\xi,2}\varphi_{1,2}(\xi) & -l^T_{\xi,1}\varphi_{2,2}(\xi) - l^T_{\xi,2}\varphi_{1,2}(\xi) & \dots & \dots \\
0 & -l^c_{\xi,2}\varphi_{1,2}(\xi) & 2\lambda_{2,1} & -l^c_{\xi,2}\varphi_{2,2}(\xi) & \dots & \dots \\
-l^c_{\xi,1}\varphi_{2,2}(\xi) & -l^T_{\xi,2}\varphi_{1,2}(\xi) - l^T_{\xi,1}\varphi_{2,2}(\xi) & -l^c_{\xi,2}\varphi_{2,2}(\xi) & 2\lambda_{2,1} - l^T_{\xi,2}\varphi_{2,2}(\xi) & \dots & \dots \\
\vdots & \vdots & \vdots & \vdots & \ddots & \\
\vdots & \vdots & \vdots & \vdots & & \ddots \\
0 & 0 & 0 & \dots & \dots & \dots \\
-l^c_{\xi,1}\varphi_{N,2}(\xi) & -l^T_{\xi,1}\varphi_{N,2}(\xi) & -l^c_{\xi,2}\varphi_{N,2}(\xi) & -l^T_{\xi,2}\varphi_{N,2}(\xi) & \dots & \dots
\end{array}\right.$$

$$\left.\begin{array}{cc}
\dots & 0 \\
\dots & 0 \\
\dots & 0 \\
\dots & 0 \\
\ddots & \vdots \\
\ddots & \vdots \\
\dots & 2\lambda_{N,1} \\
\dots & -l^c_{\xi,N}\varphi_{N,2}(\xi)
\end{array}\right.
\left.\begin{array}{c}
-l^c_{\xi,1}\varphi_{N,2}(\xi) \\
-l^T_{\xi,1}\varphi_{N,2}(\xi) \\
-l^c_{\xi,2}\varphi_{N,2}(\xi) \\
-l^T_{\xi,2}\varphi_{N,2}(\xi) \\
\vdots \\
\vdots 0 \\
-l^c_{\xi,N}\varphi_{N,2}(\xi) \\
2\lambda_{N,2} - l^T_{\xi,N}\varphi_{N,2}(\xi)
\end{array}\right] . \tag{K.16}$$

Thus it holds

$$\begin{aligned}
\frac{dE(e(x,t))}{dt} &= -\bar{e}^T \left[-2\Lambda + \left(L_\xi + L_\xi^T\right)\right] \bar{e} \\
&\leq \max\{\lambda^*_{LN},\, \lambda_{N+1,1},\, \lambda_{N+1,2}\} \bar{e}^T \bar{e} \\
&= \max\{\lambda^*_{LN},\, \lambda_{N+1,1},\, \lambda_{N+1,2}\} E,
\end{aligned} \tag{K.17}$$

according to (K.12).

Finally, remind that the dissipation corresponding to the linear dynamics (K.13) is equivalent to the linear differential part of the dissipation $\mathcal{D}_T$, so that the following

result holds

$$
\begin{aligned}
&-2\int_0^1 \left\{ \left[-\frac{1}{P_{ec}}\frac{\partial^2 e_c}{\partial x^2} + \frac{\partial e_c}{\partial x} + l_{\xi,c} e_T(\xi,t) \right] w_1 e_c + \right. \\
&\quad \left. + \left[-\frac{L_e}{P_{eT}}\frac{\partial^2 e_T}{\partial x^2} + L_e \frac{\partial e_T}{\partial x} + \eta e_T + l_{\xi,T} e_T(\xi,t) \right] w_2 e_T \right\} dx \qquad \text{(K.18)} \\
&\leq \max\{\lambda^*_{LN},\, \lambda_{N+1,1},\, \lambda_{N+1,2}\} \int_0^1 e^T(x,t) W e(x,t) dx.
\end{aligned}
$$

Appendix L

Proof of Lemma 5.2

In order to express the linear differential term $\mathcal{D}_T$ in quadratic form, note that

$$
\begin{aligned}
- \quad & 2\int_0^1 \left\{ -\left[\frac{1}{P_{e,c}} e_{c,xx} - e_{c,x}\right] w_1 e_c - \left[\frac{L_e}{P_{e,T}} e_{T,xx} - L_e e_{T,x} - \eta e_T\right] w_{1,2} e_c \right\} dx \\
= & -\left[-2\frac{w_1}{P_{e,c}} \frac{\partial e_c}{\partial x} e_c + \left(\frac{1}{P_{e,c}} \frac{\partial w_1}{\partial x} + w_1 \right) e_c^2 - 2\frac{L_e w_2}{P_{e,T}} \frac{\partial e_T}{\partial x} e_T + \left(\frac{L_e}{P_{e,T}} \frac{\partial w_2}{\partial x} + L_e w_2 \right) e_T^2 \right]_0^1 + \\
& -\int_0^1 \left\{ -\left(\frac{1}{P_{e,c}} \frac{\partial^2 w_1}{\partial x^2} + \frac{\partial w_1}{\partial x} \right) e_c^2 + 2\frac{w_1}{P_{e,c}} \left(\frac{\partial e_c}{\partial x} \right)^2 \right. \\
& \left. -\left(\frac{L_e}{P_{e2}} \frac{\partial^2 w_2}{\partial x^2} + L_e \frac{\partial w_2}{\partial x} - \eta w_2 \right) e_T^2 + 2\frac{L_e w_2}{P_{e,T}} \left(\frac{\partial e_T}{\partial x} \right)^2 \right\} dx.
\end{aligned}
\tag{L.1}
$$

Application of Wirtinger's inequality (F.2) [97, 66], bounding the integrals over the squared profile gradient by integrals over the squared profiles and their boundary values in the inlet $x = 0$ yields

$$
\begin{aligned}
-2\int_0^1 \frac{w_1}{P_{e,c}} \left(\frac{\partial e_c}{\partial x} \right)^2 dx &\leq -\frac{w_{1,*}\pi}{2P_{e,c}} \int_0^1 \left(e_c - e_c(0,t) \right)^2 dx \\
-2\int_0^1 \frac{L_e w_2}{P_{e,T}} \left(\frac{\partial e_T}{\partial x} \right)^2 dx &\leq -4\frac{L_e w_{2,*}\pi}{2P_{e,T}} \int_0^1 \left(e_T - e_T(0,t) \right)^2 dx,
\end{aligned}
$$

where $w_{i,*}$, $i = 1, 2$, are the minimal values of the weighting function's element w_i, $i = 1, 2$. After substituting the boundary conditions (5.8) in the boundary term of (L.1), one obtains an expression of the linear differential part $\mathcal{D}_T$ of the dissipation

in integral quadratic form

$$
\begin{aligned}
- \quad & 2\int_0^1 \left\{ -\left[\frac{1}{P_{e,c}} e_{c,xx} - e_{c,x} \right] w_1 e_c - \left[\frac{L_e}{P_{e,T}} e_{T,xx} - L_e e_{T,x} - \eta e_T \right] w_2 e_T \right\} dx \\
&= - \int_0^1 \varpi^T \bar{Q} \varpi dx, \\
&\varpi = [e_c(x,t),\, e_T(x,t),\, e_c(0,t),\, e_T(0,t),\, e_c(1,t),\, e_T(1,t)]^T \\
&\bar{Q} = \begin{bmatrix}
-\frac{1}{P_{e1}}\frac{\partial^2 w_1}{\partial x^2} - \frac{\partial w_1}{\partial x} + \frac{w_{1,*}\pi}{2P_{e,c}} & 0 & -\frac{w_{1,*}\pi}{2P_{e,c}} & 0 & 0 & 0 \\
\star & -\frac{L_e}{P_{e2}}\frac{\partial^2 w_2}{\partial x^2} - \frac{\partial w_2}{\partial x} + \eta w_2 + \frac{L_e w_{2,*}\pi}{2P_{e,T}} & 0 & \frac{L_e w_{2,*}\pi}{2P_{e,T}} & 0 & 0 \\
\star & \star & \mathcal{R}_{c,0} & l_{c,0} w_1(0) & 0 & 0 \\
\star & \star & \star & \mathcal{R}_{T,0} & 0 & 0 \\
\star & \star & \star & \star & \mathcal{R}_{c,1} & l_{c,1}\frac{w_1(1)}{P_{e,c}} \\
\star & \star & \star & \star & \star & \mathcal{R}_{T,1}
\end{bmatrix} \\
&\mathcal{R}_{c,0} = \frac{w_{1,*}\pi}{2P_{e,c}} + \frac{1}{P_{e,c}}\frac{\partial w_1}{\partial x}(0) + \frac{P_{ec}-2}{P_{ec}} w_1(0) \\
&\mathcal{R}_{T,0} = \frac{w_{2,*}\pi}{2P_{e,T}} + \frac{L_e}{P_{e,T}}\frac{\partial w_2}{\partial x}(0) + \frac{P_{eT} + 2l_{T0} - 2L_e}{P_{eT}} w_2(0) \\
&\mathcal{R}_{c,1} = \frac{1}{P_{e,c}}\frac{\partial w_1}{\partial x}(1) + w_1(1) \\
&\mathcal{R}_{T,1} = \frac{L_e}{P_{e,T}}\frac{\partial w_2}{\partial x}(1) + Lew_2(1)\frac{2l_{T1+P_{eT}}}{P_{e,T}}.
\end{aligned}
\tag{L.2}
$$

Appendix M

Proof of Theorem 5.1

Proof. Let N, $l^i_{\xi,k}$, $k = 1, \ldots, N$, $i = c, T$ and $\xi \in [0, 1]$ be such that (5.29) holds. As $\lambda_{0,i} < 0$, $i = 1, 2$, and $\{\lambda_{k,i}\}_{k\in\mathbb{N}}$, $i = 1, 2$ forms a decreasing series, without loss of generality[1] assume that $-2\lambda_{\max} \triangleq -2\max\{\lambda^*_{LN}, \lambda_{N+1,1}, \lambda_{N+1,2}\} > 0$. In correspondence to (5.28), the strict dissipation with rate 2λ is ensured if for all $x \in [0, 1]$ the corresponding matrix

$$Q_x \triangleq \begin{bmatrix} 2\left(\lambda - \lambda_{\max}\right) W(x) - L^2_\rho h(x) I_2 & -W(x)G \\ -G^T W(x) & h(x) \end{bmatrix},$$

is positive definite, with $G = [-D_a, \beta D_a]^T$ as given in (5.13). According to the Schur complement of $h(x) > 0$ in Q_x, this condition is equivalent to

$$h(x) > \frac{G^T W(W^{-1})WG}{L^2\rho + 2\left(\lambda - \lambda_{\max}\right)} = \frac{D_a^2(w_1^2 + \beta^2 w_2^2)}{L^2\rho + 2\left(\lambda - \lambda_{\max}\right)},$$

and as $h(x) > 0$ this is equivalent to condition (5.30). The exponential stability results from Lemma 2.1. □

[1]For l^i_ξ, $i = c, T$, it holds that $\lambda_{k,i} > 0, k \in \mathbb{N}, i = 1, 2$. Thus, the gains can always be chosen such that this assumption holds.

Appendix N

Proof of Proposition 5.1

Proof. According to the LMI in Theorem 5.2, the following Lemma is obtained

Lemma N.1. *Consider the tubular reactor (5.1)-(5.2) with the dissipative observer (5.5)-(5.6), with point injection gain $l_{\xi,T} = l^0_{\xi,T}\delta(x-\xi)$, distributed gain $l_{\xi,c}$, and let L_ρ be the Lipschitz constant of the function $\rho(z;e)$ corresponding to (5.17). The zero solution $e(x,t) = [e_c(x,t),\, e_T(x,t)]^T = [0,0]^T$ is g.e.s. with rate $\lambda > 0$, if there exist positive definite functions $w_1(x)$, $w_2(x)$, and gains $l_{c,0}$, $l_{T,0}$, $l_{c,\xi}$, $l^0_{T,\xi}$, $l_{c,1}$, $l_{T,1}$, such that the following (differential) inequalities are satisfied*

$$
\begin{aligned}
&(a) \quad M_{2,b} \triangleq \left(-\frac{L_e}{P_{e2}}\frac{\partial^2 w_2}{\partial x^2} - \frac{\partial w_2}{\partial x} + \eta w_2 - 2\lambda w_2 - L_\rho^2 h\right) h - \beta^2 D_a^2 w_2^2 > 0 \\
&(b) \quad M_3 \triangleq -\left(\frac{1}{P_{e1}}\frac{\partial^2 w_1}{\partial x^2} + \frac{\partial w_1}{\partial x} + 2\lambda w_1 + L_\rho^2 h\right) M_{2,b} + \\
&\qquad\qquad + D_a^2 w_1^2 \left(\tfrac{L_e}{P_{e2}}\frac{\partial^2 w_2}{\partial x x^2} + \frac{\partial w_2}{\partial x} - \eta w_2 + 2\lambda w_2 + L_\rho^2 h\right) > 0 \\
&(c) \quad \mathcal{R}_{c,0} M_3 > \frac{w_{1,*}^2 \pi^2}{4 P_{ec}^2} M_{2,b} \\
&(d) \quad \mathcal{R}_{T,0} > 16 w_{2,*}^2 \left(Q_4^{-1}\right)_{22} + 8 w_{2,*} l_{c,0} w_1(0) \left(Q_4^{-1}\right)_{24} + l_{c,0}^2 w_1^2(0) \left(Q_4^{-1}\right)_{44} \\
&(e) \quad l^0_{\xi,T} w_2(\xi) > l^2_{\xi,c} w_1^2 \left(Q_5^{-1}\right)_{11} \\
&(f) \quad \mathcal{R}_{c,1} > 0 \\
&(g) \quad \mathcal{R}_{T,1} > l_{c,1}^2 \frac{w_1^2(1)}{4} \left(Q_7^{-1}\right)_{77}
\end{aligned}
\tag{N.1}
$$

where the $\mathcal{R}_{ij}, i = c, T, j = 0, 1$ *are given by*

$$\begin{aligned}
\mathcal{R}_{c,0} &= \frac{w_{1,\min}\pi}{2P_{e,c}} + \frac{1}{P_{e,c}}\frac{\partial w_1}{\partial x}(0) + \frac{P_{ec}-2}{P_{ec}}w_1(0) \\
\mathcal{R}_{T,0} &= \frac{w_{2,\min}\pi}{2P_{e,T}} + \frac{L_e}{P_{e,T}}\frac{\partial w_2}{\partial x}(0) + \frac{P_{eT}+2l_{T0}-2L_e}{P_{eT}}w_2(0) \\
\mathcal{R}_{c,1} &= \frac{1}{P_{e,c}}\frac{\partial w_1}{\partial x}(1) + w_1(1) \\
\mathcal{R}_{T,1} &= \frac{L_e}{P_{e,T}}\frac{\partial w_2}{\partial x}(1) + Lew_2(1)\frac{2l_{T1}+P_{e,T}}{P_{e,T}}.
\end{aligned}$$

and Q_i *referes to the upper left* $i \times i$ *submatrix of* Q *given in (5.33), and* $\left(Q_i^{-1}\right)_{jk}$*, respectively, to the element* jk *of its inverse.*

Proof. First it is shown that the conditions (N.1) are sufficient for the positive definiteness of the matrix Q in (5.33), and then conclude the global and exponential stability of the estimation error zero solution $e(x,t) = 0$. For the positive definiteness of the 8×8-matrix Q in (5.33) in all $x \in [0,1]$, it is necessary and sufficient that all leading principal minors $M_1, \ldots, M_8$ are positive. Note that the positivity of the first three leading principal minors is equivalent to the positivity of the upper left 3×3 submatrix of Q. Furthermore, this positivity issue can be established using arbitrary rearrangements maintaining symmetry. Using the following rearrangement

$$\begin{bmatrix}
h & -\beta D_a w_2 & D_a w_1 \\
-\beta D_a w_2 & \mathcal{D}_T w_2 - L_\rho^2 h & 0 \\
D_a w_1 & 0 & \mathcal{D}_c w_1 - L_\rho^2 h
\end{bmatrix},$$

where $\mathcal{D}_i w_j - L_\rho^2 h$, $i = c, T$, $j = 1, 2$ denotes the corresponding differential expressions in Q (5.33). Applying the criterion for positivity using the leading principal minors, one obtains conditions (a) and (b), namely

$$\begin{aligned}
M_{2,b} &= h\left(\mathcal{D}_T w_2 - L_\rho^2 h\right) - \beta^2 D_a^2 w_2^2 > 0 \\
M_3 &= \left(\mathcal{D}_c w_1 - L_\rho^2 h\right) M_{2,b} - D_a^2 w_1^2 \left(\mathcal{D}_T w_2 - L_\rho^2 h\right) > 0.
\end{aligned}$$

Actually the employed rearrangement is such that $M_{2,b}$ corresponds to the determinant of the lower right 2×2 submatrix of the upper left 3×3 submatrix Q_3 of Q, and M_3 corresponds to the third leading principal minor of Q, i.e. the determinant of this submatrix Q_3. Thus, conditions (a) and (b) imply the positivity of the first three leading principal minors M_1 to M_3. Conditions (c) to (g) ensure successively

the positivity of the subsequent principal minors M_4 to M_8. The respective conditions (c) to (g) are obtained using the Schur complement: the positivity of M_i is equivalent to the positivity of the Schur complement of the diagonal element $(Q)_{i,i}$ in Q_i, thus employing the positivity of the preceding determinant M_{i-1}, which in turn imply the invertibility of the matrices Q_{i-1}. Due to the particular coupling structure, represented in the columns of the matrix Q, the conditions (c) to (g) are obtained. Consequently it holds $\frac{d}{dt}E(e(x,t)) \leq -2\lambda E(e(x,t))$ and by the comparison lemma [73] it follows $E(e(x,t)) \leq E(e_0(x,t))\exp(-2\lambda t)$. Taking into account that $w_* \left|\left|e(x,t)\right|\right|^2 \leq E(e(x,t)) \leq w^* \left|\left|e(x,t)\right|\right|^2$, with $w_* = \inf\limits_{x\in[0,1]} \min\lambda(W)$ is the minimal and $w^* = \sup\limits_{x\in[0,1]} \max\lambda(W)$ is the maximal eigenvalue of $W(x) = W^T(x) > 0$, one obtains finally $||e(x,t)|| \leq a\,||e_0(x)||\exp(-\lambda t)$, with $a = \sqrt{w^*/w_*}$, i.e. $e(x,t) = 0$ is g.e.s. with convergence rate-amplitude pair (λ, a). □

Now, choose $h = w_1$ and let w_1 and w_2 satisfy

$$
\begin{aligned}
-\frac{1}{P_{e1}}\frac{\partial^2 w_1}{\partial x^2} - \frac{\partial w_1}{\partial x} - [2\lambda + L^2 + m_1]w_1 = 0 \\
-\frac{L_e}{P_{e2}}\frac{\partial^2 w_2}{\partial x x^2} - \frac{\partial w_2}{\partial x} + [\eta - 2\lambda - \beta^2 D_a^2 - m_2]w_2 = 0,
\end{aligned}
$$

which are satisfied e.g. for

$$
\begin{aligned}
w_1(x) = e^{P_{e,c}x}\cosh(\varpi_c x),\ \varpi_c = \frac{P_{e,c}^2}{4} - P_{e,c}\left(2\lambda + L_\rho^2 + m_1\right) \\
w_2(x) = e^{P_{e,T}x}\cosh(\varpi_T x),\ \varpi_T = \frac{P_{e,T}^2}{4} + P_{e,T}\left(\eta - 2\lambda - \beta^2 D_a^2 - m_2\right),
\end{aligned}
$$

Condition (a) is automatically satisfied, and $M_{2,b} = m_2 w_2 w_1 + L_\rho^2 w_1^2$ so that (b) takes the form

$$
m_1 w_1\left(m_2 w_2 w_1 + L_\rho^2 w_1^2\right) > D_a^2 w_1^2\left(m_2 w_2 w_1 + L_\rho^2 w_1^2 + \beta^2 D_a^2 w_2^2\right),
$$

what can be rewritten to

$$
m_1\left(m_2 w_2 + L^2 w_1\right) > D_a^2\left(m_2 w_2 w_1 + L_\rho^2 w_1^2 + \beta^2 D_a^2 w_2^2\right).
$$

This condition is satisfied if it holds

$$m_1 m_2 > D_a^4 \beta^2 w_2^*$$
$$m_1 L_\rho^2 w_1 > D_a^2 (m_2 w_1 w_2 + L_\rho^2 w_1^2).$$

The maximum of the weighting functions w_1 and w_2 lies in $x = 0$ with $w_1^* = w_2^* = 1$. Furthermore these functions are positive definite, if $\varpi_i \geq 0$, $i = c, T$. Consequently under these positivity conditions, it follows that the above conditions for $M_3 > 0$ are satisfied if $m_1 m_2 > D_a^4 \beta^2$, and

$$\frac{m_1 L_\rho^2}{D_a^2} > \frac{D_a^2 \beta^2 L_\rho^2}{m_2} > m_2 + L_\rho^2, \Leftrightarrow \; m_2 < L_\rho \sqrt{(D_a^2 \beta^2 - 1)}.$$

These conditions on the constants m_1, m_2 together with the conditions for the positivity of the functions w_1, w_2 lead to the conditions on the system parameters (5.34), i.e.

$$P_{e,c} > 4 \left(2\lambda + L_\rho^2 + \frac{D_a^4 \beta^2}{L_\rho \sqrt{(D_a^2 \beta^2 - 1)}} \right)$$
$$P_{e,T} > 4 \left(2\lambda + \beta^2 D_a^2 + L_\rho \sqrt{(D_a^2 \beta^2 - 1) - \eta} \right).$$

Further note that the gradients of the weighting functions are given by

$$\frac{\partial w_i}{\partial x} = e^{-P_{e,i} x} \left(-P_{e,i} \cosh(\varpi_i x) + \sinh(\varpi_i x) \right), i = c, T,$$

so that the corresponding conditions on the weighting function w_1 on the boundaries are fulfilled under the above conditions on m_1 and m_2, and correspondingly on $P_{e,c}$ and $P_{e,T}$. □

Appendix O

Proof of Theorem 6.1

Proof. Consider the energy $E(e) = \int_0^1 e^T W e dx$ (6.12), and its dissipation according to the dynamics (6.26)

$$\frac{dE}{dt} = \int_0^1 \begin{bmatrix} e(x,t) \\ \nu(x,t) \end{bmatrix}^T \begin{bmatrix} WA + A^*W & WG \\ G^TW & 0 \end{bmatrix} \begin{bmatrix} e(x,t) \\ \nu(x,t) \end{bmatrix} dx.$$

According to the $(-R, S^T, -Q)$-strict dissipativity condition of the linear dynamic system $\Sigma(A, G, H)$, and the (Q, S, R)-dissipativity condition of the nonlinear static system $\nu = -\rho$ one has consequently

$$\begin{aligned} \frac{dE}{dt} &\leq \int_0^1 \begin{bmatrix} e(x,t) \\ \nu(x,t) \end{bmatrix}^T \begin{bmatrix} -H^TR(x)H - 2\lambda W & S^TH \\ H^TS & -Q(x) \end{bmatrix} \begin{bmatrix} e(x,t) \\ \nu(x,t) \end{bmatrix} dx \\ &\leq -2\lambda \int_0^1 e^T W e dx = -2\lambda E(e). \end{aligned}$$

The exponential stability follows from Lemma 2.1. □

Appendix P

Proof of Theorem 6.2

Proof. Introduce the energy $E(e) = \int_0^1 e^T W e dx$, which is equivalent to the standard norm in Z according to (2.18). The corresponding dissipation is given by

$$\frac{dE}{dt} = \int_0^1 \begin{bmatrix} e(x,t) \\ \nu(x,t) \end{bmatrix}^T \begin{bmatrix} WA_L + A_L^* W & WG \\ G^T W & 0 \end{bmatrix} \begin{bmatrix} e(x,t) \\ \nu(x,t) \end{bmatrix} dx.$$

According to the LOI (6.30), and the (Q, S, R)-dissipativity condition of the nonlinear static system $\nu = -\rho$ one has consequently

$$\begin{aligned} \frac{dE}{dt} &\leq \int_0^1 \begin{bmatrix} e(x,t) \\ \nu(x,t) \end{bmatrix}^T \begin{bmatrix} -H^T R(x) H - 2\lambda W & S^T H \\ H^T S & -Q(x) \end{bmatrix} \begin{bmatrix} e(x,t) \\ \nu(x,t) \end{bmatrix} dx \\ &\leq -2\lambda \int_0^1 e^T W e dx = -2\lambda E(e). \end{aligned}$$

The exponential stability results from Lemma 2.1. □

Bibliography

[1] R. E. Kalman. When is a linear system optimal? *Trans. ASME, J. Basic eng., Ser. D.*, 86:51–60, 1964.

[2] J.C. Willems. Least squares stationary optimal control and the algebraic riccati equation. *IEEE Trans. Autom. Cont.*, (16)6:621–634, 1971.

[3] R.A. Freeman and P. Kokotovic. *Robust Nonlinear Control Design: State-Space and Lyapunov Techniques*. Birkhäuser, Boston, 1996.

[4] M. Krstic, I. Kanellakopoulos, and P. Kokotovic. *Nonlinear And Adaptive Control Design*. Wiley, 1995.

[5] A. Van der Schaft. *L2-Gain and Passivity Techniques in Nonlinear Control*. Springer-Verlag, 2000.

[6] A. Isidori. *Nonlinear Control Systems II*. Springer-Verlag, 1999.

[7] W.H. Ray. *Advanced Process Control*. McGraw-Hill New York, 1981.

[8] G. Bastin and D. Dochain. *On-Line Estimation and Adaptive Control of Bioreactors*. Elsevier, Amsterdam, 1990.

[9] A. Varma and R. Aris. *Chemical Reactor Theory - A Review*, chapter 2. Stirred Pots and Empty Tubes, pages 79–155. Prentice Hall, 1977.

[10] R. Aris. *Introduction to the Analysis of Chemical Reactors*. Prentice-Hall, 1969.

[11] P.D. Christofides. *Nonlinear and Robust Control of PDE Systems - Methods and Applications to Transport-Reaction Processes*. Systems & Control: Foundations & Applications - Birkhäuser, 2001.

[12] D.J. Korteweg and F. de Vries. On the change of form of long waves advancing in a rectangular canal, and on a new type of long stationary waves. *Phylosophical Magazine*, 39:422–443, 1895.

[13] Y. Kuramoto and T. Tsuzuki. Persitent propagation of concentration waves in dissipative media far from thermal equilibrium. *Progress of Theoretical Physics*, (55)2:356–369, 1976.

[14] G.I. Shivashinsky. On flame propagation under conditions of stoichiometry. *SIAM J. Appl. Math.*, (39)1:67–82, 1980.

[15] H.S. Fogler. *Elements of chemical reaction engineering.* Prentice Hall, 1999.

[16] A.G. Fredrickson and H.M Tsuchiya. *Microbial Kinetics and Dynamics*, chapter 7. Prentice-Hall, New Jersey, 1977.

[17] G. Briggs and J.B. Haldane. A note on the kinetics of enzyme action. *Biochem J*, 19:338–339, 1925.

[18] J.J. Carberry. *Chemical and Catalytic Reaction Engineering.* McGraw-Hill, New York, 1976.

[19] S. Elnashaie and M. Abashar. The implication of non-montonic kinetics on the design of catalytic reactors. *Ch. Eng. Sci.*, (45)9:2964–2967, 1990.

[20] R. Antonelli and A. Astolfi. Continuous stirred tank reactors: easy to stabilise? *Automatica*, 39(10):1817–1827, 2003.

[21] A. Schaum and J.A. Moreno. Dynamical analysis of global obseravbility properties for class of biological reactors. In *10th International IFAC Symp. Computer Applications in Biotechnology 2007, Cancun, Mexico*, 2007.

[22] J. Diaz-Salgado, A. Schaum, J.A. Moreno, and J. Alvarez. Interlaced estimator-control design for continuous exothermic reactors with non-monotonic kinetics. In *Eighth International IFAC Symposium on Dynamics and Control of Process Systems, Cancun, Mexico*, 2007.

[23] J.D. Murray. *Mathematical Biology.* Springer-Verlag, Heidelberg, 1989.

[24] C. Delattre, D. Dochain, and J. Winkin. Observability analysis of a nonlinar tubular bioreactor. In *Proceedings of the Mathematical Theory of Networks and Systems 2002*, pages paper 12197 (CD–ROM), 2002.

[25] C. Delattre and D. Dochain adn J. Winkin. Observability analysis of nonlinear tubular (bio)reactor models: A case study. *Journal of Process Control*, 14:661–669, 2004.

[26] D. Vries. *Estimation and Prediction of Convection-Diffusion-Reaction Systems from Point Measurements*. PhD thesis, Univeristy of Wageningen, The Netherlands, 2008.

[27] Ksouri M. Boubaker O., Babary J.P. Variable structure estimation and control of nonlinear distributed parameter bioreactors. In *IEEE International Conference on Systems, Man, and Cybernetics 1998*, pages 3770–3774, 1998.

[28] R. Baratti, J. Alvarez, and M. Morbidelli. Design and experimental identification of nonlinear chemical reactor estimator. *Chem. Eng. Sci.*, 48 (14):2573–2585, 1993.

[29] I. Smets, G. Bastin, and J. Van Impe. Feedback stabilization of fed-batch bioreactors: Non-monotonic growth kinetics. *Biotechn. Prog.*, 18:1116–1125, 2002.

[30] Kokotovic P.V. H.K. Khalil J. O'Reilly. *Singular Perturbation Methods in Control: Analysis and Design*. Academic Press, 1986.

[31] I.G. Kevrekidis Shvartsman S.Y. Nonlinear model reduction for control of distributed systems: a computer-asisted study. *AiChE Journal*, (44)7:1579–1595, 1998.

[32] Shvartsman S.Y. C. Theodoropoulos R. Rico-Martínez. I.G. Kevrekidis E.S. Titi T.J. Mountziaris. Order reduction for nonlinear dynamic models of distributed reaction systems. *Journal of Process Control*, 10:177–184, 2000.

[33] P.K.C. Wang. Asymptotic stability of distributed parameter systems with feedback controls. *IEEE Trans. Autom. Control*, (11)1:46–54, 1966.

[34] E.D. Gilles. *Systems with distributed parameters (Introdction to Control Theory), in german*. R. Oldenburg Verlag, 1973.

[35] Gressang R.V. G.B. Lamont. Observers for systems characterized by semigroups. *IEEE Trans. Autom. Cont.*, pages 523–528, 1975.

[36] M. Köhne. *State-observers for systems with distributed parameters - Theory and Application (in german).* Fortschrittsberichte Nr. 8/26, 1977.

[37] R. Curtain. Finite-dimensinoal compensator design for parabolic distributed systems with point sensors and boundary input. *IEEE Trans. Autom. Cont.*, (27)1:98–104, 1982.

[38] R.F. Curtain and A.J. Pritchard. *Infinite dimensional linear systems theory.* Lecture Notes in Control and Information Sciences. Springer-Verlag, 1978.

[39] Curtain R.F. and H. Zwart. *An Introduction to Infinite Dimensional Linear Systems Theory*, volume 21 of *Texts in Applied Mathematics.* Springer-Verlag, 1995.

[40] Ajinkya M.B. W.H. Ray T.K. Yu J.H. Seinfeld. The apllication of an approximate non-linear filter to systems governed by coupled ordinary and partial differential equations. *Int. J. Systems Sci.*, 6:313–332, 1975.

[41] Shmyshlyaev A. M. Krstic. Backstepping observers for a class of parabolic pdes. *System & Control Letters*, 54:613–625, 2005.

[42] M. Zeitz. *Nonlinear Observers For Chemical Reactors (in german).* Fortschrittsberichte, 1977.

[43] M. Zeitz Bitzer, M. Design of a nonlinear distributed parameter observer for a pressure swing adsorption plant. *J. of Process Control*, 12:533–543, 2002.

[44] Vande Wouver A. M. Zeitz. State estimation in distributed parameter systems. *Enzyclopedia of Life Support Systems, http:\\www.eolss.net*, 2002.

[45] Kreutzinger Bitzer M. Marquardt W. State estimation of a stratified storage tank. *Control Engineering Practice*, 16:308–320, 2008.

[46] J. Alvarez and G. Stephanopoulos. An estimator for a class of non-linear distributed systems. *Int. J. Cont.*, (36)5:787–802, 1982.

[47] D. Dochain. *Contribution to the Analysis and Control of Distriuted Darameter Systems with Applications to (Bio)Chemical Engineering and Robotics (*Thése présentée en vue de l'obtention du grade d'agrégé de l'enseignement superieur). PhD thesis, Universidad Catolica de Louvain, Belgica, 1994.

[48] P. Ligarius and J.F. Couchouron. Asymptotic observers for a class of evolution operators. a nonlinear approach. *C. R. Acad. Sci. Paris - Automatique Théorique*, t. 327, Série I:355–360, 1997.

[49] D. Dochain. State observers for tubular reactors with unknown kinetics. *JPC*, 10:259–268, 2000.

[50] García M.R C. Villas J.R. Banga V.L. Lyubenova M.N. Ignatova A.A. Alonso. State reconstruction in spatially distributed bioprocess systems using reduced order models: Application to the gluconic acid production. In *44th IEEE CDC and European Control Conference, Sevilla, España*, 2005.

[51] P.D. Christofides and P. Daoutidis. Finite-dimensional control of parabolic pde systems using approximate iniertial manifolds. *JMAA*, (216)2:398–420, 1997.

[52] Hagen G. I. Mezic. Spillover stabilization in finite-dimensional control and observer design for dissipative evolution equations. *SIAM J. Cont. Optim.*, (42)2:746–768, 2003.

[53] Soliman M.A. H.W. Ray. Nonlinear state estimation of packed bed tubular reactors. *AIChe*, (25)4:718–720, 1979.

[54] W.H. Ray. Some recent applications of distributed parameter systems theory - a survey. *Automatica*, 14:281–287, 1978.

[55] Alvarez J., Zaldo F., and Oaxaca G. *Towards a joint Process and Control Design framework for batch processes: Application to Semibatch Polymer Reactors*, volume The Integration of Process Design and Control, chapter D6, pages 604–634. Elsevier, Amsterdam, The Netherlands, 2004.

[56] J.C. Willems. Dissipative dynamical systems: Part i - general theory, part ii - linear systems with quadratic supply rates. *Archive for Rational Mechanics and Analysis*, 45:321–393, 1972.

[57] D.J. Hill and P.J. Moylan. Dissipative dynamical systems: Basic input-output and state properties. *Journal of the Franklin Institute*, (309)5:327–357, 1980.

[58] H.K. Pillai J.C. Willems. Losless and dissipative distributed systems. *SIAM J. Cont. Optim.*, (40)5:1406–1430, 2002.

[59] B. Straughan. *The Energy Method, Stability, and Nonlinear Convection*. Applied Mathematical Sciences. Springer, 2004.

[60] Stephen P. Banks. *State-space and frequency-domain methods in the control of distributed parameter systems*. IEE Topics in Control Series 3, 1983.

[61] J.A. Moreno. Observer design for nonlinear systems: a dissipative approach. In *2nd IFAC Symposium on System, Structur and Control, Oaxaca 2004*, 2004.

[62] J.A. Moreno. Approximate observer error linearization by dissipativity methods. *Control and Observer Design for Nonlinear Finite and Infinite Dimensional Systems, Springer LNCIS*, pages 35–51, 2005.

[63] V.I. Zubov. *Methods of A.M. Lyapunov and their application*. P. Noordhoff LTD - Groningen - The Netherlands, 1964.

[64] A.N. Michel and R.K. Miller. *Qualitative Analysis of Large Scale Dynamical Systems*, volume 134 of *Mathematics in Science and Engineering*. Academic Press, 1977.

[65] A.R. Castro Figueroa. *Estabilidad de las ecuaciones diferenciales ordinarias y las ecuaciones funcionales*. IPN, Mexico, 1998.

[66] Y. Orlov. *Discontinuous Systems (Lyapunov Analysis and Robust Synthesis under Uncertainty Conditions)*. Springer-Verlag, 2008.

[67] P.V. Danckwerts. Continuous flow systems: distribution of residence times. *Chemical Engineering Science*, 2:2–3, 1953.

[68] F.G. Shinskey. *Process Control Systems 3rd. Edt.* McGraw-Hill, New York, 1988.

[69] W.L. Luyben. *Process Modeling, Simulation and Control for Chemical Engineers, Second Ed.* McGraw-Hill, Singapore, 1990.

[70] J. Alvarez, J. Alvarez, and R. Suarez. Nonlinear bounded control for a class of continuous agitated tank reactors. *Chem. Eng. Sci.*, 46(12):3235–3249, 1991.

[71] J. La Salle and S. Lefschetz. *Stability by Lyapunov's Direct Method*. Academic, New York, 1961.

[72] E. D. Sontag. *Nonlinear Control in the Year 2000*, volume 2 of *Lecture Notes in Control and Information Sciences*, chapter The ISS Philosophy as a unifying Framework for Stability-like Behavior. Springer-Verlag, berlin, 2000.

[73] H.K. Khalil. *Nonlinear Systems (Third Edition)*. Prentice Hall, Upper Saddle River, New Jersey, 2002.

[74] J. Alvarez, J. Alvarez, and R. Suarez. Nonlinear bounded control for a class of continuous agitated tank reactors. *Chemical Engineering Science*, (46)12:3235–3249, 1991.

[75] R. Hermann and A.J. Krener. Nonlinear controllability and observability. *IEEE Trans. Autom. Contr.*, pages 728–740, 1977.

[76] H. Sussmann. Single input observability of continuous time systems. *Math. Syst. Theory*, 12:371–393, 1979.

[77] H. Nijmeier and A. van der Schaft. *Nonlinear Dynamical Control Systems*. Springer Verlag, 1990.

[78] J.P. Gauthier, H. Hammouri, and S. Othman. A simple observer for nonlinear systems applications to bioreactors. *IEEE Trans. Autom. Cont.*, (37)6:875–880, 1992.

[79] J. Alvarez. Nonlinear state estimation with robust convergence. *J. Process Control*, 10 (1):59–71, 2000.

[80] R.E. Kalman, P.L. Falb, and M.A. Arbib. *Topics in Mathematical System Theory*. McGraw-Hill, 1969.

[81] S. Ibarra Rojas, J.A. Moreno, and G. Espinosa. Global observability analysis for sensorless induction motors. *Automatica*, 40:1079–1085, 2004.

[82] Arcak M. P. Kokotovic. Nonlinear observers: A cricle criterion design. In *38th IEEE CDC, Phoenix, USA*, 1999.

[83] A. Schaum, J.A. Moreno, J. Alvarez, and J. Diaz-Salgado. Dissipativity-based observer and feedback control design for a class of chemical reactors. *Journal of Process Control*, 18(9):896–905, 2008.

[84] A. Schaum et Al. Dissipativity-based observer and feedback control design for a class of chemical reactors. In *8th International IFAC Symposium DYCOPS, Cancun, Mexico*, 2007.

[85] A. Schaum, J.A. Moreno, J. Alvarez, and J. Diaz-Salgado. Output-feedback dissipative control of exothermic continuous reactors. In *IFAC International Symposium on Advanced Control of Chemical Processes, Istanbul, Turkey*, 2009. submitted.

[86] J. Alvarez-Ramirez, J. Alvarez, and A. Morales. An adaptive cascade control for a class of chemical reactors. *J. Adaptive Control Signal Process.*, 16:681–701, 2002.

[87] P. Gonzalez and J. Alvarez. Combined pi-inventory control of solution homopolymerization reactors. *Ind. Eng. Chem. Res. J.*, pages 7147–7163, 2005.

[88] J. Alvarez and P. Gonzalez. Constructive control of continuous polymer reactors. *J. Process Control*, 17:463–476, 2007.

[89] R. Sepulchre, M. Jankovic, and P. Kokotovic. *Constructive Nonlinear Control*. Springer-Verlag, London, 1997.

[90] C.I. Byrnes, A. Isidori, and J.C. Willems. Passivity, feedback equivalence, and the global stabilization of minimum phase nonlinear systems. *IEEE Trans. Autom. Cont.*, 36(11):1228 – 1240, 1991.

[91] D. Franke. *Systems with spatially distributed parameters (An introduction to modelling, analysis and control) , in german*. Springer-Verlag, 1987.

[92] R. Courant and D. Hilbert. *Methods of Mathematical Physics*, volume 4th ed. Springer-Verlag, 1993.

[93] K. Jänich. *Analysis for physicists and engineers (in german)*, volume 3rd ed. Springer-Verlag, 1995.

[94] J.W. Dettman. *Mathematical Methods in Physics and Engineering*. DoverPublications, Inc., New York, 1988.

[95] A.B. Hanson G. W., Yakovlev. *Operator Theory for Electromagnetics - An Introduction*. Springer, 2002.

[96] C. Delattre, D. Dochain, and J. Winkin. Sturm-liouville systems are riesz spectral systems. *Int. J. Apl. Math. Comp. Sci.*, (13)4:481–484, 2003.

[97] E. Schmidt. About the inequality which connects the integrals of over a power of a function and over another power of its derivative (in german). *Math. Ann.*, 117(1):301–326, 1940.

[98] G. Hardy, J.E. Littlewood, and G. Polya. *Inequalities*. Cambridge Mathematical Library, 1988.

[99] S. Boyd, L. El Ghaoui, E. Feron, and V. Balakrishnan. *Linear Matrix Inequalities in Systems and Control Theory*. SIAM Frontier Series, 1994.

[100] A. Schaum, J.A. Moreno, E. Fridman, and J. Alvarez. Observer design for a class of transport-reaction systems: A direct lyapunov approach. In *IFAC International Symposium on Robust Control Design 2009, Haifa, Israel.*, 2009. accepted.

[101] V.M. Popov. Absolute stability of nonlinear systems of automatic control. *Automation Remote Control*, 22:857–875, 1962.

[102] L. Pandolfi. Dissipativity and the lur'e problem for parabolic doundary control systems. *SIAM J. Control Optim.*, (36)6:2061–2081, 1998.

[103] Pillai H.K. J.C. Willems. Dissipative distributed systems. In *39th IEEE CDC, Sydney, Australia*, 2000.

[104] L.A. Zadeh. *The Concept of System, Aggregate, and State in System Theory*. McGraw-Hill, 1969. in: System Theory.

[105] D.C. Youla. The synthesis of linear dynamical systems from prescribed weighting patterns. *SIAM J. Appl. Math.*, 14(3):527–549, 1966.

[106] R.F. Estrada and C.A. Desoer. Passivity and stability of systems with a state representation. *Int. J. Control*, 13(1):1–26, 1971.

[107] J.S. Barras, R. W. Brockett, and P.A. Furhmann. State-space models for infinite-dimensional systems. *IEEE Trans. Autom. Control*, 19(6):693–700, 1974.

[108] C.A. Desoer and M. Vidyasagar. *Feedback systems: Inputut-Output Properties.* Academic Press INC. (London), 1975.

[109] V. Bondarko and A. Fradkov. Necessary and sufficient conditions for the passivitcability of linear distributed systems. *Automation and Remote Control*, (64)4:517–530, 2003. (Translated from Avtomatika i Telemekhanika No. 4, 2003, P. 3–17).

[110] R.F. Curtain, M.A. Demetriou, and K. Ito. Adaptive compensators for perturbed positive real infinite dimensional systems. *Int. J. Appl. Math. Comp. Sci.*, (13)4:441–452, 2003.

[111] Curtain R.F. Logemann H. Staffans O. Absolute-stability results in infinite dimensions. *Proc. R. Soc. Lond.*, A (2004) 460:2171–2196, 2004.

[112] E. Fridman and Y. Orlov. H_∞ boundary control of semilinear heat processes and distributed mechanical oscillators: an lmi approach. In *47th IEEE Conference on Decision and Control Proceedings, Cancun, Mexico*, 2008.

[113] J.J. Winkin D. Dochain P. Ligarius. Dynamical analysis of distributed parameter tubular reactors. *Automatica*, 36:349361, 2000.